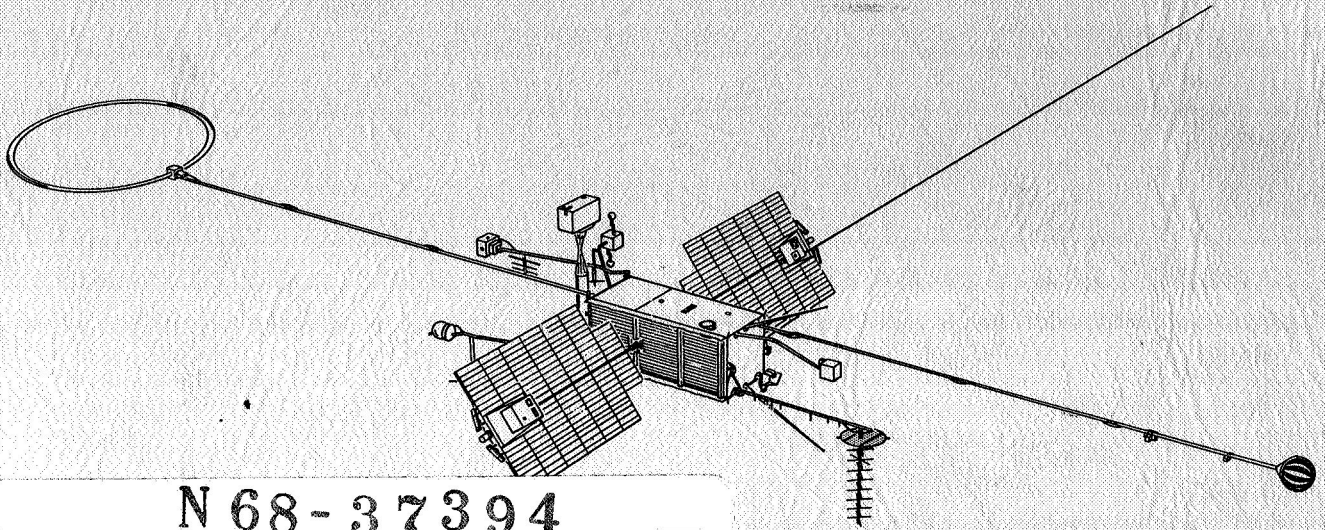


ORBITING GEOPHYSICAL OBSERVATORY ATTITUDE CONTROL SUBSYSTEM DESIGN SURVEY



FACILITY FORM 602	N 68-37394	(ACCESSION NUMBER)	(THRU)
	84	(PAGES)	(CODE)
	CR-86107	(NASA CR OR TMX OR AD NUMBER)	31
	(CATEGORY)		

NASA/ERC Design Criteria Program, Guidance and Control

Contract NAS-12-110

1968 June 28

Prepared for

NATIONAL AERONAUTICS AND SPACE ADMINISTRATION
Electronics Research Center
Cambridge, Massachusetts

GPO PRICE \$ _____

CSFTI PRICE(S) \$ _____

Hard copy (HC) _____

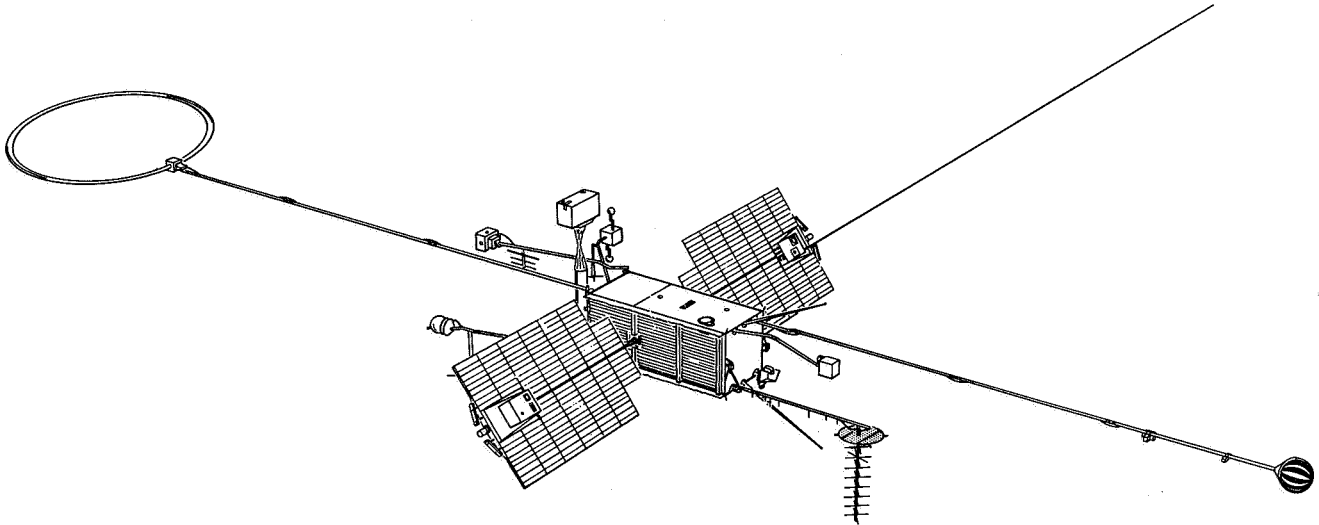
Microfiche (MF) _____



One Space Park • Redondo Beach, California



**ORBITING GEOPHYSICAL OBSERVATORY
ATTITUDE CONTROL SUBSYSTEM DESIGN SURVEY**



**NASA/ERC
Design Criteria Program, Guidance and Control**

Contract NAS 12-110

1968 June 28

Prepared for

NATIONAL AERONAUTICS AND SPACE ADMINISTRATION

Electronics Research Center
Cambridge, Massachusetts

TRW
SYSTEMS GROUP

One Space Park • Redondo Beach, California

ORBITING GEOPHYSICAL OBSERVATORY
ATTITUDE CONTROL SUBSYSTEM
DESIGN SURVEY

NASA/ERC DESIGN CRITERIA PROGRAM
GUIDANCE AND CONTROL


Prepared for
National Aeronautics and Space Administration
Electronics Research Center
Cambridge, Massachusetts

Contract NAS 12-110


28 June 1968

K. J. McKenna
H. Schmeichel

Approved:


W. J. Wellens, Manager
Control Systems
Laboratory

Approved:


T. W. Layton
Study Manager
Contract NAS 12-110

FOREWORD

This report is one of a series of design surveys being produced by industrial contractors as part of the NASA Design Criteria Program. The objective of the program is to provide a unification of design approaches for the development of space vehicles and their major components. The surveys are intended to document design experience gained from specific NASA projects and will be used as an aid in identifying suitable topics for design criteria monographs.

Acknowledgment

The authors wish to acknowledge the invaluable support given to them by many members of the OGO ACS design team. Martin S. Robinson, the OGO ACS Subproject Manager until 1967, was the prime source of much of the material within this document. Without his files and indelible memory, much would have had to be omitted. Richard E. Frazier, Senior System Engineer of the OGO project, contributed greatly to our understanding of the total spacecraft. His views on the history of flight problems with the ACS appear almost verbatim in Subsection 5.6. Robert J. Moore, the present OGO ACS Subproject Manager, provided much needed critical review of our efforts.

We would also like to acknowledge the valuable information provided by some of the many engineering personnel who participated in the OGO program: George R. Field, Patrick B. Hutchings, William N. Keller, Robert L. Wattenbarger, Robert M. Weiner, and Robert L. Winterstrom.



CONTENTS

1.	SUMMARY AND CONCLUSIONS	1
2.	SYSTEM DESCRIPTION	3
2.1	CONTROL REQUIREMENTS	3
2.1.1	General Requirements	3
2.1.2	Performance Requirements	4
2.1.3	Control Techniques and Equipment Complement	5
2.2	DESCRIPTION OF ACS OPERATION	7
2.2.1	Coordinate Systems	7
2.2.2	ACS Operation and Mode Sequencing	7
2.3	COMMAND FUNCTIONS	11
2.4	EQUIPMENT DESCRIPTION	14
2.4.1	Sensors	14
2.4.2	ACS Electronics	16
2.4.3	Torque Sources	16
2.4.4	Electromechanical Drives	17
2.5	ACS PHYSICAL PROPERTIES	17
2.5.1	Reliability	17
2.5.2	Weight	18
2.5.3	Power	19
3.	EARLY HISTORY OF ACS DESIGN DEVELOPMENT	20
3.1	OGO PROGRAM CONTRACTUAL HISTORY	20
3.2	ACS DESIGN HISTORY	20
3.3	THE OGO PROPOSAL	20
3.4	THE DESIGN MODIFICATION AND EVALUATION STUDY	22
3.5	ACS DETAILED DESIGN	23
3.6	SYSTEM ANALYSIS	25
3.7	HARDWARE DESIGN	26
3.7.1	Horizon Scanners	26
3.7.2	Sun Sensor	27
3.7.3	Pitch Rate Gyro	27
3.7.4	OPEP Gyrocompass	27
3.7.5	ACS Electronics	27
3.7.6	Reaction Wheels	28
3.7.7	Solar Array and OPEP Drives	28
3.7.8	Pneumatics	29

CONTENTS (Continued)

3.8	SYSTEMS TEST	29
3.8.1	Torsion Wire Test	29
3.8.2	Air-Bearing Test	29
3.8.3	Subsystem Laboratory Test	29
4.	DISCUSSION OF MAJOR PRELAUNCH PROBLEMS AND SOLUTIONS	31
4.1	CHRONOLOGICAL HISTORY	31
4.2	PROBLEMS UNCOVERED BY DESIGN ANALYSIS	32
4.2.1	POGO Gas Consumption	32
4.2.2	Acquisition During Eclipse	32
4.2.3	Boom Oscillations	33
4.2.4	Internal Temperature Rise of Reaction Wheel Assembly	33
4.2.5	Sun Sensor Shading	34
4.2.6	Earth Albedo Effect	34
4.2.7	Redesign of Two-Phase Inverter	34
4.3	PROBLEMS FOUND IN UNIT TESTS	34
4.3.1	Test Procedure	34
4.3.2	Horizon Scanner	35
4.3.3	Sun Sensor	36
4.3.4	Pitch Rate Gyro	36
4.3.5	OPEP Gyro	37
4.3.6	ACS Electronics	37
4.3.7	Solar Array and OPEP Drive Mechanism	37
4.3.8	Reaction Wheels	38
4.3.9	Pneumatics	39
4.4	LABORATORY SYSTEM TEST PROBLEMS	39
4.4.1	Single-Axis Simulation	39
4.4.2	Three-Axis Simulation	39
4.4.3	ACS Laboratory Evaluation Test	41
4.5	PROBLEMS IN SPACECRAFT INTEGRATION	41
4.5.1	RF Interference	41
4.5.2	SELA Switching Problems	42
4.5.3	Speed Problem With Drive Mechanism	42
4.5.4	Failure to Switch from Coarse to Fine Sun Sensors	42
4.5.5	OPEP Driving Problem	42
4.6	REVIEW OF PRELAUNCH PROBLEMS	43

CONTENTS (Continued)

5.	PROBLEMS UNCOVERED IN FLIGHT OPERATIONS	44
5.1	OGO-I	44
5.1.1	Partial Boom Deployment Problem	44
5.1.2	Corrective Action	45
5.2	OGO-II	45
5.2.1	Tracking of Cold Clouds	45
5.2.2	Horizon Scanner Modifications	47
5.2.3	The "Small Earth" Problem	48
5.2.4	OPEP Oscillation	50
5.2.5	Control Gas Time Delay	50
5.2.6	Backup Commands	51
5.3	OGO-III	51
5.3.1	Redesigned Magnetic Amplifiers	55
5.3.2	ACS Design Changes	55
5.4	OGO-IV	58
5.4.1	Operation by Ground Control	58
5.4.2	Source of OGO-IV SOEP Antenna Oscillation	60
5.4.3	Moon Tracking	61
5.5	OGO-V	61
5.6	REVIEW OF IN-FLIGHT PROBLEMS AND RELATION TO DESIGN APPROACH	63
6.	NEW CONCEPTS	66
6.1	ACS INNOVATIONS	66
6.1.1	Wobble Gear	66
6.1.2	Bang-Bang Reaction Wheel Control	66
6.1.3	Sun Orientation Control	66
6.1.4	Horizon Scanner	66
6.1.5	Sun Sensor	67
6.1.6	Testing	67
6.2	FLIGHT OPERATIONS	67
7.	THE PROGRAM IN RETROSPECT	68
7.1	SYSTEMS DESIGN	68
7.1.1	Ground Back-Up	68
7.1.2	Gas Control Law Design	68
7.1.3	Dynamic Interaction	69

CONTENTS (Continued)

7.2	EQUIPMENT DESIGN	69
7.2.1	Horizon Scanner	69
7.2.2	Magnetic Amplifiers	69
7.2.3	System Testing	70
7.2.4	Mission Changes	70
8.	REFERENCES	71

ILLUSTRATIONS

1	OGO-E Experiment Locations	3
2	OGO Attitude Control Subsystem: Coordinate System and Sign Conventions	4
3	Control System Block Diagram	6
4	Earth Acquisition Window	8
5	Nominal Yaw and Array Angles	10
6	Sun Sensor Assemblies -- Front View	14
7	OGO Horizon Scanner Geometry	15
8	OGO Horizon Scanner Detector Assemblies, Covers Off	15
9	OGO Solar Array and OPEP Drive	17
10	OGO Program Major ACS Milestones	21
11	Torsion Wire Test Table	39
12	Air-Bearing Space Simulator and ACS Table	40
13	View of OGO Looking at +Z Side	44
14	ACS Behavior with Scanner Head "D" Tracking Anomaly	46
15	ACS Behavior with Scanner Head "D" Tracking Anomaly	47
16	Revised Earth Horizon Model and Trapping Mechanism	47
17	Comparative Horizon Radiance Profiles	48
18	Telescope System	48
19	Computation of Errors for a Small Earth	49
20	Computed Versus True Roll Error for 2.3 Earth Half Angle	49
21	Typical Pitch or Roll Channel Gas Delay Logic	50
22	OGO-III Telemetry Rev. 002 Prior to Perigee Roll Wheel Oscillation Begins	52
23	OGO-III Telemetry Rev. 001 Expanded Scales Start of Array Limit Cycle	53
24	OGO-III Telemetry Rev. 001 Gas Delay Logic Command Event	54
25	Reaction Wheel Delay Logic	55
26	New OPEP Control Loop	56
27	A-C Scan Plane Rotation Geometry	57
28	Telemetry of OGO-IV SOEP Antenna Oscillation	59
29	Moon-Earth-Sun Spacecraft Positions for Moon Tracking	61
30	Telemetry of OGO-V -X SOEP Antenna Oscillation	62
31	Telemetry of OGO-V +X SOEP Antenna Oscillation	64

1. SUMMARY AND CONCLUSIONS

This design survey summarizes the history of the Orbiting Geophysical Observatories' (OGO) Attitude Control Subsystem (ACS) from the proposal phase through current flight experience. Problems encountered in design, fabrication, test, and on orbit are discussed. It is hoped that the experiences of the OGO program related here will aid future designers.

OGO was conceived as a scientific "truck" to carry large numbers (up to 50) of scientific experiments into an arbitrary earth orbit. The spacecraft is fully stabilized with one axis pointed at the earth. Orientation about this axis is controlled to maintain the spacecraft-sun line within a principal body plane. In addition, control is provided for positioning the solar array and an experiment package which is aligned with the orbit plane.

The program is managed for NASA by the Goddard Space Flight Center. TRW Systems was awarded the initial OGO contract in January 1961. The first launch was in 1964. There have been four additional launches at approximately nine-month intervals with the sixth and final launch scheduled for late 1968 or early 1969.

The ACS requirements, operation, and equipment are described in Section 2. Section 3 covers the ACS development from the proposal phase through December 1961 when the design requirements were finalized. Most of the major design decisions and equipment selections were made during this period. Many of the ACS design concepts and hardware units involved advances in the state-of-the-art. They are summarized in Section 6.

Development of the ACS hardware from January 1962 to the first launch is covered in Section 4. Because many of the components were advances in the state-of-the-art, significant problems occurred during the development phase. The most difficult problems occurred with the horizon scanner system.

Section 5 describes the problems which occurred during the first five OGO flights. A brief summary of the flights follows.

On OGO-I, an experiment boom failed to deploy fully and blocked the view of the horizon scanner. The horizon scanner locked on to the boom, preventing earth acquisition. Eventually, the spacecraft reached a spin-stabilized mode.

The horizon scanner system on OGO-II tracked cold-cloud gradients internal to the horizon. When track of these internal gradients was lost and normal horizon tracking was acquired, large transients were introduced in the ACS. As a result, the gas supply was depleted within 10 days. Subsequently, OGO-II also operated in a partially spin-stabilized mode although the final spin-rate was much less than OGO-I.

On OGO-III, dynamic interaction of two of the experiment booms resulted in a virtually continuous limit cycle of the reaction wheel system causing failure of the reaction wheel power amplifier after 45 days in orbit. A spin-stabilized mode was purposely provided in this spacecraft and has been used successfully.

This unique progression of failures prevented each succeeding problem from being determined prior to launch. In all cases, however, useful data has been obtained from the experiments.

OGO-IV developed a sustained low-frequency oscillation which was caused by a thermally-induced motion of a long (60 ft) experiment antenna. As a result, the ACS gas supply had to be disabled and reaction wheel unloading was accomplished by manual control from the ground. The spacecraft has been operated in this manner for nearly a year. This problem was not discovered earlier because fully stabilized ACS operation (OGO-III) had been achieved only with a 30-ft antenna. The antenna length on OGO-V was again reduced to 30 ft and ACS performance on this spacecraft has met or exceeded its specifications.

As a result of the flight experience, several ACS changes were made as well as changes in the flight operations philosophy. The false gradient tracking of the horizon scanner system on OGO-II and the reaction wheel power amplifier failure in OGO-III necessitated redesign of these units. Subsequent operation on orbit has been flawless.

The original concept of the ACS was for completely automatic operation with a minimum of ground intervention. The on-orbit failures clearly demonstrated the need for close ground control of critical maneuvers and flexibility in command of ACS functions. Solar array output of the spin-stabilized OGO-I and -III spacecraft has been maximized by ingenious manipulation of the ACS. Earth stabilization of

OGO-IV has been achieved only through the efforts of skilled operations personnel.

Section 7 discusses the program in retrospect. In summary, the five launched OGO spacecraft provided valuable insight into the final adequacy of the disciplines which lead to launch. The conclusion reached is that, by the time of launch, the disciplines of quality control, integration, test, engineering inspection, etc., have produced spacecraft that worked as designed. The deficiencies of spacecraft in orbit have been due to relatively obscure design deficiencies. The first three spacecraft (OGO-I, -II, and -III) disclosed the need for redesign in basic spacecraft systems as opposed to experiment payload. OGO-IV developed an anomaly which was directly the result of a change in experiment design.

In-orbit experience on the early spacecraft also showed the need for better knowledge of the earth's radiance and for more extensive dynamic simulation.

Despite the anomalies encountered, useful spacecraft life has been possible by ingenious ground command. Successive spacecraft have been fitted with an increasing array of ground back-up command capability. Manual operation has allowed full exploitation of three spacecraft (OGO-I, -III, and -IV) which would otherwise have been far less useful.

2. SYSTEM DESCRIPTION

2.1 CONTROL REQUIREMENTS

2.1.1 General Requirements

The OGO is a fully attitude-stabilized, scientific satellite. It is capable of accommodating a large number of scientific experiments in varying combinations for each launch. The ACS has the function of orienting these experiments during two basic orbits. A highly eccentric, low-inclination orbit called EGO has an apogee of 80,000 n. mi. and a perigee of 150 n. mi. It provides two crossings of the earth's radiation belts per revolution and an environment free of the earth's magnetic field. A nearly circular polar orbit called POGO (a 500-n. mi. apogee and a 200-n. mi. perigee) is suitable for aurora and magnetic field measurements in the vicinity of the magnetic poles.

The attitude control system controls five degrees of freedom: the three rotation angles of the main box, the rotation of the solar array about its axis, and the orientation of the Orbit Plane Experiment Package (OPEP). Each orientation satisfies the requirements of specific experiments. The position of the solar array also maximizes the input of solar energy. Experiments are mounted within the main box at the tips of the solar arrays within the two OPEP packages, and on six articulated booms. The OGO-V configuration is shown in Figure 1. A description of all spacecraft systems including typical experiments is given in Reference 1.

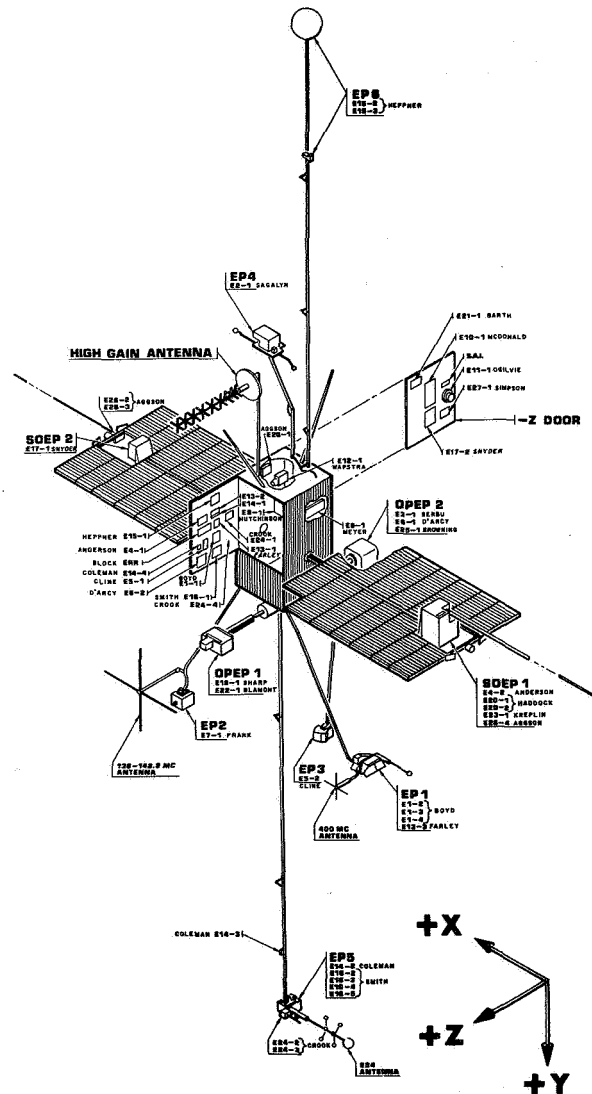


Figure 1. OGO-E Experiment Locations

Figure 2 defines the OGO coordinate systems. During normal operation, the spacecraft has the following orientation: The body yaw (Z_b) axis is aligned with the earth's local vertical; the spacecraft yaw orientation about the local vertical is maintained such that the sun is in the $Y_b - Z_b$ plane and in the direction of the $-Y_b$ or negative pitch axis; and the solar paddles are rotated such that the sun is perpendicular to the paddle face. Experiments in OPEP are aligned with the orbit plane. The ACS is required to have this control capability for a minimum of 1 year.

2.1.2 Performance Requirements

Acquisition

The spacecraft is launched in a folded configuration; that is, the experiment booms, solar arrays, antennas, etc., are folded and fastened to the main box during launch. After separation, the appendages are deployed.

Due to tip-off rates after separation from the booster, the spacecraft may have virtually arbitrary orientation at the end of the deployment sequence. Thus, the normal or earth-pointing phase must be preceded by an acquisition sequence. Requirements for acquisition are:

1. Acquisition must be accomplished from any initial spacecraft angular position.
2. Initial angular rates may be as high as $1^\circ/\text{sec}$ about each control axis.
3. Acquisition time should not exceed one orbital period.

Normal Control

In the normal control mode, the ACS is required to maintain vehicle, array, and OPEP orientations to the following orientation accuracies:

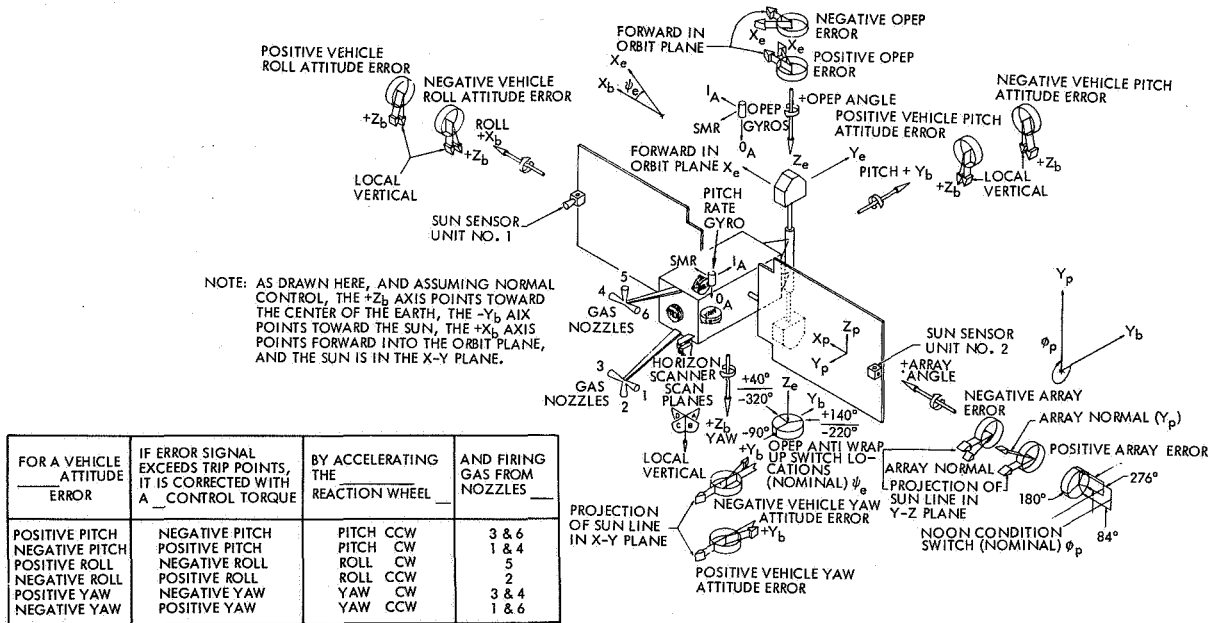


Figure 2. OGO Attitude Control Subsystem: Coordinate System and Sign Conventions

1. Earth-Pointing Accuracy. The earth's reference axis of the observatory is to be stabilized within 2° of the line from the earth's instantaneous geometric center to the spacecraft.
2. Angular Velocity of Spacecraft. The angular velocity of the spacecraft about any axis normal to the instantaneous earth reference axis is to be less than 0.001 rad/sec, exclusive of the orbital rate of the spacecraft.
3. Sun-Pointing Accuracy. The solar array and its associated experiments are to be oriented toward the sun within 5° when the sun is visible. A maximum of 10 min is allowed for sun reorientation to the above specification after emerging from eclipse.
4. Angular Velocity of Solar Array. The angular velocity of the solar array relative to the main spacecraft body is to be less than 0.03 rad/sec.
5. OPEP Accuracy. The orbit-plane experiments are to be aligned with the orbit plane within 5° . This requirement is valid for an EGO orbit only if the orbital rate exceeds or equals the minimum POGO orbital rate (0.062 $^\circ$ /sec). Large OPEP pointing errors may occur for short periods, not exceeding a total of 6 min per orbit, in both EGO and POGO orbits. (This latter requirement allows for the OPEP cables to be "unwrapped" should the spacecraft motion require OPEP travel in excess of 360°).
6. OPEP Angular Velocity. The angular velocity of the orbit-plane experiments relative to the orbit plane is to be less than 0.03 rad/sec.

2.1.3 Control Techniques and Equipment Complement

The requirements placed upon the control system are moderate in terms of accuracy and maneuvering. Consequently, the dominant consideration in designing the system was reliability and is reflected in choosing on-off rather than proportional signal processing. The on-off (or bang-bang) control system may have higher-limit cycle attitude errors and rates than a proportional system, but the errors and rates are within the allowable band. The advantages of the on-off system lie in the hardware simplification and in the resulting high reliability.

The control system, shown in Figure 3, consists of sensors, control torque sources, electromechanical drive mechanisms, and electronic circuitry. In the normal mode, sun sensors are used to obtain two error signals, the yaw and array errors. The pitch and roll control channels receive error signals from horizon scanners which track the temperature gradient between the earth's horizon and space. A single-degree-of-freedom, rate-integrating gyro, caged in the rate mode, provides a reference for the OPEP.

The control torques are generated by pneumatic jets and inertia flywheels or reaction wheels. Each channel (roll, pitch, or yaw) consists of a reaction wheel and a pneumatic system. They are operated in parallel with the pneumatic deadband set at about two and one-half times the reaction wheel deadband. The reaction wheels perform two functions. They store the periodic components of the external disturbance torques and they provide a vehicle maneuver capability, in each case without requiring the expenditure of control gas. If excess momentum builds up in a wheel, it will be decreased by firing the proper gas jet. The gas jets provide the primary torque source for the acquisition mode.

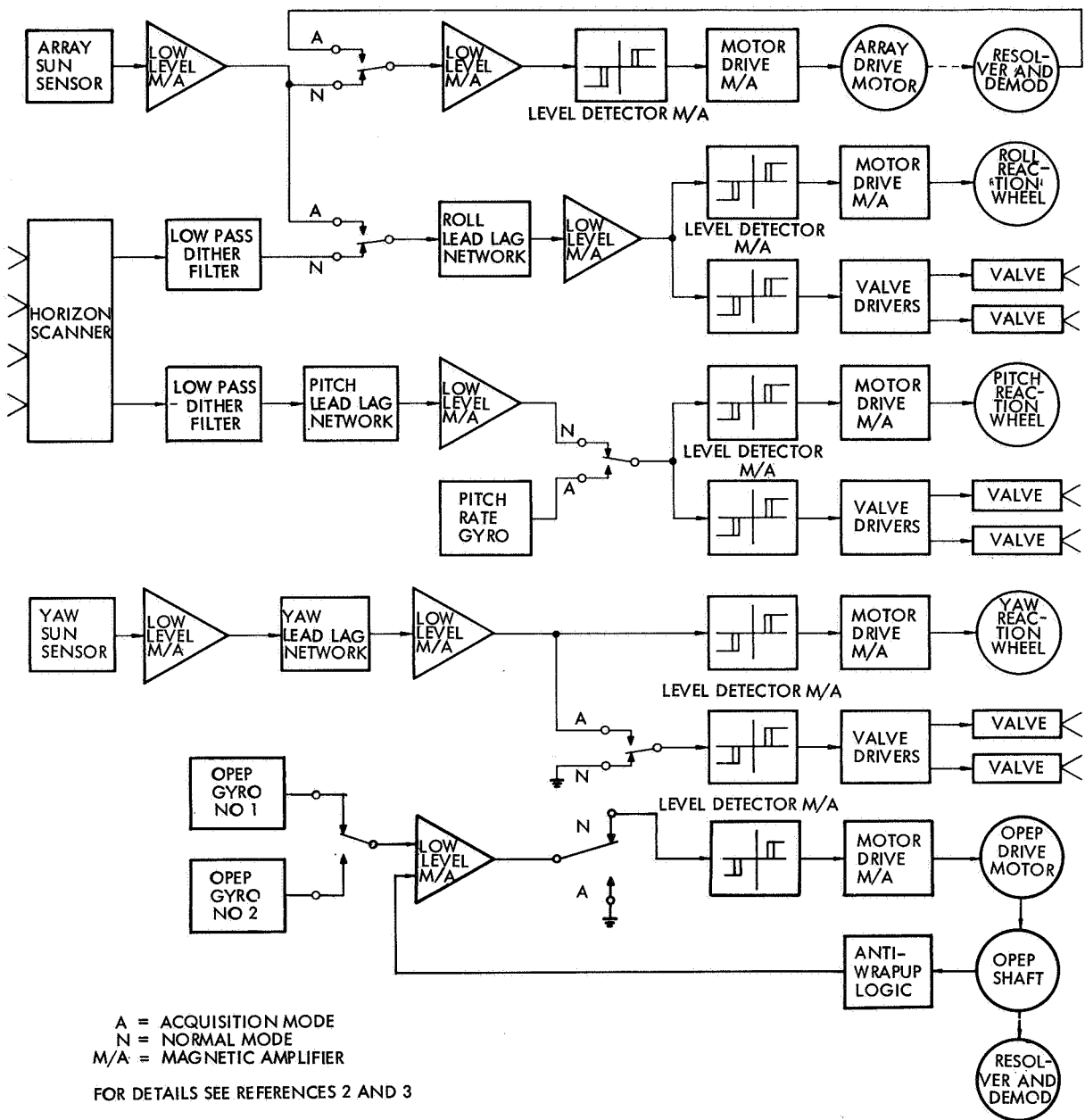


Figure 3. Control System Block Diagram

The solar array and OPEP have drive mechanisms for proper positioning with respect to the spacecraft axes. The torque for each drive comes from a small servo motor operating through a large gear reduction. Both are bang-bang systems. Details of the control system operation are discussed in the next section.

2.2 DESCRIPTION OF ACS OPERATION

2.2.1 Coordinate Systems

The body coordinate systems for OGO are shown in Figure 2. The x_b , y_b , z_b coordinate system is fixed in the body and these axes are referred to, respectively, as roll, pitch, and yaw axes. The solar paddle coordinate system is defined with respect to the X_b , Y_b , Z_b coordinate system by the paddle angle ϕ_p which is zero when the outward directed normal to the paddle surface bearing the solar cells is aligned to the $+Y_b$ axis. Similarly, the OPEP coordinate system is defined with respect to the X_b , Y_b , Z_b coordinate system by the OPEP angle ψ_e . The positive X_e axis is normal to the OPEP surface which faces in the direction of orbital motion.

2.2.2 ACS Operation and Mode Sequencing

Boost - Mode 1

During the launch or boost phase, all control functions are inhibited. The gyros are running, however, to minimize the possibility of damage from shock and vibration. The horizon scanners are also caged for the same reason.

This mode is entered only by command. The ACS configuration is as follows:

1. The pitch, roll, and yaw control channels are inhibited.
2. The solar array and OPEP control channels are inhibited.
3. The OPEP gyros and pitch rate gyro spin motors are running.

4. The horizon scanner tracker heads are caged at their mechanical null positions.

Acquisition

The ACS achieves the desired orientation by a programmed sequence of three modes: array slew, sun acquisition, and earth search. The acquisition sequence normally is initiated by an automatic timer which is started upon separation of the spacecraft from the booster although acquisition may be started by ground command.

Array Slew - Mode 2A

This mode slews the solar array so that its face is perpendicular to the $-Y_b$ or pitch axis ($\phi_p = 180^\circ$). The sun sensors located at the tips of the array are then oriented such that they indicate the sun aspect angles to the yaw (Z_b) and roll (X_b) body axis.

A resolver mounted on the array shaft is used to determine array position relative to the main box (see Figure 2). The array-positioning loop is simply a bang-bang loop. If the error signal exceeds the deadzone, the drive mechanism drives the shaft at a constant rate until the error falls below the deadzone. Drive mechanism and shaft friction are high; hence, the shaft motion is stopped immediately.

This mode is not required during the initial acquisition (ACS will automatically sequence to Mode 2B) because the solar array is released in the 180° position after separation from the booster. In the event of a reacquisition, the ACS will switch from Mode 3A to Mode 2A and the array will slew to 180° . Upon completion of the slew maneuver, the ACS will automatically switch to Mode 2B. The ACS configuration is changed from that of Mode 1 in the following way:

1. The solar array channel is enabled. The solar array position resolver provides an input to the array channel to cage the array at its 180° position.

2. The horizon scanner tracker heads are uncaged and searching. The tracker heads may track the earth's horizon if it enters their field-of-view.

Sun Acquisition - Mode 2B

Two maneuvers are accomplished in this mode. The pitch ($-Y_b$) axis is pointed toward the sun and a constant rotation rate is established about the pitch axis. The solar array is then rapidly oriented for maximum charging of the batteries.

The sun sensors mentioned above are used for roll and yaw attitude information. The sun sensors provide a continuous output over a full 4π steradian field-of-view. Roll and yaw rate information is, therefore, derived from the sun sensor attitude signals by lead-lag networks. Control torques are provided by the gas jets and reaction wheels.

A rate gyro is used to measure pitch rate. The gyro null is electrically biased such that at null, a -0.5° rate is established.

Mode 2B is entered only upon exit from the Array Slew - Mode 2A. The ACS configuration is summarized as follows:

1. The pitch error signal is provided by the pitch rate gyro assembly.
2. The roll error signal is derived from the array sun sensor.
3. The yaw error signal is derived from the yaw sun sensor.
4. The control torques for each axis are provided by the respective reaction wheel and pneumatic system.
5. The solar array is caged at 180° as in Mode 2A.
6. The OPEP drive is disabled as in Mode 1.

Earth Search - Mode 2C

Earth search is enabled by an automatic timer 70 min after initiation of sun acquisition or by ground command. The pitch axis is held aligned with the sun, with the spacecraft still rotating about this axis. As the vehicle proceeds in orbit, the yaw axis will at some point intersect the earth (see Figure 4). When this happens and the earth acquisition logic is satisfied, the ACS sequences into the normal or earth-pointing mode (Mode 3). An earth acquisition signal is obtained when three or more horizon scanners lock on to the earth and the angle between each scanner head and the $+Z_b$ axis is greater than 4.4° . The latter requirement is to prevent acquisition near apogee in an EGO orbit. The small earth size at that attitude does not allow sufficient maneuvering room to stop the pitch rate; hence, earth acquisition would be aborted.

From Mode 2B, no change in the ACS control laws is made for Mode 2C. The sequencing logic to normal mode is simply enabled.

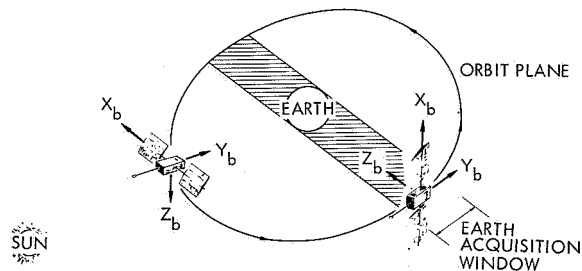


Figure 4. Earth Acquisition Window

Normal Mode - Mode 3

The normal or earth pointing is the primary spacecraft operating mode. Usually, it is entered from the earth-search mode described above or may be entered by ground command. Exit from this mode is effected only by

ground command or loss of earth lock. Should two or more of the horizon scanner heads lose earth lock, the spacecraft is switched to a standby mode (Mode 3A) where all control functions are inhibited. If this condition persists for more than 7 min, the acquisition sequence is re-initiated by switching to the Array Slew - Mode 2A and so on.

In Mode 3, the pitch and roll error signals are derived from the horizon scanner system. Yaw and array error signals are derived from the sun sensors. The reaction wheels and gas jets are used in an on-off, or bang-bang, control mode. Stable operation is achieved by deriving rate information from the error signals with lead-lag networks.

There is an additional low pass filter in the pitch and roll control channels during normal mode. This filter attenuates a $\pm 1.0^\circ$, 18-Hz tracking dither which appears on the horizon scanner signal. Operation of the horizon scanner system is discussed in Subsection 2.4.

Under typical on-orbit operation, the reaction wheels are the primary control torque source for the pitch, roll, and yaw channels. The wheels also store cyclic and noncyclic components of angular momentum. The angular momentum arises from disturbance torques which act on the spacecraft and spacecraft maneuvers which result from the particular control requirements.

Since the wheels are operated in an on-off fashion, a continual limit cycle will exist; that is, to maintain a given wheel speed or momentum, motor torque must be periodically applied. This operation is to counteract the bearing and windage friction which causes the wheel to run down.

Eventually, due to disturbances which act on the vehicle, the reaction wheel will become saturated. When it reaches maximum speed, the wheel can no longer store momentum or exert a control torque on the vehicle. As a result, the attitude error will

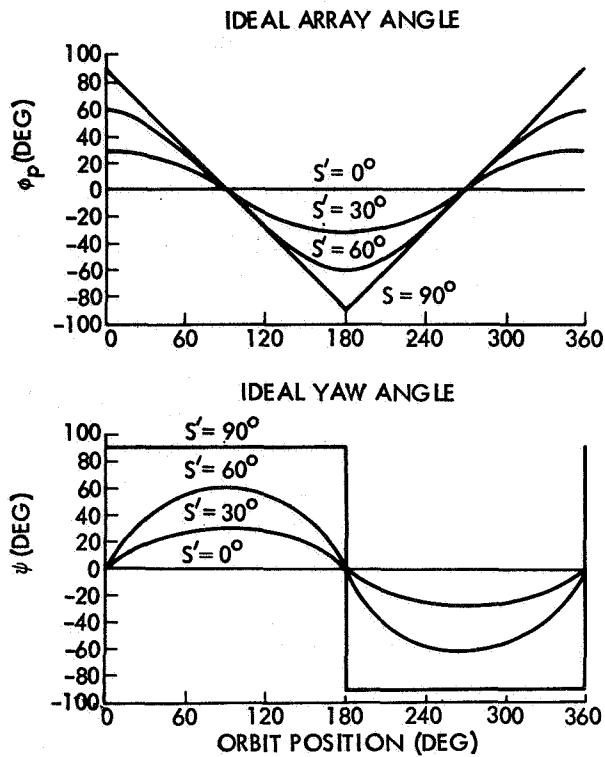
build up until the gas deadzone is exceeded. A short jet firing occurs which alters the spacecraft momentum such that the wheel will attain a new operating speed below the saturation level. Normal reaction wheel control is then reestablished and the process repeats.

In the yaw channel, however, the gas jets are disabled due to the unique maneuvering requirements of the yaw channel which are discussed below. The yaw wheel is purposely sized so that it stores approximately five times the momentum of the pitch or roll wheels. Momentum stored in the yaw wheel is interchanged to the pitch and/or roll wheels twice per orbit and vice versa by the inertial rotation of the spacecraft in orbit. Thus, the yaw wheel unloading is accomplished by the interchange of stored momentum into the pitch and roll axes. And, except in the case of the noon or post-eclipse turns the yaw wheel momentum is 1/5 or less of its maximum momentum storage capability.

The yaw angle is controlled such that the sun is always in the $Y_b - Z_b$ plane and in the direction of the $-Y_b$ or negative pitch axis. This position results in a yaw angle which varies with the spacecraft position in orbit and the position of the sun relative to the orbit plane. The ideal yaw angle versus orbit position is shown in Figure 5.

The effect of varying sun positions relative to the orbit plane is indicated in Figure 5. S' is the angle between the earth-sun line and a vector normal to the orbit plane. (For a derivation of these relationships, see Reference 2).

When S' equals zero, the earth-sun line is normal to the orbit plane and no yaw motion is required. The other extreme is when S' equals 90° or the earth-sun line is identically in the orbit plane. Here, the spacecraft must undergo a so-called "noon turn" as the sun passes overhead. The spacecraft yaw angle must change rapidly by 180° to keep the sun on the $-Y_b$ side of the box. Theoretically, the yaw rate is infinite at precisely noon.



NOTE: PRINCIPAL ANGLES ONLY ARE SHOWN

Figure 5. Nominal Yaw and Array Angles

The yaw control system accomplishes the noon maneuver by utilizing the excess momentum storage capability of the yaw wheel. As the spacecraft approaches noon, the yaw wheel will be commanded on, speeded up to saturation, and a yaw rate established. The yaw rate is limited by the wheel momentum storage capability to approximately $0.5^\circ/\text{sec}$. Thus, under "high-noon" conditions, the spacecraft yaw angle will lag somewhat the ideal yaw angle. Approximately five minutes are required for the maneuver. For other sun positions (S') relative to the orbit, the yaw maneuvers are less violent and ideal sun-pointing control can be maintained.

This form of yaw control has a particular advantage in that the solar arrays must only travel over a $\pm 90^\circ$ range. The ideal array angle versus orbit position is shown in Figure 5 for various values of S' . The arrays reach their full 90° of travel in the high-noon orbit; but, when the noon turn occurs, their travel is reversed.

This allows the use of cabling between the solar arrays and the main box. Slip rings would be required if the arrays were forced to move continuously in one direction.

A special logic is in fact provided to ensure that the high-noon turn maneuver is completed. If the arrays reach the 270° position, (i.e., the sun is directly overhead) a switch is activated which turns on the yaw wheel if it has not already been commanded to start the noon-turn maneuver.

The yaw control system loses its reference when the spacecraft enters eclipse. Because the momentum stored in the yaw wheel cannot be maintained, the yaw wheel will run down imparting a low-level turning rate to the spacecraft. When the spacecraft reenters the sunlight, it may have virtually arbitrary yaw orientation and sun orientation must be reacquired. This reacquisition is known as a "post-eclipse" turn. It is performed in the same manner as the noon turn. The large yaw attitude error causes the wheel to be commanded full on and the wheel runs up to saturation. An approximate $0.5^\circ/\text{sec}$ turning rate is imparted to the yaw axis and then is removed by the wheel when sun orientation is regained.

If yaw gas were enabled during the maneuvers described above, a prohibitive amount of gas would be required over the 1-year spacecraft lifetime. Hence, yaw gas is disabled in the normal mode and all maneuvers are accomplished with reaction wheel alone.

The control laws of the OPEP and solar array shafts are bang-bang systems. The main difference is in the error-sensing device; sun sensors for the solar array and a gyrocompass system for the OPEP. The operation of this type of loop was discussed in the Array Slew - Mode 2A paragraph. After OGO III, a reversal delay logic was added to the array control system, and a filter and feedback loops were added to the OPEP system. Those additions prevented participation of the control loops in boom oscillations. (See Section 5.)

In summary, the ACS configuration for the normal control mode is as follows:

1. The pitch and roll error signals are generated by the horizon scanners and the control torques by the pitch and roll reaction wheels and gas jets.
2. The yaw error signal is derived from the yaw sun sensor and the control torques come from the yaw reaction wheel.
3. The yaw gas jets are disabled.
4. The array error signal is generated by the array sun sensor and controls the array drive motor operation.
5. The OPEP error signal is generated by the OPEP rate gyro system and controls the OPEP drive motor.

A detailed description of the ACS is given in Reference 2. This document does not contain, however, descriptions of the special logic and command functions which were added after the initial OGO launches. References of this nature are listed in Section 5.

2.3 COMMAND FUNCTIONS

The ACS commands for the OGO I spacecraft are listed in Table I. Note that there are seven ACS mode control commands: two enables, four mode selections, and an execute. The ACS can be commanded and locked into any of Modes 1, 2A, 2C, or 3. To command a given mode, three instructions must be issued to the spacecraft in the following order:

1. ACS Mode Control Enable
2. ACS Mode Select Mode "X"
3. ACS Mode Control Execute

Unless additional commands are sent, the ACS is not free to select its future modes automatically. If this is

desired, the sequence listed above must be followed by an ACS Mode Control Normal command.

The sun sensor commands are instructions regarding the choice of fine or coarse sun sensors. Whenever the sun is outside the fine sensor field-of-view, the ACS automatically selects the coarse sensors to control the array and yaw channels. These commands were provided as an override in the event the fine sun sensor failed.

The OPEP Control Enable and Disable and OPEP Slew On and Off commands allow the OPEP shaft to be slewed to and stopped at any desired position. This control allows the experiments to maintain a fixed orientation relative to the spacecraft which is occasionally desirable for some experiments.

The remaining commands in the table represent commands which have been added since the launch of OGO I. Certain commands will only be activated if the Control Switching Assembly (CSA) bus has first been armed (+28 V applied to the CSA bus). The commands affected are indicated in Table I. The CSA Bus Safe command removes the +28 V from the CSA bus and thereby prevents the ACS from responding to the above-mentioned commands.

The ACS Power On and Off, Pitch Rate Gyro On and Off, OPEP Gyro Power Off, and OPEP Gyro Heater and Spin Motor On commands were added to enable complete shutdown of the ACS. Thus, in the event of a failure or emergency, spacecraft power could be conserved.

The delay logic which was mentioned above and whose function is discussed in Section 5 is commandable as indicated in the table. In addition, a command was provided to inhibit all gas-jet activity.

As a result of the successful operation of the OGO-I spacecraft in a spin-stabilized mode, commands were provided expressly for that purpose. The Yaw Select (\pm) commands provide the capability to spin-up or despin the

Table I. ACS Commands for OGO-V

Commands	Commands In Effect At Launch	CSA Bus Arm Required
ACS Mode Control Normal	X	
ACS Mode Control Enable		
ACS Mode Control Execute		
ACS Mode 1 Select	X	
ACS Mode 2A Select		
ACS Mode 2C Select		
ACS Mode 3 Select		
Sun Sensor Normal	X	
Sun Sensor Switched		
OPEP Enable		
OPEP Disable	X	
OPEP Slew On		
OPEP Slew Off	X	
CSA Bus Safe	X	
CSA Bus Arm		
ACS Power On (gas jet control normal)	X	
ACS Power Off		X
Pitch Rate Gyro On	X	
Pitch Rate Gyro Off		
Gas Delay Enable		X
Reaction Wheel Delay Enable		X
Array Drive Delay Enable		
Array Drive Delay Disable	X	
Gas Jet Control Normal	X	
Gas Jet Control Disable		X
-Yaw Select		
-Roll Select		
+Yaw Select		
Spin Execute		X
Array Slew CW		
Array Slew CCW		X
Array Slew Normal	X	
OPEP Gyro Heater On	X	
OPEP Gyro Power Off		
OPEP Gyro Spin Motor On	X	
OPEP Gyro Slect Auto	X	
Sun Aspect Indicator On		
Sun Aspect Indicator Off	X	

spacecraft about the yaw axis by activating the proper jets. The resulting spin-stabilized mode is a possible back-up mode of operation if the gas supply is nearly exhausted or if the ACS functions improperly. In addition to yaw spin-up, a precession capability is available to optimize solar array exposure to the sun by activating a roll jet (-Roll Select). The Array Slew commands were added to allow move-

ment of the solar array in a spin-stabilized mode to optimize solar array orientations. Also, as a part of this mode of operation, a digital sun aspect indicator was added to assist in determining spacecraft spin-axis attitude.

A list of telemetered items with their respective word numbers and sampling rates is given in Table II. The sample rates are shown for the 64-kbit/sec

Table II. Telemetered ACS Items

Item	Function	Sampling Period (in Sec)		
		64 kbit/sec Real Time	Data Stored (POGO)	Data Stored (EGO)
A1	Argon High Pressure	2.3	36.9	147.5
A2	Argon Low Pressure	1.15	18.4	73.7
A3	Argon Pressure Vessel Temperature	2.3	36.9	147.5
A4	Pitch Error Signal	1.15	18.4	73.7
A5	Roll Error Signal	1.15	18.4	73.7
A6	Horizon Scanner Sun Alarm	1.15	18.4	73.7
A7	Horizon Scanner Tracking Check	1.15	18.4	73.7
A9	Horizon Scanner Tracker Head "A" Temperature	2.3	36.9	147.5
A10	Yaw Error Signal	1.15	18.4	73.7
A11	Array Error Signal	2.3	36.9	147.5
A12	Solar Array Shaft Angle (Sine)	2.3	36.9	147.5
A13	Solar Array Shaft Angle (Cosine)	2.3	36.9	147.5
A14	OPEP Shaft Angle (Sine)	1.15	18.4	73.7
A15	OPEP Shaft Angle (Cosine)	1.15	18.4	73.7
A16	Solar Array and OPEP Drive Motors, ON-OFF	1.15	18.4	73.7
A17	Roll Reaction Wheel Speed	1.15	18.4	73.7
A18	Pitch Reaction Wheel Speed	1.15	18.4	73.7
A19	Yaw Reaction Wheel Speed	1.15	18.4	73.7
A20	Reaction Wheel Direction	1.15	18.4	73.7
A21	Gas Valve Actuation - Valves 1, 2 and 5	0.29	4.6	18.4
A22	Gas Valve Actuation - Valves 3, 4 and 6	0.29	4.6	18.4
A23	ACS Mode and Sun Sensor Intensity	1.15	18.4	73.7
A24	Pitch Gyro Rate Indication (Pitch Rate Gyro Demod. Output)	1.15	18.4	73.7
A25	Sun Sensor No. 1 (RTT) Temperature	2.3	36.9	147.5
A26	Sun Sensor No. 2 Temperature	2.3	36.9	147.5
A27	OPEP Gyro 1 or 2	1.15	18.4	73.7
A28	OPEP Gyro Spin Motor Monitor	1.15	18.4	73.7
A29	OPEP Error Signal	1.15	18.4	73.7
A30	OPEP Gyro Bracket Temperature	2.3	36.9	147.5
A31	Reaction Wheel Energized/ De-energized	0.58	9.2	36.9
A32	ACS Inverter Temperature	1.15	18.4	73.7
A33	Yaw Reaction Wheel Temperature	2.3	36.9	147.5
A34	Pitch Reaction Wheel Temperature	2.3	36.9	147.5
A35	Pitch Rate Gyro Spin Motor Monitor	1.15	18.4	73.7
A37	OPEP Drive Shaft Temperature	2.3	36.9	147.5
A40	Horizon Scanner Tracker Head "A" Position	2.3	36.9	147.5
A41	Horizon Scanner Tracker Head "B" Position	2.3	36.9	147.5
A42	Horizon Scanner Tracker Head "C" Position	2.3	36.9	147.5
A43	Horizon Scanner Tracker Head "D" Position	2.3	36.9	147.5
A44	Control Switching Assembly Status	2.3	36.9	147.5
A46	Sun Aspect Angle	1.15	18.4	73.7
D46	ACS Inverter 400 Hz Regulated Voltage	2.3	36.9	147.5

"main-frame" rate. In this mode, the ACS telemetry words are sampled from a subcommutator. An additional mode is provided where the ACS subcommutator replaces the main-frame and sample rates are 128 times faster. Lower telemetry sample rates are commandable and allow better signal-to-noise ratios when the spacecraft is far out in the EGO orbit or an omnidirectional antenna is used. One of these lower sample rates is also used for the data storage mode where all telemetry data are recorded for playback over a ground station.

For a detailed description of the command and telemetry functions, refer to Reference 3.

2.4 EQUIPMENT DESCRIPTION

A complete description of the ACS components can be found in References 4 through 12. The following paragraphs describe briefly the functions and operation of each unit.

2.4.1 Sensors

Four different types of sensors are used on OGO: sun sensors, horizon scanners, gyros, and resolvers.

Sun Sensor

A two-stage sun sensor (see connection on Figure 6) is used; the coarse stage provides full spherical coverage and the fine stage provides more accurate error signals in a 17° cone about null.

The coarse sun sensor consists of two groups of silicon solar cells. The cells are mounted on the faces of rectangular boxes and their outputs are summed in resistor networks. The accuracy of the coarse sensor is primarily dependent upon the thermal stability of the solar cells. A heat sink is incorporated for each set of cells.

The fine sensor utilizes a single two-axis detector called the Radiation Tracking Transducer (RTT). This detector is used in conjunction with pin-hole optics and receives a single spot of

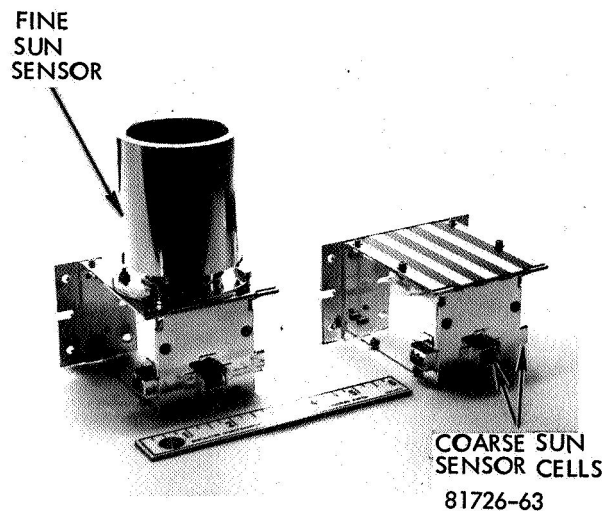


Figure 6. Sun Sensor Assemblies — Front View

sunlight on its face. Current is induced through the detector in the vicinity of the light bundle in much the same manner as in a solar cell. This current diffuses through the detector into its dark regions setting up a lateral voltage field across the detector face. The field is measured about the periphery of the detector and provides two voltages proportional to vector components of the deviation of the image from the center of the detector. The output is reasonably linear over the sensor's 17° field-of-view. Null accuracy is on the order of 0.1° .

Horizon Scanners

The horizon scanner consists of two assemblies; each contains two infrared detectors. The position of the detector scanning mechanisms allows one assembly to scan approximately 90° , from the $+Y_b$ to $+Z_b$ and $-Y_b$ to $+Z_b$ axes. The second assembly is mounted so that it can scan from $+X_b$ to $+Z_b$ and $-X_b$ to $+Z_b$ axes. The scanner mounting is shown in Figure 7 and the scanner heads are shown in Figure 8. Each head measures the angle between the yaw axis of the spacecraft and the line-of-sight to the edge of the earth. The difference in angular measurement between opposite heads is the attitude error in one axis.

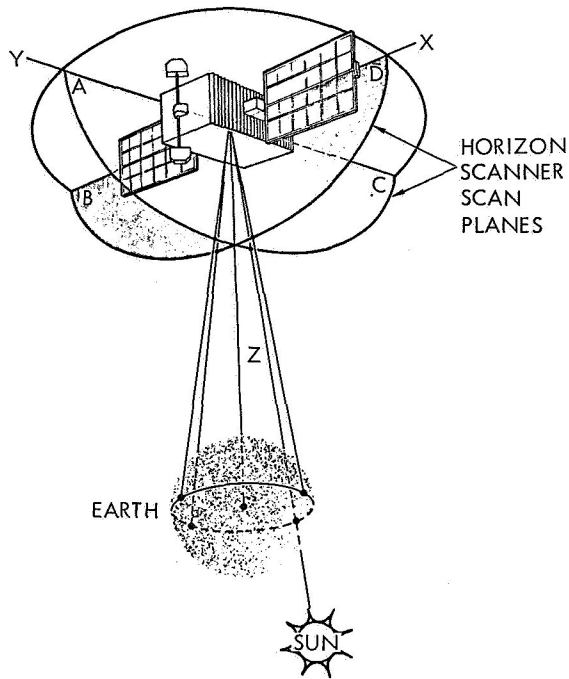


Figure 7. OGO Horizon Scanner Geometry

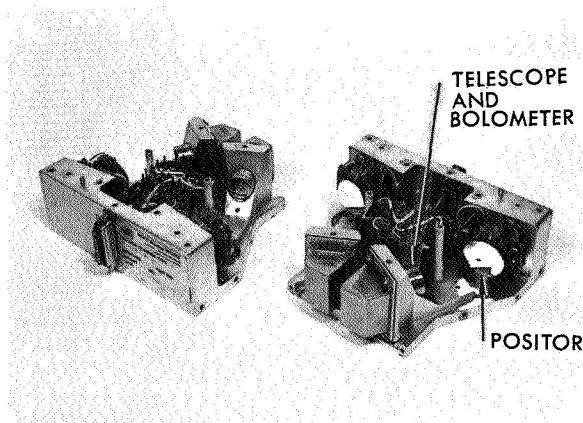


Figure 8. OGO Horizon Scanner Detector Assemblies, Covers Off

Each head utilizes a thermistor bolometer detector. Scanning is effected with a flexure-mounted mirror driven by a coil. This device, called a positor, is used to avoid bearings in

the mirror drive. The detectors, positors, and preamplifiers are mounted in two packages which are placed external to the spacecraft main box. A third electronics package which includes the tracking loop electronics is mounted internal to the main box.

Each positor scans over its 90° travel until the earth's edge is located by the detector logic. At this point, the head locks on to the earth's edge and the positor dithers across a narrow angle ($\pm 1.0^\circ$) centered on the horizon. The frequency is about 18 Hz.

Positor position is controlled by the scanner tracking loop electronics. When tracking the horizon, the dither is achieved by operating the tracking loop in a limit cycle. The radiation gradient at the horizon alternately commands changes in the direction of the positor motion. The angular measurement is made by averaging the positor position.

When no radiance signal is detected by the bolometer, the positor is commanded to scan through its full 90° travel. A complete cycle occurs once every 4 sec.

The scanner can be operated over a range of apparent earth sizes from 5° to 150° . Its accuracy is 0.25° exclusive of uncertainties in the horizon. The system is redundant in that three of the four heads will supply the required attitude information in two axes. Logic has been included which permits operation using any three heads.

Pitch Rate Gyro

A pitch rate gyro is used to establish a reference angular rate about the spacecraft pitch axis during sun and earth acquisition. The complete gyro assembly consists of a subminiature spring-restrained rate gyroscope, signal amplifying, demodulating electronics, and telemetry processing circuitry. The gyro itself is of an advanced design, incorporating both a motor speed sensor and a gimbal torquer through which the required rate bias is applied.

OPEP Gyro

The OPEP gyro assembly detects errors in the alignment of the OPEP shaft with the orbital plane. This assembly consists of two separate sub-assemblies, the OPEP gyro electronics assembly and the OPEP inertial reference assembly. The latter contains two MIG gyros which are operated in the caged or rate gyro mode. Only one is needed, but two are used to provide redundancy. When the gyro input axis (IA) is located in the orbital plane and is pointing in the direction of travel, there will be no error signal output. If the IA is not in the orbit plane, the gyro will sense a component of the spacecraft orbital rotation rate proportional to the attitude error.

Resolver

The OPEP and solar array shaft positions relative to the main spacecraft box are measured with ac pancake resolvers. Each has two outputs, one proportional to the sine and the other proportional to the cosine of shaft angle. The resolvers are excited by 2461-Hz, 28-Vac square wave. To obtain a dc voltage for telemetry and ACS use, the resolver outputs are summed with the 2461-Hz ac reference phase, then rectified and filtered.

2.4.2 ACS Electronics

It is beyond the scope of this report to give a complete description of the ACS electronics; only the major electronic packages are identified and their primary functions are pointed out.

Sensor Electronics and Logic Assembly

The Sensor Electronics and Logic Assembly (SELA) is one of the most complex ACS assemblies. It amplifies and filters the error signals for the roll, pitch, yaw, and array control channels. In addition, it defines the switching between the various modes of the control system, controls the redundant states of the horizon scanner, and processes a number of telemetry signals. In terms of hardware, the assembly contains welded electronic modules with

both analog and digital transistor circuits, and magnetic amplifiers.

Attitude Control Assembly

The Attitude Control Assembly (ACA) controls the two-phase, 400-Hz, ac power to the roll, pitch, and yaw reaction wheel motors, and dc power to the gas jet valve solenoids. All control signal inputs to the ACA are supplied by the SELA and by the pitch rate gyro assembly.

Drive Electronic Assembly

The Drive Electronic Assembly (DEA) controls the two-phase, ac power to the solar array shaft and the OPEP shaft motors. The DEA also processes the signals from the solar array shaft, OPEP shaft position resolvers, and OPEP anti-wrap up logic.

Inverter

The ACS Inverter supplies ac power to the magnetic amplifiers, reaction wheels, solar array shaft, and OPEP shaft drive motors. It is also used for pitch rate gyro excitation. The inverter provides unregulated 400-Hz power to operate the reaction wheels and motors and regulated 400-Hz power for the magnetic amplifiers requirements in SELA and DEA.

2.4.3 Torque Sources

Reaction Wheels

The reaction wheels are motor-driven inertia wheels enclosed in hermetically sealed cases. The case is filled with argon gas at a pressure of 5.9 psia. The inertia wheels have the weight concentrated in the rim to attain a maximum inertia-to-weight ratio. The reaction wheel motor is an "inside-out," two-phase induction motor. An electrostatic tachometer produces eight pulses per revolution of a reaction wheel. The tachometer signal is conditioned for telemetry to provide wheel speed and direction of rotation.

The yaw reaction wheel has greater torque and momentum storage capabilities than the roll and pitch wheel be-

cause it provides the entire maneuvering control about the yaw axis during normal operation. On the other hand, the roll and pitch wheels are each backed up by a pneumatic system in the normal mode. The roll and pitch axes interchange positions in inertial space and, therefore, the momentum storage capabilities of the roll and pitch wheels must be identical. The low limit on this momentum storage was set at 1.5 ft-lb-sec. The yaw reaction wheel stores approximately five times the momentum of the pitch and roll wheels.

Pneumatics

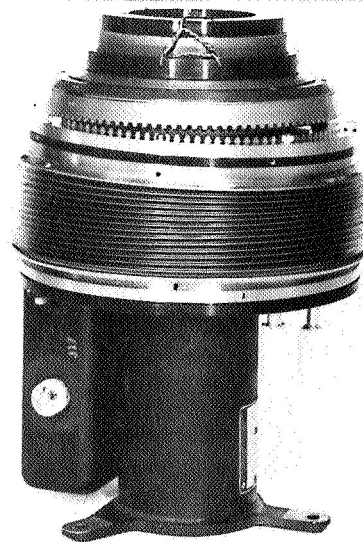
The pneumatic assembly is a cold gas ejection system which applies on-off torques about the three control axes. After receiving signals from the ACA, the appropriate solenoid valves open to allow gas ejection through the nozzles. The nozzles are mounted on booms which provide a longer lever arm, therefore reducing the nozzle thrust level required to produce the desired torque.

The pneumatic system consists of a storage vessel (gas bottle) filled with argon under high pressure, a pressure regulator and relief valve, six solenoid valves, six pressure switches, six nozzles, a high and low pressure transducer, a loading valve, and the appropriate tubing and manifolding necessary to connect the parts.

2.4.4 Electromechanical Drives

The OGO drive mechanism is an electromechanical device which uses the unique wobble gear principle. Figure 9 is a photo of the mechanism assembly. The prime mover is a size 11 servo motor with gearhead. The output rotation is approximately $1.6^\circ/\text{sec}$ with no load torque. The stall torque of the drive is approximately 35 ft-lb. The system application on OGO uses the drive in an on-off mode of operation.

The final drive members of the mechanism are the wobble gears. The input wobble gear is constrained to its irrotational wobbling motion by the bellows assemblies. This gear has 100 teeth. The output wobble gear is in



81139-63

Figure 9. OGO Solar Array and OPEP Drive

mesh with the input gear at one point only. The output gear has 99 teeth, and is mounted so that it rotates about the centerline of the drive mechanism. The wobble gear mesh provides 99:1 reduction because one complete wobble motion of the drive gear causes the output gear to move one gear tooth. Total speed reduction, a motor to output shaft, is about 24000:1.

2.5 ACS PHYSICAL PROPERTIES

2.5.1 Reliability

TRW employed an integrated reliability program to increase the probability of success for OGO. A reliability number for each individual subsystem was chosen as a design goal. For the ACS, this number is 0.85 and it indicates the probability of successful ACS operation over a period of 1 year. The actual reliability number is computed on the basis of component failure rates. The latest available reliability estimate computed in this way is 0.79 for the ACS and thus falls short of its design goal. However, the reliability assessment for the total OGO system slightly surpasses its design goal of 0.70.

Little redundancy in design is used in the attitude control system because of weight limitations. The sun sensors are somewhat redundant with both

coarse and fine sensors available. The horizon scanner system has one redundant tracking head. Reliability considerations also dictated the use of magnetic amplifiers instead of solid-state devices for switching and amplification in the control channels.

Life-confidence tests were conducted during the design and development stage of the OGO program. The purpose of these tests was to obtain data on the wear-out characteristics and failure modes of the critical assemblies of the OGO spacecraft. The life-confidence tests were carried out on boom-actuating mechanisms, pneumatics, OPEP and solar array drive mechanisms, reaction wheels, gyros, horizon scanners, bearings, battery cells, battery and charge controller, tape recorder, time delay modules, etc. The only significant failure of an ACS component that occurred was the burnout of a magnetic amplifier during a reaction wheel life test. Since the test was considered only a test of the reaction wheel life, failure analyses of the magnetic amplifier were not made at that time. The significance of this test will be discussed further in Section 5.

On orbit, two premature failures of an ACS unit have occurred. The first was the failure of the horizon scanner system on OGO-II to track the horizon properly. While scanner operation was reliable, it has been classed as a failure because its design did not anticipate

horizon anomalies. (See Section 5.) Subsequent redesign has corrected this problem. The second failure was the roll reaction wheel motor driver magnetic amplifier on OGO-III. The failure was due to a high-duty cycle which overstressed the thermal design. The magnetic amplifiers have also been redesigned. The pitch rate gyro on OGO-I failed after 2200 hr of operation, but expected gyro life is only 1500 hr.

2.5.2 Weight

The original estimate of total ACS weight made in February 1961 was 156 lb. Table III gives the data of ACS weight for all the OGO spacecraft. OGO-I was slightly under the original estimate, OGO-II and OGO-III were precisely at the weight estimate. The difference in pneumatic system weight is due to a larger gas bottle used on POGO spacecraft. More gas is required for the low-attitude POGO orbit since disturbance torques, particularly aerodynamics, are higher. On OGO-III, which was an EGO, the larger gas bottle size was retained to provide a greater margin for unexpected gas usage.

The significant weight increase for the remaining spacecraft resulted from redesigns and requirements for more gas in the POGO orbits. The electronics weight increase was due to increases in magnetic amplifier sizes and the addition of the digital sun aspect

Table III. ACS Weight for all OGO Spacecraft

	Electronics and Drive Mechanisms (lb)	Pneumatics (lb)	Total (lb)
OGO-I (EGO)	114.9	26.6	135.5
OGO-II (POGO)	119.3	36.6	155.9
OGO-III (EGO)	118.5	37.8	156.3
OGO-IV (POGO)	132.1	96.8	228.9
OGO-V (EGO)	132.5	37.8	170.3
OGO-F (POGO)	132.5	96.0	228.5

indicator. These changes are discussed in Section 5. Analysis indicated that disturbances in a POGO orbit would consume the ACS gas at a higher rate than anticipated in the original design. Krypton, which has a higher impulse than argon, was substituted and the bottle pressure was increased from 3000 to 4000 psia. Krypton is about three times heavier per unit volume than argon, hence the large increase in pneumatics weight on OGO-IV and -F.

2.5.3 Power

Power for the ACS is derived from the inverter which supplies regulated and unregulated 400-Hz ac, a converter which supplies ± 20 and ± 10 Vdc as well as 2461-Hz ac, and +28 V power

from the spacecraft bus is used directly. Total power drawn from the spacecraft bus varies with the mode of operation. Table IV summarizes the total ACS power consumption for the major modes of operation.

Table IV. ACS Power From the 28-V Bus

Mode of Operation	Power (Watts)
Boost - minimum	77
Acquisition - peak	205
Normal Mode - peak	170
Normal Mode - average	100

3. EARLY HISTORY OF ACS DESIGN DEVELOPMENT

3.1 OGO PROGRAM CONTRACTUAL HISTORY

The OGO proposal (Reference 13) was submitted to NASA Goddard Space Flight Center on 23 September 1960. As the result of this proposal, a letter contract was received dated 6 January 1961. This contract authorized a further 8-week study of spacecraft design and specified certain areas of concern. Near the end of the study, the letter contract was modified to permit development of the spacecraft hardware. The final definitive contract was received on 3 August 1962. On 23 November 1963, the contract was converted from a cost plus incentive fee to fixed price incentive fee. This contract required delivery of three flight observatories (OGO-A, -B, and -C) plus a variety of ground support equipment and an engineering model spacecraft. The follow-on OGO (FOOGO) contract was received 26 August 1964. This contract was also fixed price incentive fee and required delivery of two additional flight observatories, OGO-D and -E. A third flight observatory, OGO-F, was authorized later.

3.2 ACS DESIGN HISTORY

For purposes of this design survey, the OGO history is in six distinct phases: (1) the proposal, (2) the design modification and evaluation study, (3) the detailed system design, (4) hardware development, (5) unit and system test, and (6) post-flight re-designs.

Figure 10 shows more of the major program milestones from the submission of the proposal to the present time as they were actually achieved.

The sections which follow discuss ACS design evolution from the proposal through the detailed design phase. The majority of the hardware development will be covered in Section 4. Changes to the system prompted by flight experience are discussed in Section 5.

3.3 THE OGO PROPOSAL

The original OGO proposal was submitted to NASA Goddard Space Flight Center on 23 September 1960. This proposal was based upon rather general specifications (Reference 14) issued by NASA with the Request for Proposal No. GS-1014. These specifications included:

- A 1-year lifetime with a 6-month so-called "operating" life or all subsystems in on condition.
- The EGO and POGO orbits were mission requirements.
- The reaction wheel and gas jet control torquing system conceived at GSFC was specified for use in the attitude control system.
- Earth-pointing errors of less than 2° were required.
- The OPEP was to be pointed within 5° of the orbit plane throughout the orbit.
- The Sun Oriented Experiment Package (SOEP) was to be oriented to the sun line to within $\pm 20^{\circ}$.

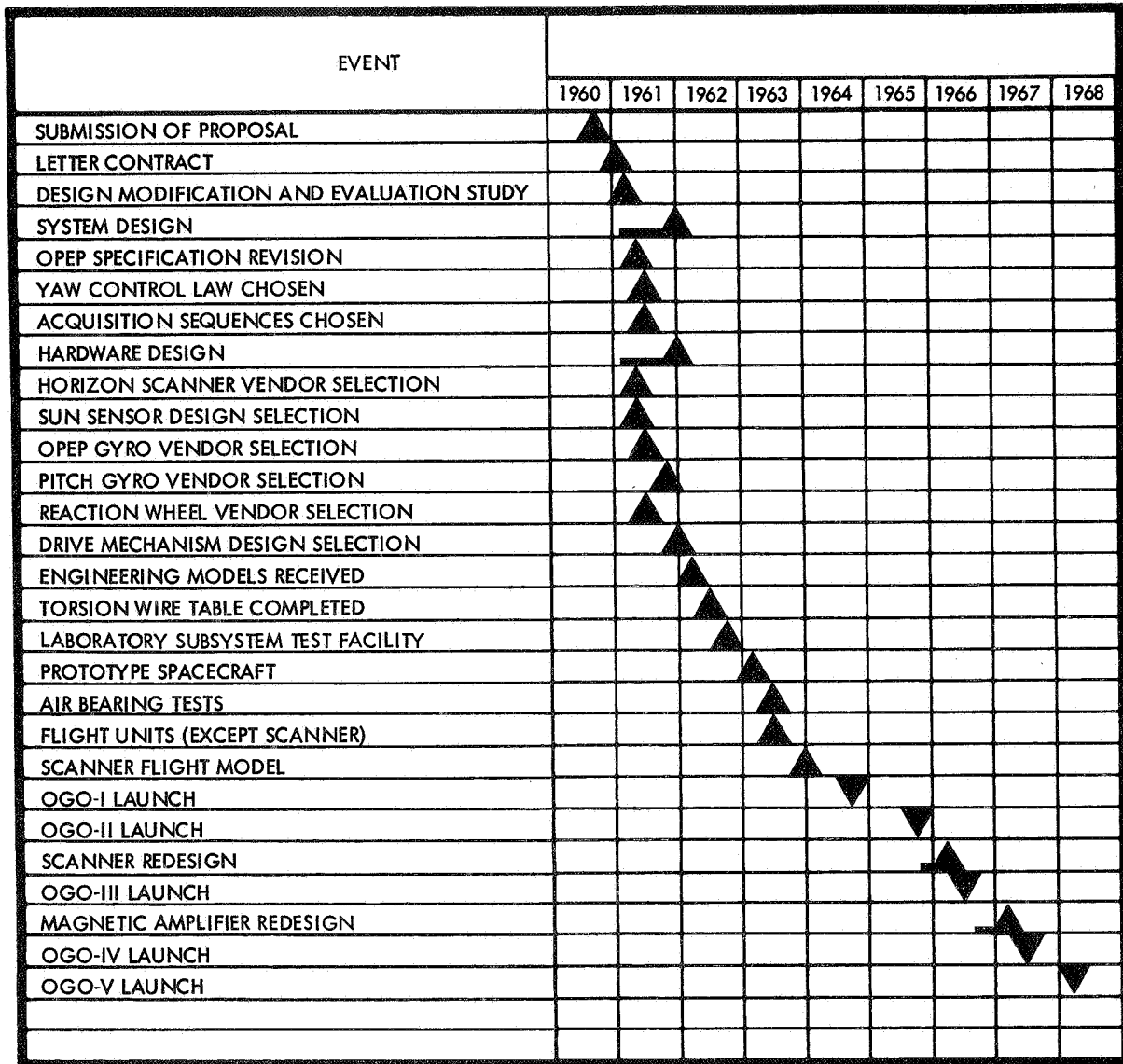


Figure 10. OGO Program Major ACS Milestones

- A full-scale prototype test of the ACS system, possibly on an air bearing.

The OGO attitude control requirements were similar to those of the Advent Communications Satellite which was under study by TRW. In fact, the concept of a two-stage acquisition sequence (sun, then earth) and the sun-referenced yaw control system were adapted directly. By mounting the

SOEP on the solar array, the experiment-pointing requirements could be met. The OPEP required a third body controlled to point in the orbit plane. While these basic concepts have remained unchanged, the details of the system design from that originally proposed changed significantly. The section which follows discusses the ACS design items considered during the 8 weeks after receipt of the Letter Contract.

3.4 THE DESIGN MODIFICATION AND EVALUATION STUDY

The letter contract authorizing the go-ahead required that some specific studies be made in the area of ACS design (as well as others). Most of the areas requested for study eventually led to changes in the ACS system from that originally proposed though the changes generally were not conceived during the initial 8-week study.

To meet the original OPEP-pointing requirements in an EGO orbit, an attitude reference or integrating gyro was necessary. Because pointing errors were induced by gyro drift, it was necessary to correct or update the gyro reference periodically. This correction required a complex onboard or a ground-assisted system. Ultimately, the customer elected to eliminate the OPEP pointing accuracy requirement over the whole EGO orbit except near perigee. This elimination allowed the use of a gyrocompass system for the OPEP control loop and greatly simplified the control logic required; however, the decision was not made until approximately May 1961. Thus, the customer requested a restudy of the updating schemes for the OPEP gyro.

Two other significant changes in system design occurred. They were the acquisition sequence and the noon and post-eclipse turn control methods.

The original acquisition sequence was proposed as follows:

1. Slew the solar array to -90° (i. e. , $-Z_b$ spacecraft axis normal to paddle face).
2. Acquire the sun with the $-Z$ axis using sun sensors for pitch and roll control and the OPEP gyro in a caged or rate gyro mode for yaw control.
3. Rotate about the yaw axis until the pitch axis intersects the earth.

4. When pitch axis "sees" the earth, stop yaw rotation and rotate about roll axis until all four scanners "see" the earth.
5. Enable earth-pointing control.

The acquisition logic required was fairly complex and would require some open-loop maneuvers, i. e. , the roll rotation. The sequence apparently was motivated by the desire to use the OPEP gyro in the rate mode, hence, avoiding the second gyro package now used. The customer expressed concern over the complexity of the acquisition sequence and requested additional analysis.

Control of the noon and post-eclipse maneuvers was also changed significantly from the original proposed design. The so-called noon turn occurs when the sun is nearly in the orbit plane. As shown in Figure 5, the spacecraft must undergo a rapid reorientation in yaw to keep the sun on the $-Y_b$ axis side of the body. This reorientation occurs when the sun passes over the spacecraft at high noon in the orbit. At this same time, the paddles are looking upward along the $-Z$ axis so that the sun sensors no longer are a precise measure of yaw orientation. In fact, with the paddles precisely aligned with the $-Z$ axis, no sensitivity to motion about the yaw axis exists. In the proposal, a system was proposed to monitor paddle angle. As the paddle angle approached within 20° of the $-Z$ axis, signaling the approach of a noon turn, a special control loop would be activated. This loop, using a separate reaction wheel, would through a timed maneuver perform the large-angle reorientation required near noon in the orbit. Upon completion of the turn, the yaw attitude would be held constant relative to the OPEP shaft. Control would revert to the normal yaw axis controller once the array angle indicated high-noon conditions had passed.

It was originally proposed that yaw orientation during eclipse be maintained through use of the OPEP shaft

transducer. This again was an awkward and complex control law. It required two yaw reaction wheels, complex logic circuitry, and placed heavy reliance on a multitude of sensors (i. e. , OPEP and array shaft position transducers). Thus, analysis of the yaw noon and post-eclipse turn control was specifically requested.

Other items which were included in the study request were:

1. Consider the use of argon rather than nitrogen for control gas. An inert gas was desired to minimize experiment interference.
2. Consider ACS system redundancy and determine the effect on overall system reliability.
3. Consider servo requirements of the Solar Array Drive. Apparently the customer was concerned over the feasibility of achieving the slow drive rates required ($6^{\circ}/\text{min}$) with the proposed drive mechanism.
4. Authorization was given to proceed with generation of design specifications for all sensors.

The results of the design modification and evaluation study are documented in Reference 15. The results of the study are summarized as follows:

- A detailed re-examination of system sizing was performed. Gas-jet torques were increased to reduce acquisition times. Impulse requirements due to disturbance torques were refined. Original sizing for the reaction wheel specifications were verified.
- No changes were proposed to the acquisition system.
- Preliminary reliability studies were made of the system components with and without redundancy.

- New noon and post-eclipse turn control laws were proposed. The second yaw reaction wheel was eliminated. Mixing the OPEP shaft angle and sun sensor outputs was proposed which reduced the severity of the noon turn. It also eliminated open-loop maneuvers. Eclipse control utilized a yaw angle holding mode to minimize the post-eclipse yaw sun reorientation.
- At this time, the decision to use a gyrocompass for OPEP control had not yet been made. Hence, further studies of methods to reset the integrating gyro were made.
- Argon was determined to be an acceptable substitute for nitrogen as a control gas.
- ACS weight as originally proposed was 216 lb. Estimates were revised to 156 lb. The entire difference was due to a downward adjustment in on-board gas impulse requirements, hence, reduction in pneumatics system weight.

During the preliminary study, plans for the development of the ACS were drawn up (Reference 16). This program plan called for the completion of the basic system design by the end of 1961.

The following subsections discuss the design progress and hardware development decisions through 1961.

3.5 ACS DETAILED DESIGN

From March through December 1961, most of the basic design decisions and tradeoff studies were made. Considerable simplification of the system design was effected as well as simplification of the hardware component design. The several system design changes will be discussed in the following paragraphs.

The final design of the acquisition control sequence was chosen about July 1961. The sequence was described in Section 2. Although this method required the addition of a rate gyro along the pitch axis, it also provided for continuous closed-loop control of the entire acquisition sequence. The rate gyro was required only for acquisition, however, and could be turned off upon switch to normal earth pointing. The sequence also permitted acquisition of the earth in an EGO orbit where earth angular size may be small. Analysis of the original acquisition sequence showed that acquisition of small earth sizes was difficult. Finally, the original acquisition sequence was based upon a rotating head scanner design, whereas, an edge tracker type scanner was found to satisfy other system operating constraints better.

Another change in the system configuration was made which later proved significant. In the original proposal, the scanner scan planes were set at 45° to the principal X_b - Y_b spacecraft axis. Since the $-Y_b$ axis was to be in the direction of the sun, sun interference on the horizon scanners was minimized by canting the scan planes away from the sun-pointing axis. During evaluations of various acquisition sequences, it was decided to align the horizon scanners with the principal axes to improve the scanner geometry for earth acquisition. It also had the obvious benefit of permitting computation of pitch and roll error signals directly from the head angles. However, it did place the C scanner head scan plane in line with the sun.

Analyses were performed during the system design phase to determine a method of preventing sun interference on the C scanner head. It was recommended that a small angular offset (-1.6°) be placed in the sun sensor to move the scanner scan plane away from the sun line. In addition, a sun alarm was incorporated into the C scanner head to activate a logic signal. This signal causes the yaw wheel to turn on to move the C scan plane away from the sun.

This analysis made certain assumptions regarding the scanner field-of-view and the sun alarm activation. The assumptions could not at that time be supported by either analysis or test nor were they in retrospect conservative. It was not until the scanner optics redesign after the second OGO launch (OGO-C) that tests or analyses were performed to evaluate the sun interference problem. This evaluation is covered in Section 5.

The final design decisions were made in July 1961 on the redesign and simplification of the yaw control system. Basically, a large reaction wheel was installed in the yaw channel which could store approximately five times the pitch or roll wheel momentum. Gas is disabled in yaw during normal earth-pointing control. The excess momentum storage capacity of the yaw wheel is used to control the spacecraft to follow the rates required during the noon turn and to impart approximately a $0.5^\circ/\text{sec}$ rate during the post-eclipse turn. The yaw wheel is heavy and consumes a significant amount of power but it permits an extremely simple control law; thus, control law simplicity was traded off against weight and power.

Another aspect of the yaw control law which required consideration was the time required to complete the post-eclipse turn. Since the spacecraft was allowed to drift uncontrolled during eclipse, at sunrise the sun could be at virtually any azimuth with respect to the spacecraft. The originally proposed controller tended to minimize the yaw error at the end of eclipse. Design studies indicated that, with the simplified control law, post-eclipse turn times would be typically less than 6 min. Evaluation of power, thermal, and experiment interfaces indicated no operational problems would exist with the simplified controller.

Another basic change to the system design significantly simplified the control electronics throughout the system. The original proposal considered linear servo type reaction wheels with

tachometer feedback. Servo type drive mechanisms were also proposed for the OPEP and Solar Array Drive (SAD). The change was to use bang-bang or on-off control for the reaction wheels and shaft drive mechanisms. The ramifications of this change in terms of hardware design are discussed in Subsection 3.6.

The controller design for the attitude control channels now was quite straightforward since on-off control was to be used for both gas jets and reaction wheels. Lead networks were used for rate stabilization. This form of reaction wheel control results in continuous limit cycling of the reaction wheel controller. Typically, the reaction wheel will retain some stored momentum, or in other words, run at some nonzero speed. Windage and friction losses in the wheel force the wheel to slow down imparting an equal and opposite momentum to the spacecraft. This results in the build up of an error signal which eventually turns on the wheel drive motor for a short period. The wheel speeds up and in turn reduces the attitude error. The process is virtually continuous. Design studies indicated that all system requirements could be met easily with this form of controller including maximum rate limitations.

The concept of the bang-bang reaction wheel controller was an idea originated at TRW. Previous control systems using reaction wheels for attitude control had considered only the so-called proportional wheel. This type controlled wheel speed proportional to the attitude error by comparing the commanded wheel speed to that measured with a tachometer.

The drive mechanism (OPEP and SAD) controllers were also simplified since the drive mechanisms selected (see Subsection 3.6) were constant velocity drives with high frictional levels. The controller need only to operate when the error input exceeded the deadzone. The drive would move the package at constant rate until the error fell to some increment below the deadzone, then turn off. The high

friction within the drive stopped package motion almost immediately. The drive could then remain quiescent until the error again exceeded the deadzone. As with the reaction wheels, a significant amount of power was saved since the drives were quiescent much of the time. A bang-bang controller did require a relaxation in the upper limit of rate allowable (0.005 rad/sec to 0.03 rad/sec) for the OPEP and SOEP experiments. However, this relaxation apparently did not impose any severe performance penalties.

3.6 SYSTEM ANALYSIS

The previous subsection described the major design decisions which were made during the initial design phase. Most of the major decisions had been made by July 1961. Design verification through analysis and simulation was performed during the period of July through December 1961.

Two major simulations were developed. The first was a three-axis, small-angle, digital simulation including disturbance torque models. The second was a large-angle analog simulation for study of sun and earth acquisitions.

Primarily, the digital simulation determined the gas consumption rate due to disturbance torques. It also provided a tool for evaluation of the reaction wheel system under simulated on-orbit conditions. The most important result was verification of the yaw system operation, particularly the ability to handle momentum build up from disturbance torques without gas jets.

The analog simulation was used for verification of the acquisition system performance under nominal and non-nominal conditions. Gas impulse requirements for sun and earth acquisition were determined.

To complement these large-scale simulations, single-axis simulations were performed to evaluate individually pitch, roll, and yaw control system

performance. Some of these simulations were also used during the earlier design phases.

Design of the control loops for the OPEP and SAD was carried out through phase plane type of analysis. Since these control loops were extremely simple, no simulations were made.

One addition to the lead-lag compensation filters in the pitch and roll channels was required for earth pointing. The horizon scanner error signals contained a $\pm 1.0^\circ$, 18-Hz sinusoidal signal caused by the dither motion used in the horizon scanner head tracking loop. To attenuate this signal to a level which would not interfere with ACS operation (e. g., cause valve chatter) required a low pass filter. The filter design was optimized through a preliminary hand analysis with final verification via a single-axis analog simulation.

An analysis and an analog simulation of the horizon scanner tracking loop performance were performed. The primary benefit of the analysis was a considerable increase in understanding the horizon scanner operation. Critical parameters and loop characteristics which affected the tracking loop performance were determined. Effects of noise and variation in altitude were also evaluated.

Other analyses of a system's nature were performed during this initial phase. They included the tradeoff and selection of a logic scheme to prevent wrap-up of the OPEP cabling, definition of duty cycles for drive mechanisms and reaction wheels, and the previously mentioned analysis to determine a method of minimizing sun interference of the C scanner head.

These analyses culminated in the issuance of Reference 2, the ACS system description, specifications, and logic. The NASA-approved ACS specifications were not issued in final form until Reference 17. They have essentially been listed in Section 2. Additional limited analyses and simulations were performed on a sustaining

engineering basis throughout the development program and are described in Section 4. From this point until the launch of OGO-I, analytical support to the program was minimal.

The problems of spacecraft flexibility were not considered during this initial design phase. All system design was made on the basis of rigid body spacecraft models. This probably was due to lack of definition of experiment boom design. Analysis of the effects of the flexible experiment booms was made later in the development phase. (See Section 4). Another area which apparently received insufficient attention was the horizon scanner performance, particularly under conditions of sun or moon interference or variation in the earth's radiance profile. The problems of spacecraft flexibility and scanner performance are well recognized today as a result of the OGO flight experience. Historically, however, these problems were not analyzed in the initial design phase.

3.7 HARDWARE DESIGN

The hardware and component design and development were well advanced by the end of 1961. Major design decisions and tradeoffs were for the most part completed with most units well into the breadboard or engineering model stage. The following paragraphs briefly describe the tradeoffs which affected the final design decisions on the ACS components and their status at the end of 1961.

3.7.1 Horizon Scanners

The horizon scanner was a purchased item. The requirements and work statement for the proposal request were completed in mid-February. Eight proposals were submitted. The design submitted by the Advanced Technology Laboratories (ATL), a Division of American Standard, was selected. The unique feature of the ATL design was that the scanner utilized a mirror mounted on a flexure pivot to obtain the required scan capability. Thus, the scanner

system required no bearings or hermetic seals associated with motor-driven scanner designs and resulted in a greater system reliability. NASA contract approval was received on 9 August 1961 although ATL was given a preliminary go-ahead on 5 June 1961.

Throughout 1961, some significant redesigns were required, both in the electronics as well as mechanical configuration. Some of these redesigns were the result of redefinition of interface requirements; error signal computation was revised and packaging requirements were changed. Some electronics redesigns were necessitated since some transistors used in the original design were not acceptable for use in the OGO program. Finally, difficulty was experienced in fabricating the flexure support (called a positor) for the scanner mirror. Delivery of an engineering model horizon scanner originally scheduled for early December 1961 was delayed and actual delivery was in mid-February 1962.

3.7.2 Sun Sensor

The sun sensor design was frozen in June 1961. The design consisted of silicon solar cells to provide coarse attitude information with a Radiation Tracking Transducer (RTT) produced by Micro Systems Inc. to provide fine attitude information (i. e., the sun within $\pm 17^\circ$ of the solar paddle normal). The fine sensor was necessary to meet system null accuracy constraints. The coarse sensor design was adapted to provide a nonsaturating attitude error with a 4π steradian field-of-view. The nonsaturating requirements were necessary since vehicle rate information during acquisition is derived from the attitude error signals. If saturated, no rate information would be available. With the basic design of the sensor frozen early, development of engineering models proceeded smoothly.

3.7.3 Pitch Rate Gyro

The acquisition approach which defined the requirement for the pitch rate gyro was not selected until July.

Therefore, procurement steps for the rate gyro occurred significantly later than the other components. It was not until November 1961 that a Minneapolis-Honeywell rate gyro was selected. Fortunately, the gyro requirements were considerably less stringent than other system components (i. e., the gyro did not have to operate continuously over the year lifetime) and gyros in current production were adequate.

3.7.4 OPEP Gyrocompass

Work on the OPEP gyro specification was initiated during the 8-week study contract. Selection of a vendor was made in May but NASA approval of contract go-ahead was not obtained until August. The Minneapolis-Honeywell GG-49 type gyro was selected. At the time of the gyro selection, the OPEP design was still to use the gyro as an attitude reference with periodic resets to trim drifts. Although this scheme was eliminated in favor of a gyrocompass scheme, no major change was required in the gyro. The electronic caging loop was simply designed for the rate mode. The gyro is one of the few cases in the ACS where redundancy is provided due to the limited operating life of the gyros.

The electronics which provided caging of the gyro, temperature control, and switching for the redundant gyro were designed and developed at TRW. Design of this unit proceeded smoothly throughout 1961 with engineering model tests including a gyro conducted early in 1962.

3.7.5 ACS Electronics

Although the proposal specified a single electronics package, this plan was revised early in the development stages to divide the electronics into three packages: Sensor Electronics and Logic Assembly (SELA), Attitude Control Assembly (ACA), and Drive Electronics Assembly (DEA). This division facilitated fabrication and checkout and, more importantly, conformed to spacecraft integration requirements.

The major decision, however, in the electronics design was to use magnetic amplifiers. The original motivation for using magnetic amplifiers came from the desire to use bang-bang wheel control. Previous applications of the bistable magnetic amplifier had shown it to be ideally suited for the deadzone function required in the bang-bang control. Reliability assessments of the electronics with magnetic amplifiers versus solid-state elements showed significant reliability improvements with magnetic amplifiers. As design evaluations progressed, it was found that magnetic amplifiers could be used for low-level signal amplification, and as power switches for the reaction wheel motor as well as the bistable function. Compared to all solid-state electronics, the number of system components were reduced significantly. Solid-state circuits were used only for specialized circuits such as the telemetry, logic, valve drive amplifiers, and the horizon scanner electronics.

Use of magnetic amplifiers did impose a significant weight penalty. At the time of the original design, the weight penalty for the ACA was estimated to be a factor of two based upon components alone (i. e., neglecting chassis weight). On the other hand, estimates of unit reliability for 1 year increased significantly. The reliability based upon parts count increased from 0.82 for a solid-state design to 0.942 for magnetic amplifier implementation. The magnetic amplifiers also had the aesthetic reliability attractiveness of being "iron and wire." Thus, the magnetic amplifier implementation was chosen on the basis of the significant gain in reliability and the inherent weight penalty accepted.

By the end of 1961, circuit design was for the most part complete as were breadboards of all the electronics units (SELA, ACA, DEA, gyro electronics). All the breadboards lacked the magnetic amplifiers, although limited circuit testing had been accomplished with the engineering model magnetic amplifier units.

3.7.6 Reaction Wheels

In the original proposal, the reaction wheels were two-phase ac servo-type motors with a flywheel mounted to the shaft and were to be produced at TRW. Investigations after the proposal showed that several companies had performed considerable development work on reaction wheels. This fact combined with limited manpower available at TRW prompted a "buy" rather than "build" decision. Preliminary requirements for the wheel torques were increased significantly over the original proposal. Detailed studies of the post-eclipse and noon-turn requirements dictated the change. As previously discussed, the yaw control design necessitated an increase in the yaw wheel size.

The reaction wheel vendor, Bendix Corporation Eclipse Pioneer Division, was selected about July 1961. Since the request for proposals was based upon the original reaction wheel parameters defined during the design modification study, some significant revisions of specifications occurred after vendor selection. This resulted in no significant program delays, however, since the wheels were not off-the-shelf items. Delivery of the first wheel assembly for engineering evaluation was scheduled for early January 1962.

3.7.7 Solar Array and OPEP Drives

The drive mechanisms required for the OPEP and solar array were the object of considerable review during and subsequent to the design modification study. It was concluded that no off-the-shelf drive was directly adaptable to the OGO drive requirements. Therefore, an inhouse effort was initiated to develop a drive mechanism, the most promising being the TRW-developed "wobble" gear design. However, evaluation efforts continued in parallel on vendor-supplied drive units.

In July, a tentative decision was made by TRW to pursue only the inhouse development based upon the

results of the parallel evaluation program. However, TRW was directed by NASA to pursue the vendor-supplied drive mechanisms. This NASA direction was based primarily upon the lack of previous TRW experience in building drives. As a result, an RFP was initiated for (1) a vendor to build the TRW wobble gear design and (2) alternate designs to be proposed by the vendor. In any case, at this time the wobble gear drive appeared to be the most promising drive system.

Several companies responded to the wobble drive RFP but no other directly applicable drive proposals were received. Meanwhile, the inhouse development of the wobble gear drive had progressed significantly with build up of an engineering model well under way. After evaluation of the proposals and the TRW design-and-build potential, approval for an inhouse development was given by NASA. This occurred in December 1961. Although the final decision on the drive was not made until December 1961, development of the drive mechanism was sufficiently advanced so that tests of the first engineering model were performed in January 1962.

3.7.8 Pneumatics

The development of the pneumatics system was relatively straightforward. With the exception of the pneumatic lines and nozzles, the pneumatic system equipment was purchased. For the most part, the purchased items (e.g., valves, pressure regulators, and pressure sensors) were within the state-of-the-art and required no development.

One significant change in the pneumatic system was the placement of the nozzles at the end of two 4-ft booms, permitting a reduction in jet thrust and, hence, a savings in on-board gas required. The valves were kept inside the spacecraft to ensure adequate thermal control. Careful evaluation was made of thrust rise and decay times to verify that there was no degradation in system performance.

3.8 SYSTEMS TEST

As outlined in the proposal, three tests of the ACS system were planned. They were: (1) a single-axis test using a torsion wire supported table, (2) a complete systems test using an air bearing, and (3) a laboratory evaluation test of the complete ACS before integration into the spacecraft.

3.8.1 Torsion Wire Test

The torsion wire table was to provide an early dynamic test of the ACS. To limit size and weight, the inertias and torque sources were scaled to 1/20 of actual value. Preliminary tests of the bang-bang type of reaction wheel control loop were run by October 1961. These tests provided a qualitative verification of the bang-bang reaction wheel system. No detailed design verification type of tests with parameter variations were made. Plans were formulated for simulation of the high-noon and post-eclipse turn yaw channel response on the torsion wire table. Ultimately, this proved to be the only other test run on the torsion wire table. Cost and schedule limitations prevented tests of the pitch or roll loops using the horizon scanners.

3.8.2 Air-Bearing Test

The air-bearing space simulation was to provide a three-axis test that would duplicate the on-orbit conditions. It was meant to be a development tool for providing confidence in the ACS system design, logic, and sequencing. Design of the air bearing and layout of the ACS components were performed during 1961. Inertias and torque sources were scaled to 1/10 actual value. Procurement of the air bearing and fabrication of the table to support ACS components were initiated early in 1962.

3.8.3 Subsystem Laboratory Test

Prior to spacecraft integration, each ACS system was laboratory tested to evaluate parameters such as system gains, deadzones, dynamic characteris-

tics, and logic threshold levels as well as to check the logic functions. During 1961, the requirements for this test were defined and procurement and fabrication of the necessary equipment were initiated.

A great deal of flexibility was designed into the subsystem laboratory (S_L) tests. The test console was designed to provide all command functions normally supplied from the spacecraft command distribution unit. It also permitted static simulation of error signals derived from the horizon scanners and sun sensors. Unit (e. g., SELA) outputs or interface signals were also simulated. This approach permitted portions of the system tests to be performed even if all units were

not available at the same time. This capability proved to be very valuable in many cases. It should also be pointed out that the division of the unit functions also facilitated this approach.

Provisions were made for dynamically checking the ACS operation by mounting the sensors (horizon scanners, sun sensors, pitch rate, and OPEP gyro) on single-degree-of-freedom rate tables. Dynamic inputs in the form of constant rates could be applied to sensors. The sun sensors and horizon scanners were, of course, moving with respect to the stimuli. The tables were accurately calibrated such that null and gain measurements could be made. Final checks of telemetry output calibrations were also made during the S_L test.

4. DISCUSSION OF MAJOR PRELAUNCH PROBLEMS AND SOLUTIONS

Most prelaunch problems discussed in this section fall into the time period from the beginning of 1962 to September 1964 when the first OGO was launched. During this time period, ACS flight systems were checked out for the first three observatories. Additional ACS testing took place before each launch, but the major prelaunch problems for OGO-I, -II, and -III had been solved by that time.

As a result of the OGO-III flight experience, a major redesign of the attitude control system was performed beginning in July 1966. The redesigned ACS was subjected to a complete series of tests, during which some noteworthy problems were encountered which are also described in this section.

4.1 CHRONOLOGICAL HISTORY

In January 1962, an engineering model of the wobble gear drive was completed at TRW. Engineering models of the remaining ACS units, such as the horizon scanner and sun sensor, were received during the following 2 months and development testing started immediately. At the same time, testing facilities were built up for complete system tests. The torsion wire table for a single-axis simulation of the control system was available by April 1962. The first S_L test console was used in November 1962. About two-thirds of the control system, which was initially tested, consisted of pro-

totype or engineering model assemblies.

An air-bearing table for a three-axis simulation was near completion at the end of 1962. In January 1963, an engineering model control system was checked out on the air-bearing simulator.

Prototype models of most ACS units were available at the beginning of 1963, and a prototype spacecraft was constructed. In March, the first complete ACS system was checked out. By this time, the air-bearing simulator still had some difficulties with the precision air bearing and the sun simulator. Finally, in June, the air-bearing simulator was ready for simulating OGO attitude maneuvers.

Construction and acceptance testing of flight units proceeded throughout the first few months of 1963. At least one flight model of each ACS unit, with the exception of the horizon scanner system, had been successfully acceptance tested by June 1963. The first horizon scanner flight unit was ready in December 1963.

Qualification and acceptance testing continued in 1964. Three complete flight systems were also checked out in the laboratory and in spacecraft integrated system tests. The actual flight system for OGO-I was sent to Cape Kennedy for thorough and complete integrated tests several weeks before the September launch.

4.2 PROBLEMS UNCOVERED BY DESIGN ANALYSIS

4.2.1 POGO Gas Consumption

Early investigations of the pneumatic impulse requirements for a 1-year OGO lifetime gave the following results: (1) 100 lb-sec for each acquisition, (2) 440 lb-sec for normal control in a POGO orbit, and (3) 50 lb-sec for normal control in an EGO orbit. The difference in estimated gas consumption between a POGO and an EGO orbit is mainly due to the greater aerodynamic drag torques in the lower POGO orbit.

Since OGO-I was launched into an EGO orbit, a gas impulse capability of approximately 500 lb-sec was believed to be more than sufficient for a 1-year operational lifetime. Unfortunately, no data became available on normal gas consumption from the OGO-I flight experience because the spacecraft was never fully stabilized.

Although the initial POGO orbit perigee was specified as 200 n. mi., it was lowered to 140 n. mi. after the initial design phase had been completed. However, gas consumption estimates were not revised. As the launch of OGO-II approached, the question of gas consumption was again raised. A review of earlier analysis showed that the gas supply was insufficient to achieve a year's life with the 140-n. mi. perigee. Thus, the perigee altitude of OGO-II was raised again to the original design value of 200 n. mi.

The premature depletion of gas on OGO-II, due to unexpected attitude disturbances, did not allow verification of data on gas consumption. Additional analysis of gas consumption for a POGO orbit indicated that the gas supply for future spacecraft might be marginal. This was due in part to changes in the experiment configuration and orbit parameters. The atmospheric density at perigee altitudes was expected to increase due to an increase of sun spot activity. Finally, additional margin for unexpected gas usage was obviously desirable.

Investigations were conducted to determine the suitability of other inert gases for increasing the total impulse capability of the OGO Pneumatic Assembly. It was concluded that it was feasible to directly substitute krypton for argon and thereby roughly double the impulse capability.

The only expected change in functional performance of the pneumatic system, as a consequence of using krypton instead of argon, was an increase in the internal leakage rate of the regulator following the acquisition maneuver. However, this increased leakage rate should be a temporary result of the reduced regulator housing temperature and should become normal within a maximum time of half an hour after acquisition.

Krypton gas was first used on OGO-IV with an initial pressure of 4000 psi. Despite a boom oscillation problem, OGO-IV has been in orbit for nearly a year with sufficient gas left to last for at least another year.

4.2.2 Acquisition During Eclipse

A study, including an analog computer simulation, was performed early in 1963 to examine the behavior of the ACS during the initial acquisition under an eclipse condition. Two potential problem areas were discovered.

First, the case was considered where the spacecraft entered a brief sunlight period after injection into orbit and had insufficient time to acquire the sun before eclipse. Computer results showed that the transient vehicle angular rates could reach values as large as $4^\circ/\text{sec}$ during sun acquisition. If the vehicle entered eclipse before the completion of sun acquisition, the tumbling rates could be that large. Since the pitch rate gyro operates whether or not the sun is visible, excessive gas would be expended in controlling the pitch rate in eclipse.

Earth search for OGO-I was automatically initiated 27 min after the start of acquisition. Assuming earth

acquisition was successfully completed in eclipse, yaw stabilization following eclipse would be attempted. It was observed that for initial body rates of $3^\circ/\text{sec}$ and a 180° initial attitude error, the system did not converge to the desired equilibrium condition.

When the observatory is injected into a long eclipse, similar difficulties with acquisition are encountered. However, in this case the rates imparted to the vehicle at separation should be less than $1^\circ/\text{sec}$ by specification. With initial roll and yaw rates of $1^\circ/\text{sec}$, less than 25 lb-sec of pneumatic impulse would be expended in controlling the pitch rate during a 30-min eclipse according to analog computer results.

4.2.3 Boom Oscillations

Several brief studies investigated the effects of spacecraft appendage oscillations on the OGO attitude control system performance before the first OGO launch. In June 1963, an analysis was made of boom oscillations about the roll axis induced by gas or reaction wheel limit cycles. The conclusion of this analysis was that the boom motions induced by ACS activity were not large enough to justify further investigations, in particular an extensive three-axis analog simulation.

The results of the above-mentioned study were based on a 2% structural damping for the booms as estimated from deployment tests of the booms. Heavy reliance on this assumed damping factor created the false impression that no potential problem existed. It is briefly mentioned in the analysis report that much lower damping would result in boom motion amplitudes sufficiently large to fire the reaction wheels. From later flight experience, it was found that less than 0.5% structural boom damping existed in EP-5 and EP-6 booms.

Flight data from OGO-II indicated vibrations of the EP-5 boom. A magnetometer experiment, located at the tip of the EP-5 boom, sensed this motion and was adversely affected by it. A study of the EP-5 motion concluded with several recommendations

for reducing the vibration which obscured the magnetometer experiment data. Apparently, the oscillation problem was not considered very serious since no action was taken.

The failure to make a complete stability analysis of the flexible spacecraft dynamics with the attitude control system had severe consequences for OGO. On OGO-III, a reaction wheel limit cycle which involved the EP-5 and EP-6 booms developed and eventually caused the roll wheel motor driver magnetic amplifier to fail, shorting the ACS inverter. (See Section 5.)

On OGO-IV, another form of oscillation occurred. In this case, a 60-ft experiment antenna mounted on the -X solar paddle excepted into a self-sustained oscillation. This problem is discussed in detail in Section 5. Analyses were made of the antenna interaction with the ACS in the 1963 studies, and more complete stability analyses and simulations were made after the OGO-III failure. In both cases, stable performance was predicted. Post-flight analysis revealed the oscillations were caused by a thermo-elastic instability of the boom which was virtually an unknown phenomena prior to the OGO-IV flight.

4.2.4 Internal Temperature Rise of Reaction Wheel Assembly

The reaction wheel motor windings were initially specified to be wound with Formvar magnet wire. Under extreme conditions, thermal calculations indicated that the temperature rise within the reaction wheel would result in internal temperatures exceeding the rating of the wire. The pitch and roll reaction wheel temperatures were expected to be the highest because of the poor thermal path from the motor to the mounting base. As a result, Isonel magnet wire, which has a higher temperature rating, was substituted for the Formvar wire. Thermal vacuum tests indicated that the reaction wheel internal temperatures at maximum qualification temperature and maximum expected power drain are well below the temperature rating of the Isonel wire.

Interestingly, a Formvar wire that was also used in the magnetic amplifiers later failed on orbit. The failure was due in part to inadequate thermal design which caused the wire temperatures to exceed temperature ratings. Redesign of the magnetic amplifiers after OGO-III resulted in the use of wire similar to the Isonel used in the wheels.

4.2.5 Sun Sensor Shading

OGO-I has a 30-ft long, 1/2-in. diameter antenna mounted at the end of the -X solar array paddle extending parallel to the X-axis. The location of the antenna is such that shading of the yaw and roll coarse sun sensors will occur for particular array orientations. No shading of the fine sun sensor is possible.

The shading problem was recognized and studied before launch. The conclusions of this analysis were that the sensor shading will probably result in slightly increased time for post-eclipse maneuvers and cause a local gain reduction in the yaw channel. These effects were not believed to seriously disturb normal ACS performance.

4.2.6 Earth Albedo Effect

In July 1966, a study was made to examine the effect of reflected sun light from the earth on the OGO sun sensors. Results showed that both the gain and null position outputs are changed on the coarse sun sensors. However, the fine sun sensor remains unaffected because it does not see the earth albedo.

When the ACS switches from the coarse to fine sun sensor, the yaw error signal may suffer a sudden change on account of the albedo effect. A single-axis analog simulation verified that the control system will remain stable with this switching transient.

4.2.7 Redesign of Two-Phase Inverter

The Static Inverter Assembly (SIA) supplies ac power to the magnetic amplifiers, the reaction wheels, the

solar array and OPEP drive motors, and the pitch rate gyro. The original inverter design was not considered satisfactory because of an excessive no-load input power drain of 25 to 28 W. In May 1962, the design was changed by adding a low-power output channel and gating the high-power output channel on or off in response to output power demands. The no-load power level was reduced to about 9 W. The design change added 29 components to the inverter assembly, including five power transistors and two toroidal output transformers. The package volume was maintained at the same level, resulting in increased packaging density.

During assembly and checkout of the SIA, an excessive number of problems arose directly related to the packaging density. Kinetics Corporation proposed to redesign the output transformers using a core with lower-loss materials. The new transformers were heavier and somewhat larger than the old ones, but the no-load power drain dropped from 25 to 28 W to 11 to 14 W. Subsequently, the low power channels and also the gating circuitry for high power outputs were eliminated. In this way, the overall weight was slightly reduced and the packaging density was considerably lowered.

4.3 PROBLEMS FOUND IN UNIT TESTS

4.3.1 Test Procedure

In general, test operations for all ACS units (horizon scanner, sun sensor, etc.) went through three major phases: development, qualification, and acceptance testing. In the development phase, the main effort was concentrated on building a workable hardware unit. The final version of this unit, known as the prototype model, was used in ACS system tests (S_L) and preliminary integration and spacecraft tests of the prototype observatory. A first flight-type unit was then fabricated and subjected to qualification tests to determine whether or not it satisfied all specifications. When a qualification model passed the qualification phase successfully, a flight unit was constructed and

then acceptance tested before it was installed on the spacecraft.

Qualification testing usually involved a functional test, an environmental test, and another functional test. The first functional test evaluated the unit performance under normal conditions. The environmental tests included thermal vacuum, vibration, and radiation tests among others. After each environmental test, the functional test was repeated. The second functional test exposed the unit to extreme environmental conditions to detect any degradation in performance.

The acceptance tests were similar to the qualification tests except that the environmental tests on the flight unit were not as severe as those on the qualification unit.

4.3.2 Horizon Scanner

After the horizon scanner engineering model was received in February 1962 from Advanced Technology Laboratories, alignment checks and functional tests on this unit were successfully completed. Temperature control tests also gave satisfactory results. However, trouble developed during the vibration tests.

Positor evaluation testing was performed at the design vibration levels of 13 g rms over a frequency range of 400 to 3000 Hz. Both flexure pivot springs on the magnetic damper side of the positor broke at 400 Hz and 500 Hz. Each flexure pivot consists of two flat springs attached to the mirror shaft and the positor base structure so as to form an X. These springs serve as the mirror shaft support and as the electrical connection to the drive coils.

Because the springs failed, an extensive mechanical and materials investigation of the flexure pivots was undertaken. As a result, a new material, a beryllium-copper alloy, was recommended to replace the Elgeloy used for the springs. All future pivot flexure springs were made from the beryllium-copper alloy.

Furthermore, it was found that the positor can withstand significantly higher sinusoidal vibration levels when the drive-coil input is shorted. This short inhibits the mirror motion. A relay package, which shorts the input to the positor drive coils during Boost-Mode 1, was added to the horizon scanner assembly.

The second testing phase of the horizon scanner system was started when ATL delivered a prototype model in December 1962. This qualification unit performed satisfactorily when electrically and optically tested, but it failed to survive the vibration test and was returned to ATL for damage inspection and repair. Again, the main problem was the failure of a pivot flexure spring.

To alleviate the vibration problem, several design changes were made to the tracker head mechanical structure. All functional elements of the tracker (positors, electronics, telescopes, and connectors) were mounted on a single-piece, K1-A magnesium plate. An aluminum casting was designed to fit over this plate to provide a dust cover with window openings. The Be-Cu springs, employed by the flexure pivots, were made twice as stiff as those previously used. In addition, the pivots were coated with an RTV material to reduce the motion at the resonant frequencies. Finally, a lightweight beryllium mirror was installed on the positor. With these modifications the horizon scanner assembly successfully passed vibration testing. Random vibration times were reduced from 12 to 4 min and the 4-min period represented the actual launch environment.

A thermal vacuum test for the scanner system simulated low and high temperatures in space. The system malfunctioned at a high temperature of 120° F and a low temperature of 0° F. In both cases, the A and B tracking channels indicated tracking when no temperature gradient was present. The cause of this failure was a large signal

amplifier noise at high and low temperatures which kept the tracking check logic in the tracking state. To remedy this situation, the signal amplifier output was passed through a low-pass filter.

4.3.3 Sun Sensor

Testing of the sun sensor engineering model, which was received in March 1962, revealed nonlinearities in the fine sensor response due to internal reflections. A redesign of the shading structure improved the response considerably.

Another early difficulty was encountered in the fabrication of the Radiation Tracking Transducer (RTT). The RTT is a silicon p-n junction similar to a solar cell except that it makes use of a photo current flowing parallel to the junction. Micro Systems, Inc., had trouble in manufacturing silicon ingots with a uniform resistivity. Quality control of the manufacturing process had to be improved before all RTT specifications were met.

During the acceptance test of the first flight unit, a thermal problem developed. The sun sensor stabilized at a temperature of about 140° F which exceeded the specified value of 100° ±15° F. The sun sensor has passive thermal control with heat sinks, insulative wrapping, and an outer case with a thermal coating. It was found that almost every unit had a different stabilization temperature. As a first improvement, the bottom plate of the sensor assembly was coated with black anodize instead of vacuum-deposited aluminum. In addition, sufficient aluminized Mylar insulation was placed around each unit to stabilize the temperature within the acceptable range.

In one of the sun sensor units, a short circuit in the thermistor circuit occurred. After removing some of the RTV potting compound from the terminal board, one of the Cicoil harness wires connected to a thermistor terminal was shorted to a terminal board retaining screw. Once the short was located, it was easily repaired, but from this

experience it became obvious that a clear, transparent potting compound would facilitate the job of troubleshooting. All future units did use a clear potting compound on the terminal board.

4.3.4 Pitch Rate Gyro

The first engineering model of the pitch rate gyro, MS 130 B1, was received from Minneapolis-Honeywell in April 1962. Evaluation tests performed on this unit gave satisfactory results. Development, qualification, and acceptance testing on subsequent gyro assemblies proceeded without any serious difficulties. By January 1963, the first flight unit had successfully completed all acceptance tests.

Trouble developed for the pitch rate gyro when Minneapolis-Honeywell decided to discontinue building the MS 130 B1 gyroscope. The quality of those gyros, which were still manufactured for OGO, suffered noticeably. Many gyro failures during testing were directly traceable to poor quality control. For example: a spin motor failed because it had incorrect bearings, one gyro was received with a bent pivot, the damping fluid of a few gyros was contaminated, and a gimbal stuck because it did not have adequate clearance. These malfunctions were uncovered during acceptance testing of flight units for the first five OGO's. However, no pitch rate gyro has failed prematurely in orbit although it has been necessary to select the flight gyros carefully from all available spares.

Since Minneapolis-Honeywell was the sole supplier of the gyros selected for OGO, it was not possible to choose another vendor. The pitch rate gyro has two unique features, namely, a self-test torquer and a Spin Motor Rotation Detector (SMRD) circuit. The self-test torquer and SMRD circuit greatly facilitate testing of the gyro. The SMRD circuit indicates whether or not the spin motor is running at synchronous speed. At the time the pitch rate gyro was selected for OGO, Minneapolis-Honeywell was the only manufacturer of a subminiature rate gyro with those two features.

4.3.5 OPEP Gyro

Minneapolis-Honeywell supplied the first Miniature Integrating Gyro (MIG) in February 1962. Some trouble was encountered in attaching a connector of a test cable to the gyro, a few gyro pins were covered with solder, and one pin pulled out completely. Also, the concentric terminal arrangement was unsatisfactory so the vendor agreed to redesign it for future gyros.

Early difficulties with gyro engineering models arose because square wave instead of sinusoidal voltages was used to power the gyro. In some cases the spin motor did not reach synchronous speed with square-wave excitation. This problem was solved by properly adjusting the value of the phase-splitting capacitor for each individual gyro. Also, the SMRD circuit did not function correctly at first because of the large harmonic content of the 400-Hz voltage driving the spin motor. A maximum distortion of the 400-Hz voltage which could be tolerated for the SMRD circuit was specified.

Noise became a problem for the OPEP gyro because of a beating effect between the 400-Hz and 2461-Hz power supplies. If these two voltages were harmonically related, there would be no beating effect, but since this solution was not feasible, the noise problem was solved by filtering.

Qualification and acceptance testing for the OPEP gyro assembly proceeded smoothly. During one acceptance test a transistor in the heat control circuit burned out because of an inadequate heat sink. A simple redesign eliminated this failure. Besides several minor workmanship problems, the remaining gyro testing was completed without any further difficulties.

4.3.6 ACS Electronics

There were no serious problems with the ACS electronics which required major redesign during the testing phase. The failures which occurred were due typically to defective components, bad connections, or inadequate testing equipment.

A relay with an open coil wire is a good example of a component failure. The break was located under the coil wrapping at the point where the coil wire connects to an interconnecting lead wire. The break may have resulted from fatigue caused by excessive longitudinal movement of the coil bobbin, or it may have been induced in the coil wire by thermal stress. Later, the relay was replaced by a more reliable type.

A different kind of component failure is a capacitor which lacked adequate stability under temperature extremes. This ceramic capacitor was used to control a pulsewidth in the digital decoder of the Command Module. At high or low temperatures, the capacitance changed sufficiently to bring the pulsewidth out of tolerance. A porcelain capacitor was selected as a replacement because it was more stable in the same temperature range.

The magnetic amplifiers presented no serious difficulties before OGO-III. Unfortunately, the temperature tests for the magnetic amplifiers were not severe enough to uncover an inadequate thermal and magnetic core design. After the magnetic amplifier failure during the OGO-III flight (see Section 5), the redesigned amplifiers performed satisfactorily.

4.3.7 Solar Array and OPEP Drive Mechanism

The bellows were the most critical mechanical part of the drive mechanism because little basic design theory was available. Their function is to provide a load-carrying, flexible hermetic seal and to prevent rotation of the input wobble gear. The initial engineering model of the drive mechanism utilized a welded metallic bellows which failed after about fifty hours of operation. Metallurgic and micrographic examination showed that the fatigue failures were always at a point where the metal had been thinned during the manufacturing process.

Modified bellows were procured, one convoluted type and one welded, "nesting ripple" type. Load tests

resulted in failures in the convoluted bellows, but the welded bellows survived the 10,000-hr life test. Consequently, the improved welded bellows (consisting of annealed, corrosion-resistant steel), were used for the OGO drive mechanism.

Some difficulty was experienced with the hermetic seal provided by the bellows during qualification tests for OGO-IV. The maximum allowable leak rate for the drive assembly was set at 1×10^{-6} std cc/sec. The sealed unit is filled with 90% argon and 10% oxygen at a pressure of 1/2 atm through two filler tubes. These tubes are pinched off so that the ends are forged into a perfect seal. The pinched ends are quite sharp and are therefore covered by a silicone rubber (RTV) potting. It was found that the RTV material, which is used as the sealant throughout the drive mechanism, outgasses and, as a result, gives a false indication of leakage. For purposes of the leak test, the maximum leak rate was simply relaxed to 5×10^{-6} std cc/sec, which still provides adequate on-orbit pressurization lifetime.

4.3.8 Reaction Wheels

The first yaw reaction wheel presented a problem to the Bendix designers. Gyroscopic torques caused the rim of the wheel to hit support shoulders which hold the stationary wheel in place during shock and vibration. The clearance between the rim and the support shoulders was increased to eliminate this interference. An engineering model was delivered to TRW in January 1962.

The earliest reaction wheel motors assembled with Isonel wire failed to pass the dielectric strength requirements placed on the motor; i. e., no breakdown of insulation shall result from the application of 1,000 V rms at 60 Hz between each motor winding and the case and between motor windings. Tests indicated that capacitive coupling between the two motor windings was sufficient to cause an insulation breakdown. This coupling apparently originated from an area in the end loops

of the windings. Additional insulation between the windings in this area was added to increase the dielectric strength to an acceptable level.

After vibration of the first yaw reaction wheels, considerable difficulty was experienced in maintaining a hermetic seal. Immediately after soldering of the seals, the original assembly procedure specified a leak test consisting of internal pressurization of the reaction wheel to more than one atmosphere and then submerging the unit in a freon-filled tank for detection of bubbles. Leak detection with more sensitive equipment was not performed until after the unit had been painted. All units assembled to this procedure developed leaks following the vibration tests. The assembly procedure was therefore revised to require leak testing with the sensitive equipment after the final hermetic sealing and both before and after the unit is painted.

Magnetic field tests on the reaction wheel assembly indicated that the unit had an unacceptably large magnetic field. The main source of the magnetic field was a magnetic slug used for the tachometer. Efforts were made to somehow shield the magnetic field of the tachometer. A proposal to use a nonmagnetic tachometer was followed by the selection of a capacitance pickoff tachometer. It was found that at low speeds the capacitive tachometer was noisy. This was considered acceptable since the tachometer was used only as a monitoring device. The tachometer development then proceeded smoothly. An evaluation of the complete reaction wheel assembly with the new tachometer showed that the magnetic field was well within the tolerable limits.

The life test requirement for the reaction wheels is a minimum operating time of 10,000 hr. Reaction wheels were operated at a 100% duty cycle and with a reversal of direction every 30 min. Four pitch or roll wheels and two yaw wheels successfully completed operation for more than twice the required minimum lifetime.

4.3.9 Pneumatics

The development testing of the pneumatic system proceeded smoothly except for typical problems such as contamination. The first serious failure occurred during a thermal-vacuum acceptance test when the high pressure regulator did not operate properly. An investigation revealed that the internal damping was too low and caused the regulator to become unstable. To increase the damping, the diameter of an orifice in the regulator was made smaller by placing a plug, with a hole in the center, into the orifice.

The design of the solenoid valve was improved to increase its reliability. Sometimes a valve leaked because the ball did not move into place properly. To eliminate this problem, two guide-pins for seating the ball correctly were added. When it was determined that the solder seal on the valve nose section also leaked, this problem was solved by using a harder solder material.

4.4 LABORATORY SYSTEM TEST PROBLEMS

As outlined in the proposal, three ACS system tests were performed: (1) a single-axis simulation using a wire-suspended table, (2) a three-axis test using an air-bearing space simulator, and (3) a laboratory evaluation test of the complete ACS before integration into the spacecraft.

4.4.1 Single-Axis Simulation

The single-axis simulator consisted of a circular platform suspended from the ceiling by a torsion wire (see Figure 11). The 9-ft torsion wire was made up of several highly stressed wires rectangular in cross-section and separated from each other by a few thousandths of an inch to prevent their rubbing and adding damping to the system. The control system was mounted on the platform to control its angular position about the axis defined by the torsion wire. In order to eliminate

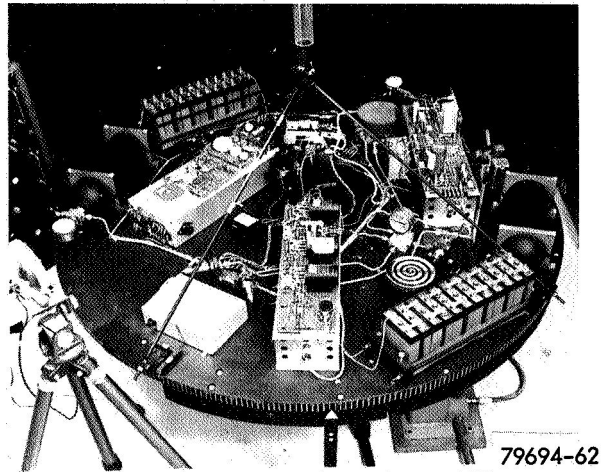


Figure 11. Torsion Wire Test Table

cable twist, the top support of the torsion wire was rotated by a servo system to match the angular position of the platform.

The simulator was not built full size because it was felt that this would result in a structure too large and unwieldy to be practical. The inertias and torque sources were scaled by a factor of 1/20. The parasitic torques associated with the simulator were larger than the disturbance torques expected to act on the vehicle in space. This fact limited the usefulness of the simulator to testing of large-angle maneuvers and system sequencing.

The initial acquisition sequence for the yaw channel was tested, and the high-noon and post-eclipse turns were also checked out for the same axis. These tests provided gross data on the limit cycle behavior of the system. The mathematical model of the control system was refined and minor gain changes were made to the design.

Cost and schedule limitations prevented similar tests of the pitch and roll control loops using the horizon scanners.

4.4.2 Three-Axis Simulation

The three-axis simulator consisted of a rigid, stainless-steel table supported from below by a spherical air

bearing (see Figure 12). The table was capable of free rotation about its yaw axis and a $\pm 92^\circ$ rotation about the pitch and roll axes. The control system was mounted to the table and controlled its attitude with respect to simulated sun and earth sources. Inertias and torque sources were scaled by a factor of 1/10 of their actual value.

The air-bearing space simulation was to provide a three-axis ACS test simulating the on-orbit conditions. The simulator was meant to be a development tool for qualitatively checking out the ACS system design, logic, and sequencing; although it was not suitable for producing accurate quantitative performance data such as gas consumption, power requirements, etc. However, the test results brought out several shortcomings in ACS operation due to nonlinearities and irregularities of the real electronic and mechanical components.

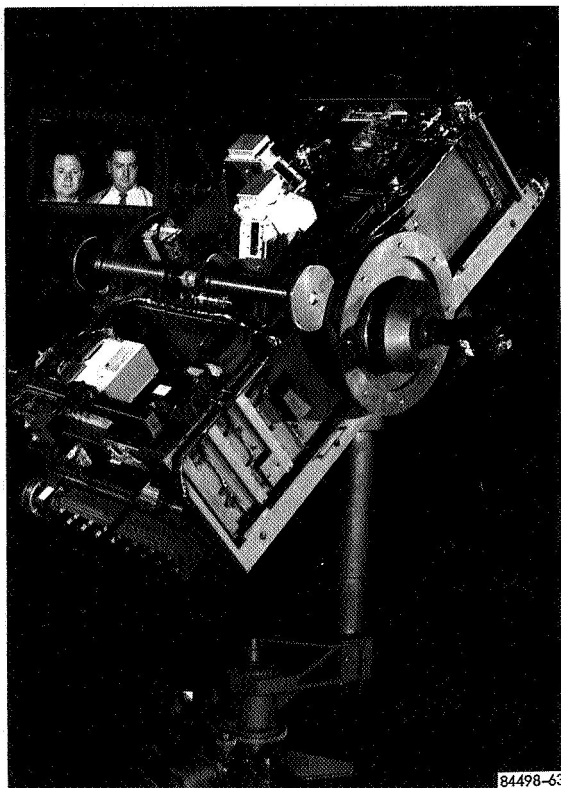


Figure 12. Air-Bearing Space Simulator and ACS Table

In checking out the acquisition logic, the horizon scanner unit gave the most trouble. In the first few acquisition runs, the control system switched directly from Mode 2B to Mode 3 without ever being in Mode 2C. This would be expected if the scanners were locked on the earth, but it happened when the scanner heads could not see the earth. After some experimentation, it was discovered that the scanner heads sometimes put out tracking check signals when they were still searching. At first, the telemetry transmitter was suspected as the trouble source, but the scanner heads behaved the same way when the transmitter was turned off. Eventually this problem was solved by putting an RC noise filter in the horizon scanner central electronics box.

Another problem was that the C scanner head stayed locked on the sun during Modes 2B and 2C. When two other heads locked on the earth, generating tracking check signals and changing the mode of operation from 2C to 3, the control system started to point the yaw axis toward a spot that was not the center of the earth. This difficulty was overcome by putting a piece of masking tape at the edge of the C scanner head window, cutting off its view by a few degrees so that it could not see the sun.

It was concluded then that it was unlikely the C head sun interference would occur during an actual OGO acquisition. In the simulation, the sun interference was blamed on geometric inaccuracies in the test set-up. In reality, the sun could not enter the nominal field-of-view of the horizon scanner during acquisition.

Some of the acquisition runs were unsuccessful because three scanner heads locked on temperature gradients other than the earth's edge. The horizon scanner was found to be extremely sensitive; even locking on edges and corners of the room.

The first few attempts at simulating a post-eclipse turn were not successful. Initially, an overshoot of about 160° resulted and it took almost half an hour

before the table settled down. In one run the table overshot so far that it continued to rotate in the same direction. It was noticed that the yaw wheel passed through zero speed when the table still had a large angular velocity. The only explanation for this behavior was that the system was picking up momentum from a torque source external to the table. It was finally concluded that air friction on the exposed high-speed reaction wheel was causing the momentum change. To solve this problem, a plexiglass cover was made to completely enclose the yaw wheel.

The control system operated satisfactorily for a simulation of the noon turn. The sun, earth, and satellite lie in a straight line for the noon condition. The control system properly rotated the table 180° (see Figure 5).

4.4.3 ACS Laboratory Evaluation Test

Test Description

Each ACS system underwent a detailed S_L test prior to spacecraft integration. The test involved precise evaluation of parameters such as system gains, dynamic characteristics, deadzones, and logic threshold levels, as well as a complete check of the logic functions.

In S_L and unit testing the horizon scanners a parallax error developed because two scanner heads were mounted on one base (see Figure 8). Rotation of the assembly, regardless of the center of rotation, will cause at least one of the heads to be translated as well as rotated. Analysis indicated the parallax error introduced would be significant. To circumvent this problem, four separate thermal gradient sources were set up. The scanner heads "looked" at the sources through collimating parabolic mirrors. With the collimated source, parallax was eliminated.

Problem Uncovered

A closed-loop test was performed on the OPEP control system to verify that the Drive Electronics and OPEP

Gyro Assembly operated correctly together. On the first flight unit, performance was as expected from analysis except for a chatter in the drive. When large error angles exceeded the deadzone angle by 10° or more, the shaft rotated at full speed. However, as the error approached the deadzone angle within 10° to 15°, the drive began to chatter and the average speed decreased to one half full speed. The chatter repetition rate was about 1.2 Hz. For brief intervals of perhaps 1° the chattering ceased and the drive operated at full speed. Chattering of this sort was explained by coupling of OPEP shaft rate into the gyro input axis, and by shaft acceleration into the gyro gimbal. In addition, some backlash of about 1/2° magnitude was observed in the shaft of the wobble drive gear.

Because the chatter could affect the life of the OPEP drive in space, efforts were made to eliminate it. A change was made to reduce the loop gain of the OPEP control system by increasing the deadzone, and special care was taken to minimize the backlash in the drive gear. Although the deadzone was enlarged, overall system accuracy was within specification. Subsequent tests on the OPEP control system gave satisfactory results.

4.5 PROBLEMS IN SPACECRAFT INTEGRATION

4.5.1 RF Interference

During the Integrated System Test (IST) on the first flight spacecraft, it was observed that the horizon scanner operation was grossly degraded whenever the spacecraft's 10-W transmitter was on. Tests performed on the horizon scanner system in the prototype spacecraft screen room indicated that the interference arose from radiated RF pickup rather than from internally generated or conducted noise. The method of carrying shield and ground wires through the scanner system was altered to provide isolation from the transmitter. With these changes, the RF pickup was reduced to an acceptable level.

4.5.2 SELA Switching Problems

At Cape Kennedy, Florida, a strange mode-switching problem was encountered during systems testing for OGO-I. Under normal environmental conditions, the following three malfunctions were observed in a single test: (1) improper switching from Mode 3A to 2C (proper switching is from 3A to 2A), (2) ambiguous telemetry readings in the mode telemetry channel, and (3) lock-up in Mode 2C when the conditions were proper to switch to Mode 3. It was impossible to cause the problems to repeat. After some investigation, it was concluded that a marginal relay possibly caused all three symptoms. Testing in the TRW laboratories with the marginal relay briefly reproduced all three malfunctions. The relay was replaced, incorporating a pulse-stretching capacitor in the flight unit as a precaution.

4.5.3 Speed Problem With Drive Mechanism

During a cold thermal-vacuum test of the OGO-I spacecraft, it was observed that both the solar array and OPEP drives ran at slower than expected speeds. The trouble was traced to excessive viscous drag in the four angular contact bearings of the gear head. To use the drives already installed on OGO-I, thermostatically-controlled heaters were mounted on these particular drive mechanisms. All other flight drive mechanisms were reworked to use a lower viscosity oil in the angular contact bearings.

4.5.4 Failure to Switch from Coarse to Fine Sun Sensors

In a thermal-vacuum test of OGO-IV, the SELA was not switching from coarse to fine error signals upon RTT stimulation. In subsequent testing it was not possible to obtain a switch to the fine signal with any of the usual stimuli. Only when the 180° lamp was operated at an over voltage of 35 V did SELA switch, and then the indication was one of a marginally low intensity.

When the spacecraft was removed from the chamber, investigation showed that the pinhole at the bottom of the RTT was almost completely obscured by the soldered end of a wire that had been snipped off and had fallen into the RTT cylinder. The RTT was cleaned and laboratory tested before being reinstalled on the spacecraft; it was also enclosed by a plastic bag cover at all times except when under actual test.

4.5.5 OPEP Driving Problem

The OGO-IV OPEP experienced severe problems in driving. It was not possible to reach the +140° limit switch. In several tests, the shaft stopped moving although the drive motor continued to drive it. When the chamber was opened, it was found that the OPEP experiment cables were interfering with the frame and the collar at the base of the bellows on each end of the OPEP. The cables were also rubbing and binding severely against the wrapping on the cupola housing. When the shaft cable and bellows collar interferences were removed, the OPEP drive operated normally.

There was some difficulty with the OGO-V OPEP. During one test, it overran a limit switch and wrapped up. It was found later that the limit switch did not operate because the dc voltage (+28 V) supplied by the DEA was missing. The OPEP wrap-up had to be replaced.

For the first three OGO's, a keyway was used to interlock the wobble gear drive output with the shaft. Sometimes the keyway was cocked and an excessive backlash developed. To eliminate this problem, the keyway was replaced by a bracket riveted to the shaft and then screwed to the drive output piece.

The S_L tests for OGO-IV and OGO-V only encountered minor difficulties. For the OGO-IV test, two successive rate gyros were rejected during the pitch channel test. The first gyro

exhibited unusually high levels of noise because it had bad bearings. The second gyro assembly would not repeat its null rate due to a sticky gimbal.

The roll gas delay times were slightly below specifications when measured during the laboratory test. However, this was attributed to partial charging of the time-delay capacitor by null offset voltages and by insufficient waiting periods for discharge between measurements.

A problem common to both OGO-IV and OGO-V testing was that of hardware delivery, especially for the DEA and ACA units. These two assemblies required the most extensive rework and were, therefore, the last to arrive. As a result, the S_L test procedure was performed out of sequence. Since the OGO-IV OPEP and Solar Array Shaft assemblies were tested in January 1967, they were returned to the spacecraft area for installation and testing well before the rest of the ACS was received. Engineering shaft assemblies were used as substitutes during testing of the ACS electronics, and a similar situation existed for OGO-V.

4.6 REVIEW OF PRELAUNCH PROBLEMS

Most of the critical prelaunch problems were discovered during the development stages of the individual ACS units. However, there were two notable exceptions.

The speed problem with the drive mechanism, due to the high viscosity lubricant, was not discovered until it was integrated into the first flight

spacecraft. Previous cold temperature testing had not shown the problem. Proper temperature testing should have detected this difficulty at a much earlier stage and in this way eliminated the need for a last-minute fix on OGO-I.

The magnetic amplifiers were not adequately tested for worst-case thermal conditions, and this resulted in a failure during flight. In this case, the qualification requirements were not stringent enough to uncover an inadequate design. The testing did not include continuous cyclic operation of the magnetic amplifiers as a worst case. During normal attitude control, the magnetic amplifiers would not operate continuously, but the original design should have incorporated this possibility.

A valuable asset of the OGO testing program was the emphasis on system tests. Early system tests in the laboratory prevented interface problems later in spacecraft integration. The separate ACS units were put together as a system as soon as engineering models were available, with the result that any incompatibility problems of the individual units were detected early and the necessary modifications were made. As an example, the chatter in the OPEP drive was observed in a closed-loop test toward the ends of 1962. This system problem was discovered and corrected before most of the prototype models were available.

In view of the flight data from five observatories, the testing procedures used for the OGO ACS have generally been effective. Except for the magnetic amplifier failure, there has been no known component failure in flight due to a testing oversight or deficiency.

5. PROBLEMS UNCOVERED IN FLIGHT OPERATIONS

5.1 OGO-I

The first OGO was launched into an EGO orbit in September 1964. The ACS initiated the acquisition phase at a predetermined time after separation from the booster; but while Sun acquisition was successful, earth acquisition was not.

5.1.1 Partial Boom Deployment Problem

The first indication of trouble occurred immediately after ACS start. Three of the horizon scanner heads indicated almost constant tracking even in Mode 2B. Obviously, the earth could not constantly be in the field-of-view of the four tracking heads while the spacecraft was rotating about its pitch axis. Later, it became clear that the horizon scanner heads were tracking the EP-1 experiment boom which failed to deploy fully. Figure 13 shows the location of the EP-1 boom before deployment and the location of the horizon scanner. Although they did not directly affect ACS operation, the EP-6 and one solar paddle also failed to deploy fully.

This "false earth" fooled the horizon scanner momentarily so that the ACS automatically switched to the normal operation mode, Mode 3. However, since operation was far from normal, the ACS almost immediately entered Mode 3A. In this mode, the wheels and gas jets are inhibited. The switch from Mode 3 to 3A took place because fewer than three scanner heads were tracking the false earth. After ex-

piration of the Mode 3A timer, the entire acquisition cycle started over.

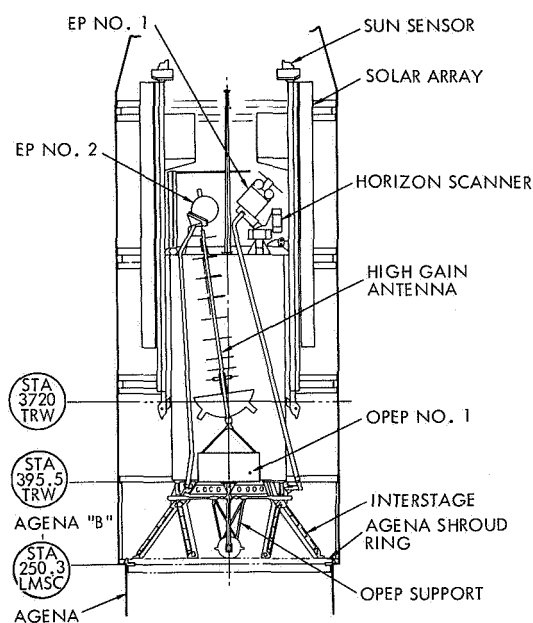


Figure 13. View of OGO Looking at +Z Side

During the second attempt at acquisition, real-time telemetry was lost for about 18 min. This loss was rather unfortunate because in the meantime virtually all control gas was expended. A tape recorder on board the spacecraft kept a record of what happened during the telemetry blackout. Evaluation of the tape recorder data proved very valuable in subsequent ACS design changes.

When ground control realized the low level of control gas, the ACS was commanded into Mode 2A. In this mode all reaction wheels and gas jets are inhibited. Of course, the spacecraft was still tumbling about some uncontrolled axis because earth acquisition had never been accomplished. Eventually, the spacecraft spin momentum was transferred to the axis of maximum moment-of-inertia (yaw axis) and OGO-I was reduced to a spin-stabilized observatory. From time to time, though, the position of the solar array has been changed in order to increase the solar energy input.

5.1.2 Corrective Action

Several mechanical changes were introduced into the boom deployment design for subsequent spacecraft. These changes have been effective and no faults have been observed.

The horizon scanner was relocated on the spacecraft to achieve a clear field-of-view with all surrounding appendages either fully folded or deployed. In investigating the horizon scanner malfunction, it was also discovered that tracking of the scanner housing might become a problem. So the field-of-view of each tracking head was reduced by readjusting the mechanical stops of the positers.

A detailed discussion of the OGO-I performance and system modifications may be found in References 18 and 19.

5.2 OGO-II

OGO-II was launched October 14, 1965, into a POGO orbit. The OGO-II ACS operated satisfactorily during the initial acquisition phase. As a precaution, ground control operators delayed earth search for about four hours while they scrutinized the tracking behavior of the horizon scanner. Once it was ascertained that all tracking indications

were due to the earth, earth acquisition began by ground command.

In Mode 3, ACS performance was excellent most of the time. However, on several occasions one of the horizon scanner heads apparently tracked a false thermal gradient over the earth's surface. At such times, the solar array departed noticeably from its expected position indicating that the spacecraft Z_b axis was being deflected away from the center of the earth. When the delinquent scanner head abandoned the false thermal gradient and returned to the horizon, a large step error in the roll and pitch control channels resulted. The control channels reacted by firing the gas jets to correct the errors. Unfortunately, the cumulative effect of these occurrences during many orbits was a serious gas loss. After 129 orbits, the control gas supply was depleted in spite of attempts to conserve gas.

The OPEP control depends upon smooth and correct earth tracking of the spacecraft. Naturally, it was disturbed during tracking lapses and resultant body motion. But, during normal ACS operation, the OPEP control channel also exhibited a small shaft oscillation which occurred at an amplitude of approximately 0.8° and a frequency of 0.4 Hz. In any event, this oscillation did not affect the basic OPEP pointing performance.

5.2.1 Tracking of Cold Clouds

The major problem of OGO-II was the erroneous tracking of cloud-covered regions on the earth. The horizon scanner is designed to sense the sudden change in temperature between the earth's edge and cold space. Similar temperature jumps appear between clouds or cloud and clear earth interfaces. In any case, the horizon scanner was tracking thermal gradients over the earth's surface besides tracking the earth's horizon.

ACS pitch and roll error signals are derived from any three of the four tracking heads which are pictured in Figure 7. If A, B, C, and D are the position angles of the respective heads, the error signals are determined from the following algorithms:

Case	Pitch Error Formed By:	Roll Error Formed By:
All heads tracking or C head not tracking	$\frac{B - D}{2}$	$A - \frac{B + D}{2}$
A head not tracking	$\frac{B - D}{2}$	$\frac{B + D}{2} - C$
B head not tracking	$\frac{A + C}{2} - D$	$\frac{A - C}{2}$
D head not tracking	$B - \frac{A + C}{2}$	$\frac{A - C}{2}$

The effect of cold cloud tracking on pitch and roll errors is illustrated in Figures 14 and 15. To explain the step changes in the pitch and roll errors, one has to consider previous ACS activity not shown in Figures 14 and 15. The first indication of false tracking came from the solar array which departed from its correct and nearly static position of about 195°. The D scanner head was viewing forward in the orbital path at that time and apparently detected some atmospheric thermal gradient near or at the true horizon. As the spacecraft proceeded in orbit, the D head tracking this gradient was led away from the true horizon. Consequently, the spacecraft's Z_b axis was pulled away from the local vertical. Figure 16 illustrates the "trapping" of OGO-I by a cold cloud.

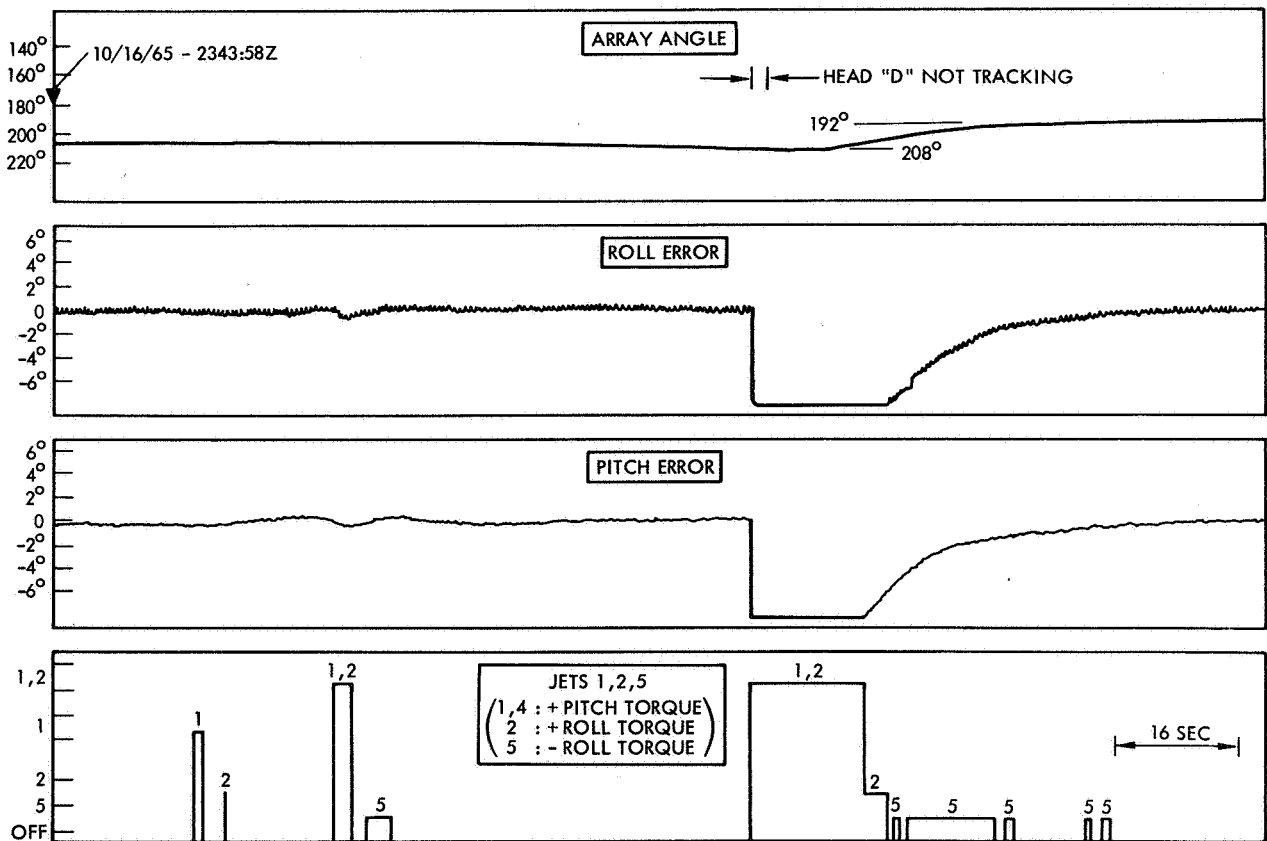


Figure 14. ACS Behavior with Scanner Head "D" Tracking Anomaly

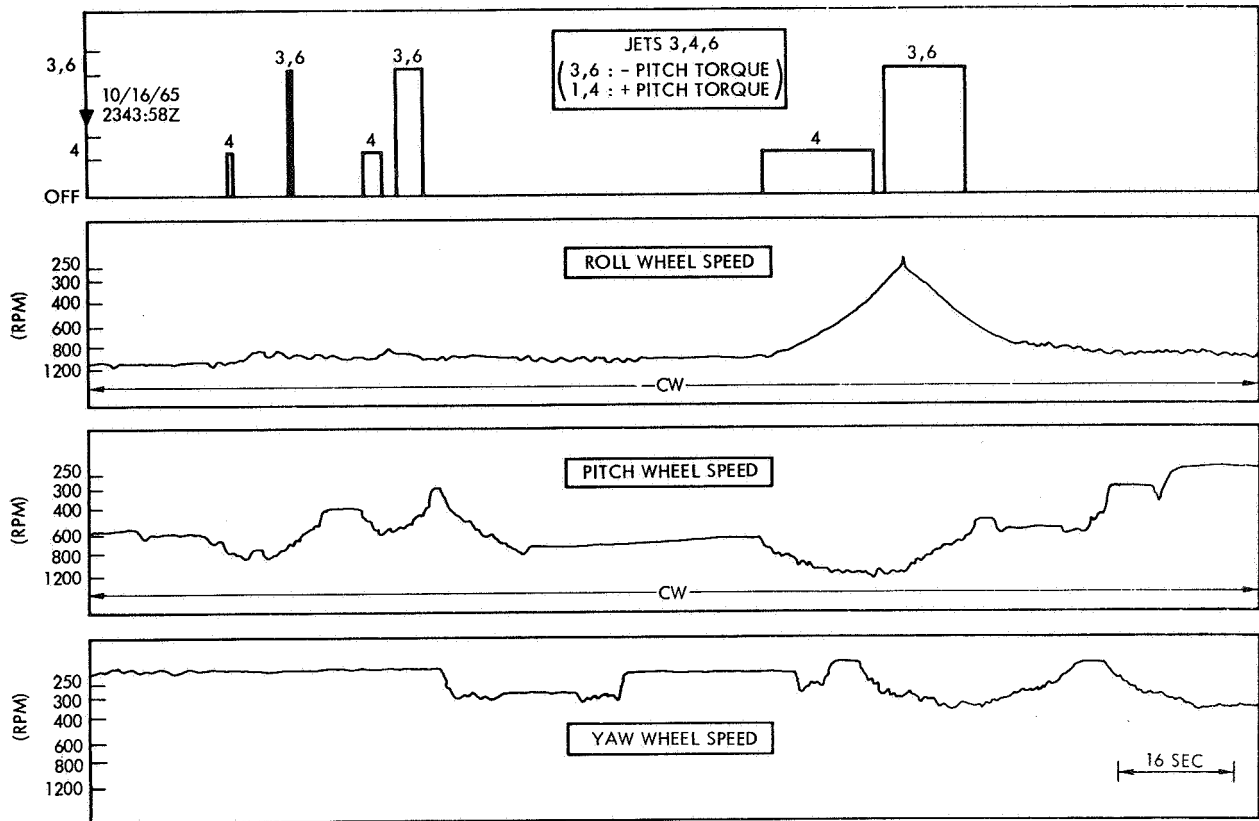


Figure 15. ACS Behavior with Scanner Head "D" Tracking Anomaly

After about seven minutes, the D head lost the false horizon and was not tracking at all for approximately two seconds. Thus, the ACS selected heads A, B, and C for error computation. Those heads were tracking the true horizon. The pitch and roll error signals suffered sudden, large changes when the true earth-pointing situation of the spacecraft was recognized. The telemetry traces in Figures 14 and 16 depict the ACS reaction to these errors. In less than 1 min, the ideal orientation of the observatory was restored.

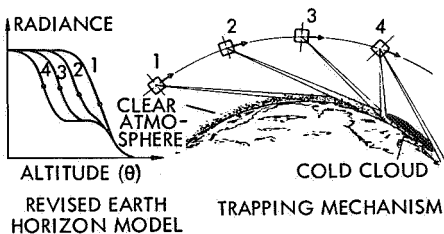


Figure 16. Revised Earth Horizon Model and Trapping Mechanism

There was considerable wheel and gas activity before the large transient. It is believed that the unsteadiness in error signals results from slight wanderings of the head as it attempts to follow an ill-defined thermal gradient. The error fluctuations were large enough to require frequent gas jet actuations because of the lead networks in the control channels. The ACS behaved as expected in the presence of these disturbances, but in the process it lost an unacceptably large amount of control gas. For example, the tracking anomaly shown in Figures 14 and 15 caused the gas jets to fire a total of about eighty-five seconds. The OGO design, with an operational lifetime of 1 year, is based on gas firings of 1 to 2 sec per orbit.

5.2.2 Horizon Scanner Modifications

An analysis of current atmospheric radiance characteristics confirmed that large variations in radiance occur at locations other than the horizon. The horizon scanner of OGO-II, with

a spectral acceptance band of 8μ to 24μ , responded to these radiance variations. It was found that a considerable improvement in the rejection of false thermal gradients could be expected by narrowing the spectral acceptance band to 14μ to 24μ . In addition, the scanning motion of the tracking heads about the horizon is biased toward space to favor the earth-space gradient over any other gradient.

The two extremes in atmospheric radiance that might have been encountered by OGO-II in its polar orbit are plotted in Figure 17. The spectral response curves for OGO-II were convolved with radiance data from Goddard Space Flight Center. As shown by these curves, the scanner may have experienced maximum to minimum radiance ratios of as much as 4:1.

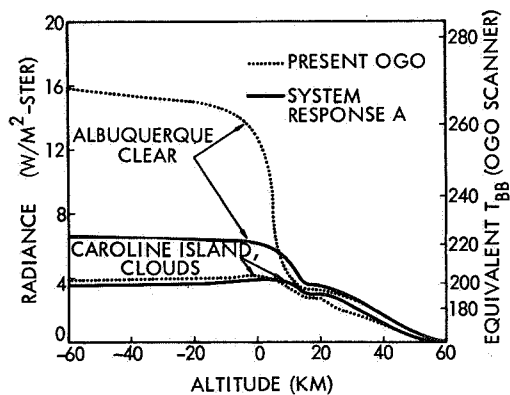


Figure 17. Comparative Horizon Radiance Profiles

The effect of restricting the spectral response to wavelengths from 14μ to 24μ is illustrated in Figure 17 by the solid-line curves. The maximum to minimum radiance ratio for this case is only about 2:1 mainly because the narrower spectral band rejects ozone radiation. Ozone radiation varies widely over different parts of the earth and has its maximum radiance in a tropical atmosphere.

Implementing the horizon scanner design changes involved installing a new lens with correct filter coatings in the scanner telescope system. For comparison Figure 18 shows both the

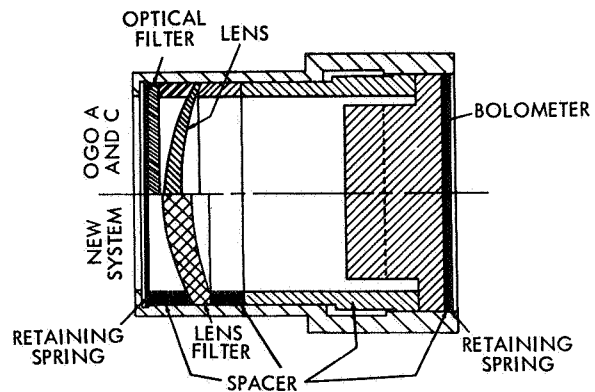


Figure 18. Telescope System

old and the new telescope systems. Note that the new system has no separate infrared filter; a coating on the lens provides the proper filtering.

The second horizon scanner modification was the offset tracking of the scanner heads. The tracking loop employs a binary level detector which detects both cold-to-hot and hot-to-cold transitions corresponding to space-to-earth and earth-to-space transitions. Detection of a space-to-earth transition reverses the positor drive voltage to drive the positor back toward space. This is followed by detection of an earth-to-space transition which drives the positor back toward the earth. The same process continues in a limit cycle at about 18 Hz. Average position of the positor is used to determine the angular position of the horizon.

If the scanner is biased in such a manner that the positor spends more time looking at space, the probability of tracking the space-earth interface is increased. For this reason, the output of the level detector was unbalanced to cause the positor to scan more toward space.

5.2.3 The "Small Earth" Problem

When OGO is in the apogee region of an EGO orbit, the earth occupies only a 4.6° arc of the horizon scanner field-of-view. The EGO orbit has an apogee of 80,000 n.mi. While the observatory is at that attitude, the

noticeable curvature of the earth, even for small attitude errors, presents a potential problem to the horizon scanner. The pitch and roll error signals, formed by certain combinations of three tracking head signals, do not always indicate the actual attitude errors.

Figure 19 illustrates the track points of the four scanner heads when a pitch and roll error exists. The pitch error signal is determined by the formula

$$\epsilon_p = \frac{B - D}{2}$$

This algorithm will give correct pitch error. However, the roll error is given by $\epsilon_R = A - (B + D)/2$ which is not equal to the actual roll error in this case. From the geometry of Figure 19, the following relation

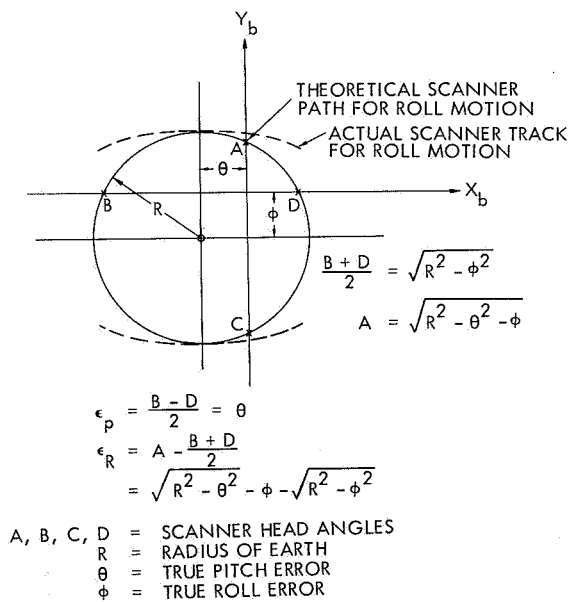


Figure 19. Computation of Errors for a Small Earth

between the computed and actual roll error is derived:

$$\frac{\epsilon_R}{R} = \sqrt{1 - \frac{(\theta)^2}{(R)^2}} - \sqrt{1 - \frac{(\phi)^2}{(R)^2}} - \frac{\phi}{R}$$

A plot of this relation for zero pitch error and an earth radius of 2.3×10^7 is shown in Figure 20. The curve reveals that for position roll errors up to 2.3° , the computed value is always less than 1° . If the roll reaction wheel should become saturated and a gas-jet firing be necessary, the spacecraft could drift off the earth without generating enough error to activate the gas jet.

In reality, the situation is not as bad as depicted by the plot in Figure 20. The scanner heads do not exactly follow the curvature of the earth. They tend to track along the path which is shown by the dashed line in Figure 19. As a result, the roll error curve is actually more linear.

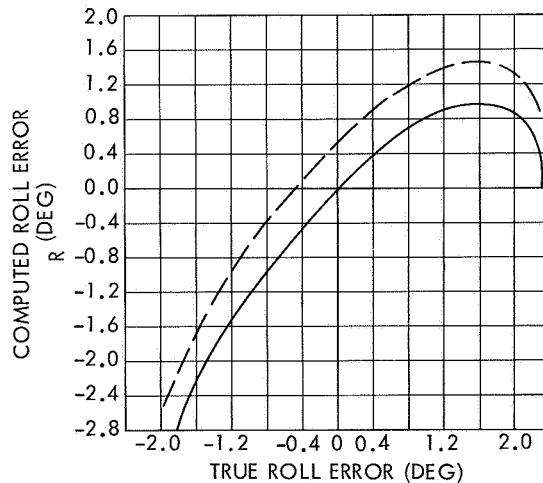


Figure 20. Computed Versus True Roll Error for 2.3×10^7 Earth Half Angle

This problem was considered in the original selection of the error signal algorithm. However, at that time the apogee attitude was only 60,000 n.mi. Subsequently, apogee was raised but the effect on scanner performance was not re-evaluated. The detailed review of the horizon scanner after the flight of OGO II revealed this potential problem. As a result, apogee of OGO III was lowered to 66,000 n.mi. Analysis and test indicated this was the maximum altitude at which a greater than 1.0° error could be generated reliably.

On the subsequent EGO (OGO V), a bias of 0.5° was added to the algorithm terms $(B + D)/2$ and $(A + C)/2$. The roll error is now computed by the formula $\epsilon_R = A - [(B+D)/2 + 0.5]$. The new curve is drawn in Figure 20 by a dashed line. Apogee was again raised to 80,000 n.mi.

5.2.4 OPEP Oscillation

As mentioned, the OPEP shaft was observed to oscillate at a small amplitude with a frequency of 0.4 Hz. Several causes for this behavior were postulated, including flexible-boom vibrations. However, since this problem was overshadowed by the more dramatic and serious problem of cold-cloud tracking, time did not permit a detailed evaluation of it. It was believed that the OPEP disturbance would be alleviated by reducing the shaft drive speed from $1.6^\circ/\text{sec}$ to $0.8^\circ/\text{sec}$. This was implemented by simply inserting a resistor in series with one of the motor windings.

5.2.5 Control Gas Time Delay

The erroneous horizon tracking by OGO II strongly affected the pneumatic system because the lead network in each control channel amplified relatively small but sudden changes in the error signal. The lead networks help to provide system stability, but gas expenditure for minor vehicle attitude excursions, which could be handled by the reaction wheels alone, is ultimately unnecessary and detrimental to the ACS performance. To prevent needless gas consumption in future

flights, gas actuation was isolated from the normal control loop by a time delay. The delay logic was provided for the pitch and roll channels and is used only in Mode 3.

The delay logic for a particular gas jet is initiated when the corresponding reaction wheel switches on. For a period of 12 sec, the gas delay logic inhibits the gas jet. If the error persists steadily with no wheel drive interruptions lasting longer than 3 sec, the delay logic enables the gas jet. If the reaction wheel is turned off for longer than 3 sec, the delay logic is reset. Otherwise, the gas jet fires after 12 sec, provided the error still exists.

This gas logic is implemented by four (\pm pitch and \pm roll) R-C delay circuits which are housed in a new electronic package, the Control Switching Assembly (CSA). The circuits receive their drive from the outputs of the reaction wheel bistable magnetic amplifiers. They inhibit gas jet firings by grounding the input to the valve drive amplifiers through a transistor switch. Figure 21 shows how the delay logic is incorporated into the control system.

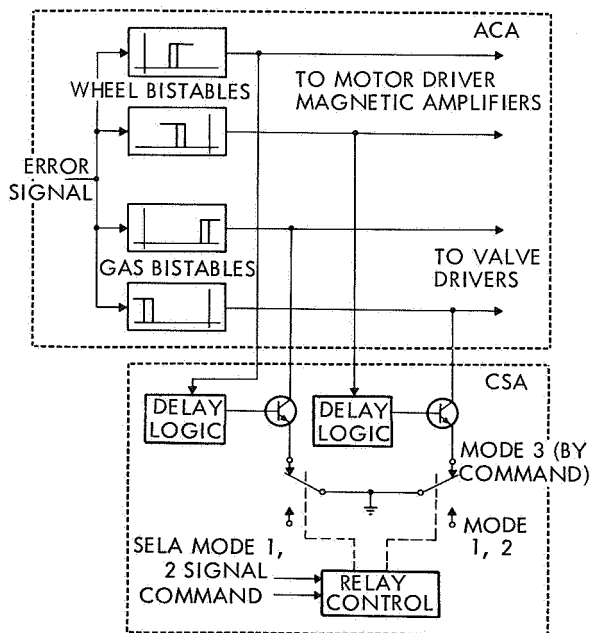


Figure 21. Typical Pitch or Roll Channel Gas Delay Logic

The delay is automatically disabled by the SELA in Modes 1 and 2 and enabled by ground command. The logic must be disconnected during acquisition as it reduces overall ACS stability significantly. For large-angle maneuvers, the delay causes a large increase in gas consumption over the normal control system configuration.

5.2.6 Backup Commands

The OGO II light experience pointed out the need for operational flexibility of the spacecraft. Ground operators should have the ability to cope with unforeseen flight problems in a more effective way. By establishing several backup modes of operation, a single ACS failure does not completely render the observatory useless. The functions of the new backup commands are:

1. Spin up the spacecraft in yaw
2. Remove ACS power
3. Slew the solar array
4. Disable the control gas jets
5. Disable the pitch rate gyro

The first three commands are intended to put OGO in a spinning mode in case of total ACS failure or at the end of the normal mission. Their operation is discussed in Subsection 2.3. The fourth command is for prevention of needless gas loss especially as a result of erratic error signals. A gas inhibit command would have been valuable on OGO-I and OGO-II. The rate gyro disable command makes Mode 2C available as a backup mode of operation in the event that earth-pointing control is lost. Normally, the gyro is employed to establish a pitch rotation of $-0.5^{\circ}/\text{sec}$. But if the spacecraft is continuously kept in Mode 2C, it is better to shut off the gyro and thus save it for future use.

A detailed discussion of the horizon scanner malfunction and modifications as well as other ACS modifications can be found in Reference 20.

5.3 OGO-III

OGO-III was launched into an EGO orbit on 7 June 1966 from Cape Kennedy. The ACS proceeded smoothly through sun and earth acquisition. For about two days ACS operation was normal and without incident. However, during the approach to the first perigee at an altitude of approximately 2800 n.mi., the roll reaction wheel began pulsing back and forth. The amplitude of this motion built up slowly until a definite limit cycle was reached with a frequency of 0.4 Hz. Soon the roll oscillation had grown sufficiently to cause the gas jets to limit cycle. The solar array control loop also started to limit cycle in sympathy with the oscillation.

As soon as ground operators noticed the gas activity, they sent a command to insert the gas delay logic. The pneumatics immediately stopped participating in the oscillation. As the spacecraft approached apogee, the roll reaction wheel limit cycle died out and then reappeared just before the next perigee. The ACS behavior followed the same pattern on succeeding orbits. The oscillation, when driven by the reaction wheels alone, was too small to affect the overall pointing accuracy of OGO seriously.

Figure 22 shows the OGO-III ACS telemetry at the time when the oscillation reappeared on the approach to perigee Rev. 002. The oscillation is hardly discernible in the roll error due to the high noise level produced by the horizon scanner dither. The array motion which is also a measure of roll oscillatory level when the roll wheel limit cycle begins.

Participation of the array drive in the limit cycle on Rev. 001 is shown in Figure 23. At the time period shown, the gas jets were also participating in the limit cycle. The oscillation amplitude was approximately $\pm 0.25^{\circ}$.

The effect of commanding the gas inhibit logic is shown in Figure 24. The telemetry has been traced here

2

RECEIVED

RECEIVED

1 kbs tape playback data

11 June 1966 Approx. 04:00Z

Flexible format 32

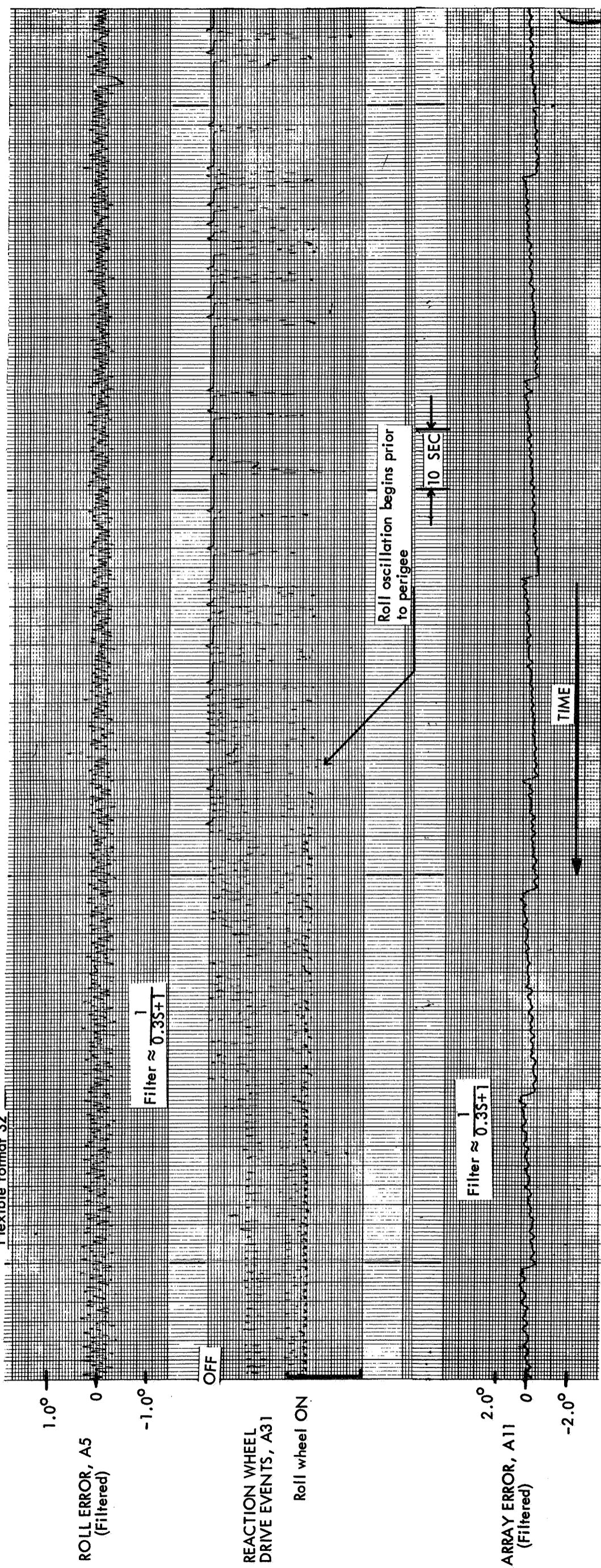


Figure 22. OGO-III Telemetry Rev. 002
 Prior to Perigee Roll Wheel
 Oscillation Begins

VOIDOUT FRAME 2

VOIDOUT FRAME 1

8 kbs accelerated subcom data
OGO III TELEMETRY DATA
REV 001 Just prior to first perigee
9 June 1966 04:37Z

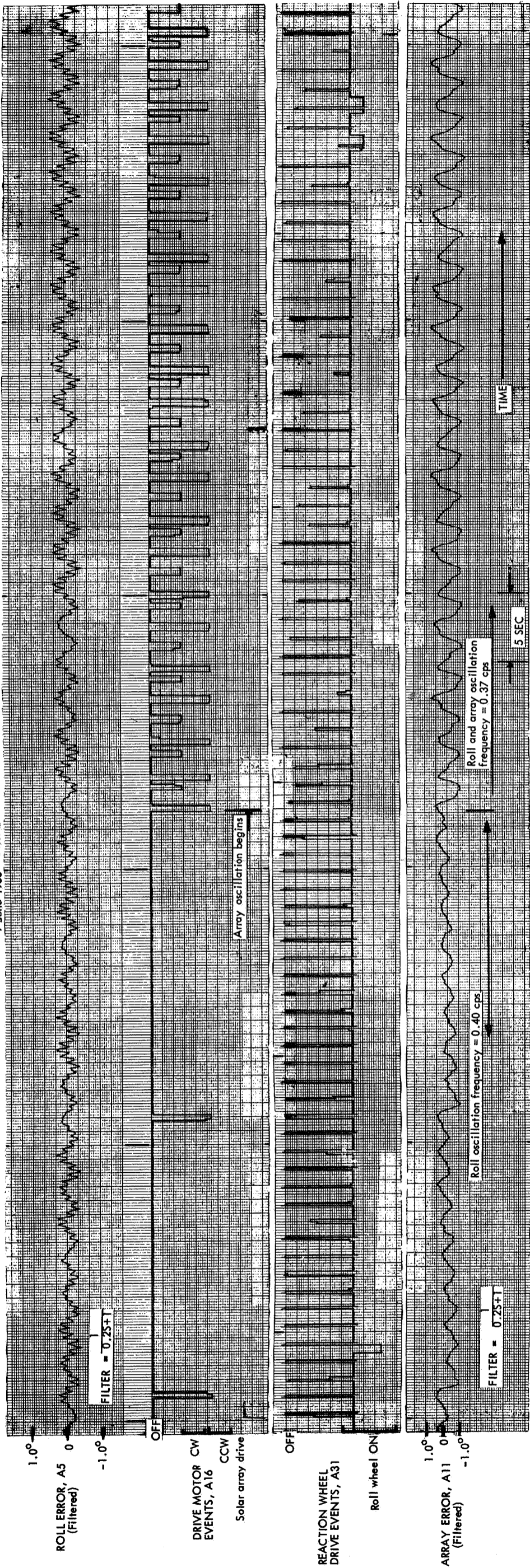


Figure 23. OGO-III Telemetry Rev. 001
Expanded Scales Start of
Array Limit Cycle

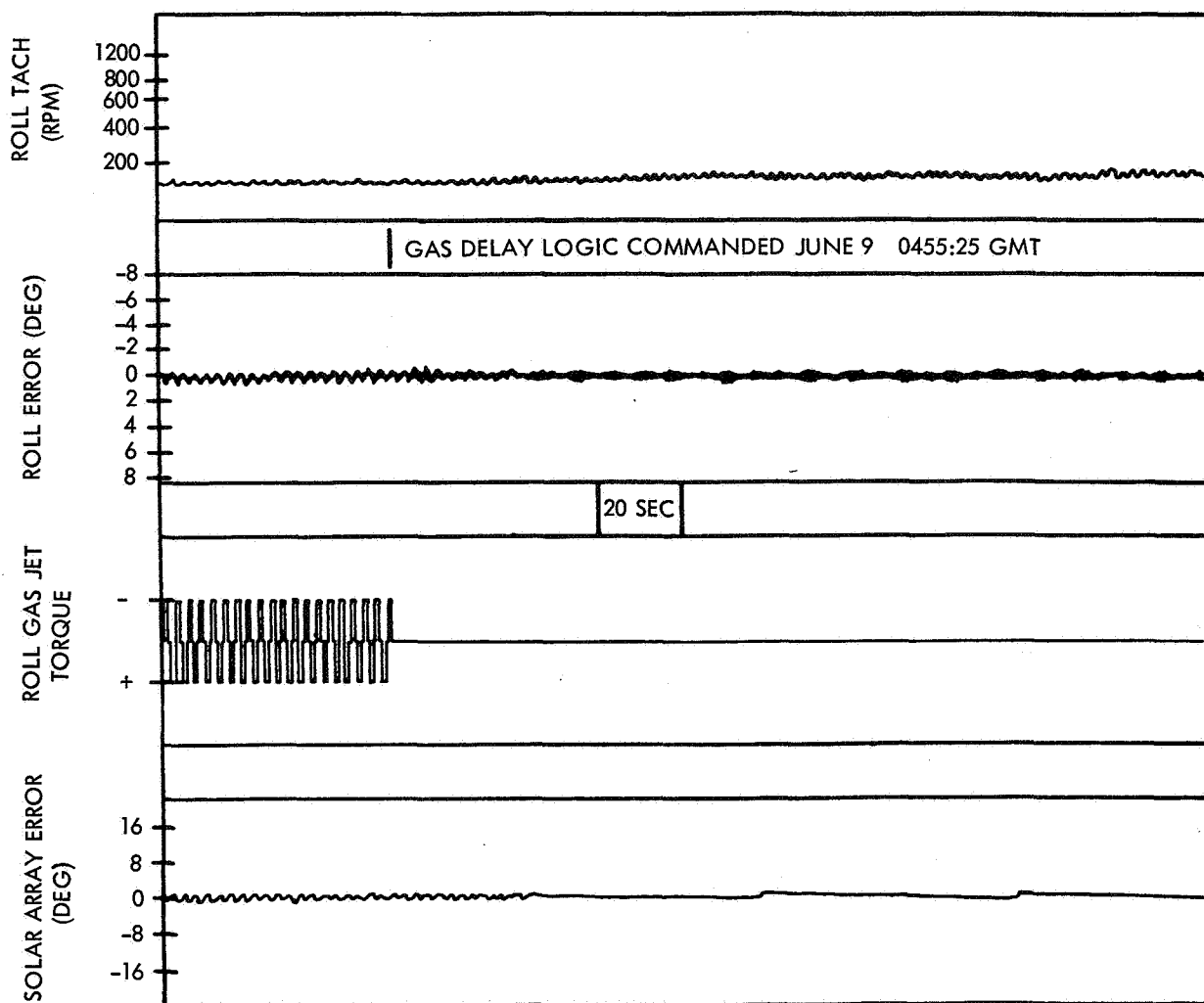


Figure 24. OGO-III Telemetry Rev. 001 Gas Delay Logic Command Event

for clarity. At this time, the oscillation amplitude was approximately $\pm 0.3^\circ$. As soon as the jet activity was inhibited, the oscillation amplitude decayed and array drive participation ceased.

Studies have confirmed that the ACS limit cycle was the result of the EP-5 and EP-6 experiment boom vibrations which rocked the spacecraft about its roll axis. The initial excitation probably came from the solar array drive system. Once the oscillation was started, it was sustained by the pulsing of the reaction wheels.

On July 23, 1966, OGO-III experienced a serious ACS failure. A roll wheel motor driver amplifier burned

out shorting the ACS inverter. Consequently, the spacecraft lost earth stabilization. It was concluded that the high duty cycle in the roll channel due to the boom oscillation accelerated the failure of the magnetic amplifier. Later tests indicated that the magnetic amplifier had inadequate thermal and magnetic core design for continuous alternating duty cycle operation.

High duty cycle operation was not, however, a normal or an expected operating condition. On the other hand, a motor-driven amplifier had burned out under similar operating conditions during early reaction-wheel life tests. Unfortunately, the failure was not analyzed because the operating conditions were considered abnormal.

5.3.1 Redesigned Magnetic Amplifiers

The magnetic amplifiers were redesigned to provide for a better heat flow, and the core design was improved to withstand the high duty cycle conditions. The wire for the new windings can withstand a temperature of 220° C as compared to 105° C for the wire used in the old design. The magnetic amplifiers were tested under worst-case power load conditions in a vacuum. Test results showed that the old magnetic amplifiers fail after operating for a period of 2 to 3 hr and the average wire temperature goes up to about 180° C. On the other hand, the wire temperatures of the redesigned magnetic amplifiers stabilized at less than 60° C. Thus, the new thermal design has a substantial safety margin.

5.3.2 ACS Design Changes

The problem of boom oscillations or interaction with the control system was considered during the design phase (see Subsection 4.2). There was a basic fault with the data used in the analysis, however. Tests of the boom had shown that for large amplitude deflections (several inches) the structural damping was 1% to 2%. That value was used in the analysis. However, the amplitudes of motion which cause control system interaction are only a few tenths of an inch. Analysis of flight data indicated that the structural damping of the OGO-III booms was actually less than 0.5%. The low damping was the result of very low stress in the booms at low amplitudes. Consequently, structural hysteresis was very small.

The original analyses of boom interaction were simply response studies. The boom response to ACS torque disturbances was determined and found to be negligibly small. The analysis did not, however, consider the solar array coggling as an input. Finally, no stability analyses were made of the ACS with flexible booms. Had these analyses been made, the sensitivity of the ACS stability to boom damping might have been recognized. Analysis performed after the OGO-III flight showed that, with low-boom damping,

both the reaction wheel and gas jet control loops would sustain a "hard" limit cycle. In conjunction with low-boom damping, the cause for the instability or limit cycle was the sizable phase lag through the low-pass horizon scanner dither filter at the boom frequency.

Increase of Boom Damping

Methods of increasing boom damping were evaluated, including tuned dampers mounted at the boom end and visco-elastic tape wrapped around the boom. The tape was put on the OGO-IV booms without apparent improvement in boom damping. The effectiveness of the tape material is highly dependent upon its temperature. Thermal design was improved for OGO-V and a significant reduction in boom motion has been observed.

Wheel Delay Logic

Redesign of the ACS filter to stabilize the control system was found impractical. Thus, to prevent ACS participation in boom oscillations, a "wheel delay logic" was added to the roll and yaw control channels (Figure 25). The delay logic makes the reaction wheels unresponsive to oscillatory error signals with periods less than 10 sec. For example, assume an oscillatory error signal is alternately turning on the bistables. When the (+) bistable is turned on, the transistor switch opens the ground path for the (-) signal. Now even if the (-) bistable turns on, no ac power is supplied to the reaction wheel. Turning off the

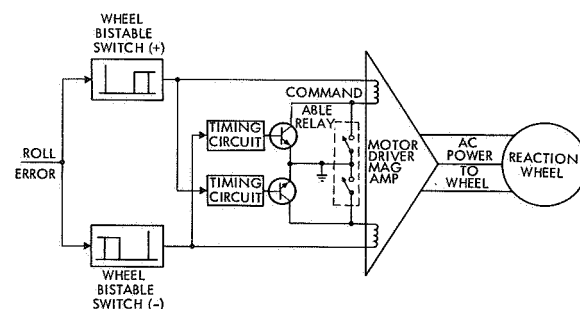


Figure 25. Reaction Wheel Delay Logic

(+) bistable initiates the timing circuit. For 5 sec, negative error signals have no effect on the reaction wheel. But a negative error (-) will also flip on the (-) bistable which opens the ground path for a (+) signal. Thus, a similar 5-sec inhibit occurs on the (+) side. Unless the bistables switch slowly enough to "outwait" the 5-sec delay, the reaction wheel remains unactivated.

Uni-directional inputs to the wheels are not affected by the wheel delay logic. The gas delay operation is also unaffected. Both the wheel and gas delay logic must be turned on by command in Mode 3. They are automatically removed by return to Mode 1 or 2.

Yaw Channel Changes

A stability analysis of the yaw control channel indicated that the gain and phase margins for the reaction wheel system were adequate. Nevertheless, a wheel delay logic was included in the yaw channel in order to forestall any possible sustained oscillations. On the other hand, the phase margin for the pneumatic system was small. Therefore, the deadzone of the yaw pneumatic bistable was doubled.

Solar Array Drive Changes

As stated earlier, it was believed that the solar array drive initially excited the boom oscillation. Moreover, at times during the flight of OGO-III, the solar array control loop participated in the roll oscillation by driving back and forth at the oscillation frequency.

A study was made of possible modifications to the solar array drive system which would prevent its participation in the boom oscillation. Chosen from several alternatives was a time delay scheme identical to the one used in the roll wheel channel. The delay may be commanded on or off independent of the ACS mode.

An analog computer study of the solar array control loop resulted in another change in this system. Using

the worst allowable set of loop parameters, the response of the control system to an initial 0.5° error was determined. Under these conditions a limit cycle occurred. The limit cycle was due mostly to the backlash in the drive mechanism. When the bistable deadzone was changed from 0.5° to $0.9 \pm 0.1^\circ$, the solar array loop response was satisfactory.

Two mechanical changes also were made to the drive assembly to reduce the backlash. One change was to firmly attach the output drive gear to the shaft and in this way replace a key which was subject to wear. The second alteration was an array hinge redesign to reduce its backlash.

OPEP Design Changes

The OPEP participated in the roll oscillation because the OPEP gyro sensed the roll motion. Since the boom motion could not be entirely eliminated, a filter was devised to smooth the bending signal from the OPEP error. It was assumed for design purposes that the largest magnitude of body-roll rate would be only one-half the value observed on OGO-III because of the wheel inhibit logic.

The large phase lag, introduced by a simple low-pass filter, presented a stability problem. It was found that a feedback from the bistable output to the filter input stabilized the control loop. Figure 26 is a block diagram of the modified OPEP control loop.

The addition of the feedback loop and the lag filter actually forms a pulse ratio modulator. If a constant error input is applied from the gyrocompass, the drive motor operates in a pulsed fashion.

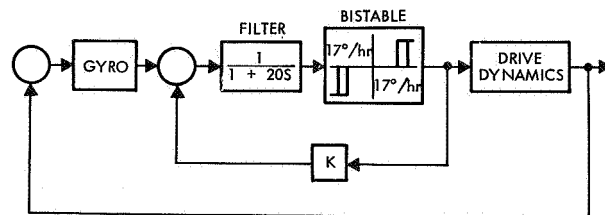


Figure 26. New OPEP Control Loop

Sun Interference

The problem of sun interference with horizon scanner operation was treated in the original design by providing sun alarm circuits for each scanner head. The sun presence is detected by observing the output level of an amplifier which processes the scanner bolometer output. This same amplifier output is also used to indicate earth tracking. Usually for sun tracking the output level is higher, and in this way the scanner can discriminate against the sun. In addition, the yaw axis null was biased 1.6° so that the C scanner head would not "see" the sun under sunrise and sunset conditions.

Although the problem of sun interference was re-examined during the horizon scanner redesign after OGO-II, no design changes were made at that time. The next spacecraft, OGO-III, was to be an EGO, and very few eclipses occur during a year's life.

A unique method was developed for testing the scanner behavior when it sees the sun. To simulate the sun's spectral response normally requires elaborate simulation techniques. The technique developed used a clear lens in the bolometer telescope in place of the coated lens (see Figure 18). The sun radiance could then be simulated by a simple electric heater coil which was masked to simulate sun diameter. Appropriate adjustments were also made to targets used to simulate the earth-space temperature gradients.

Tests performed using the above techniques showed that when the sun appeared in the edge of the bolometer field-of-view, insufficient radiance was received to trigger the sun alarm. The phenomena occurred when the sun was from 1.2° to 3.5° from the center of the scanner field-of-view. The 1.6° offset of the C scanner head from the sun line placed it squarely in the region where no sun alarm would occur though it could track the sun. It should be kept in mind that normally the C head is redundant and used only if any one of the other three heads fails. But in case of a scanner-head failure,

the sun tracking by the C head could lead to unnecessary gas consumption much in the same manner as the cold-cloud problem observed on OGO-II.

After a study of the sun interference problem, it was concluded that an A-C scan plane rotation of 5.8° away from yaw null and removal of the yaw axis 1.6° offset would clear the sun from the C head field-of-view. The A scan plane had to be rotated anyway because the field-of-view of head A was partially obstructed by OPEP. This was caused by an increase in the size of the OPEP experiment package for OGO-IV. Figure 27 illustrates the A-C scan plane rotation.

Since sun reference is lost during an eclipse, the yaw error could actually be quite large at the time of emergence from the eclipse. In that case, other heads might briefly track the sun as the yaw rotation of the post-eclipse turn sweeps the heads about the horizon. This causes a jump in the scanner track point which can fire gas. It was found, however, that if the gas delay were 15 instead of 12 sec, virtually all gas firing would be prevented during reacquisition. For this reason the gas time delay was increased to 15 sec for OGO-IV and subsequent spacecraft.

Reference 21 gives a detailed discussion of ACS design changes, and Reference 22 gives the hardware design change details made after OGO-III.

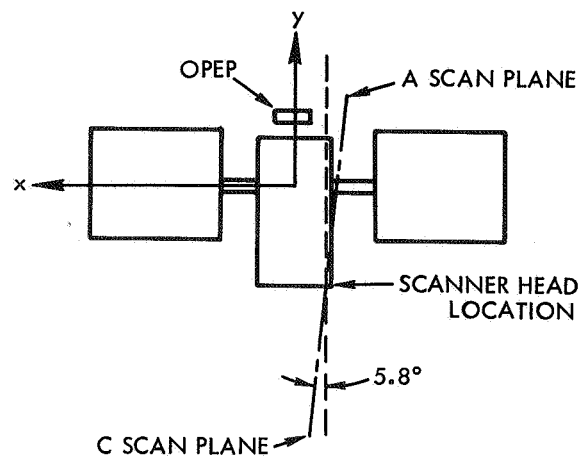


Figure 27. A-C Scan Plane Rotation Geometry

5.4 OGO-IV

OGO-IV was launched into a POGO orbit 28 July 1967. The initial operation of the OGO-IV ACS was satisfactory. The EP-5 and EP-6 booms, which caused trouble on OGO-III, occasionally induced a roll oscillation but the wheel delay logic effectively prevented a reaction wheel limit cycle. For about 40 revolutions, OGO-IV looked like a complete success.

On the 42nd orbit, the Rosman tracking station reported a pitch oscillation with a period of approximately 40 sec. The oscillation frequency immediately put under suspicion the 60-ft antenna mounted on the -X SOEP package. The antenna motion was not restricted to one plane and its vibration coupled into the pitch and yaw channels. The oscillation grew in amplitude until the gas system participated in the limit cycle. At that time, the gas jets were inhibited by command.

The growth of the oscillation can be observed in the flight data traces of Figure 28. On Rev. 042, the amplitude was low and the gas jets were not engaged. The Rev. 083 data is typical of the oscillation which has persisted for nearly a year on OGO-IV (gas jets disabled). Gradual increases and decreases of the oscillation amplitude are indicative of the antenna motion coupling from the pitch to yaw axes and vice versa.

5.4.1 Operation by Ground Control

The oscillation continued steadily with the participation of the pitch reaction wheels. There is no wheel delay logic in the pitch channel. In any case, a 5-sec delay would not be long enough to inhibit the wheels. Even the 15-sec pitch gas delay was ineffective for this slow oscillation, and the gas had to be turned off completely. However, periodic gas jet firings are needed to desaturate or "unload" the reaction wheels.

Normally, when the average wheel speed reaches the saturation region, sufficiently large attitude errors develop to fire gas. The gas pulse imparts

angular momentum to the spacecraft which is eventually transferred to the reaction wheel. Typically, the wheel momentum is reduced by about one-third of its momentum storage capacity in this way.

Since the gas jets had to be disabled for OGO-IV, a scheme for unloading the reaction wheels by ground control was developed. The spacecraft with relatively large roll and/or pitch reaction wheel speeds is first commanded into the ACS Mode 2A. Attitude control is inhibited in that mode and the wheels run down naturally due to windage and friction. Their angular momentum is transferred to the satellite body. In response, the roll and/or pitch axes develop attitude errors. When these errors are deemed large enough, the ACS is commanded back into Mode 3 with control gas disabled. After the lead networks have recovered from the mode switching transient, the gas jets are enabled for a definite time period. The remaining error signals generally are large enough to engage the appropriate gas jets. In the meantime, the wheels are back at their original high speed and the gas pulse, if it is applied in the right direction, dumps part of the total momentum stored in the wheels.

A second method which utilizes the yaw spin command is also used. Normally, when the yaw spin command is sent, the gas jet is activated by a timer which pulses the jet for 5 sec. This firing is too long since it changes the spacecraft momentum by an amount greater than the total pitch or roll wheel momentum storage capability. To reduce the yaw jet firing time, the yaw spin command is sent; a second or two later, the ACS Power Off command is transmitted. This removes power to the valve drivers turning off the yaw jet. When the timer has expired, the ACS is reactivated and normal control is resumed.

The time for dumping the wheels is determined from a time history of the wheel momentum build-up. Frequency of wheel unloading varies from once nearly every revolution to once every

REV 042
DATA STORAGE
ACCELERATED SUBCOM 2

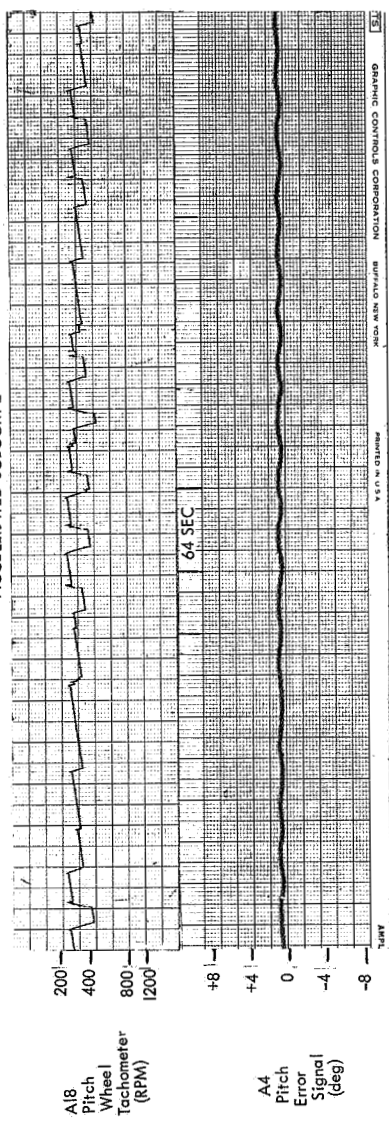
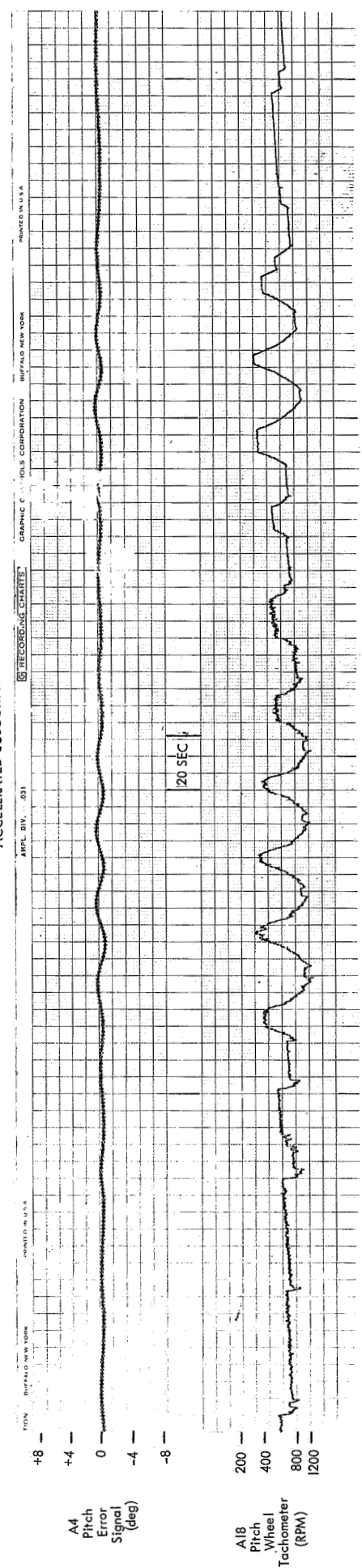


Figure 28. Telemetry of OGO-IV
SOEP Antenna Oscillation

REV 083
DATA STORAGE
ACCELERATED SUBCOM 2



15 revolutions. Since ground-station coverage is limited by virtue of the low-altitude orbit, personnel have been dispatched to remote ground stations to perform the unloading procedure.

Manual operation of OGO-IV in this way has saved a spacecraft which otherwise would have been doomed to a short lifetime of useful operation. Tape recorder data has been indispensable. Flexibility in operation by ground command, though somewhat limited, has been absolutely necessary. In fact, as a result of the OGO-IV experience, provision for individually disabling the roll, pitch, or yaw gas jets has been incorporated on OGO-F. In addition, commands will be provided for individually firing any axis gas jets in 1-sec bursts. A detailed discussion of the OGO-IV spacecraft performance and operations is given in Reference 23.

5.4.2 Source of OGO-IV SOEP Antenna Oscillation

During the OGO-III redesign, the problem of boom flexibility was given a great deal of attention, including the low-frequency antenna. Both stability analyses and analog simulation studies were made of the ACS, including all flexible appendages. These studies indicated that the system response was not highly damped at the antenna frequency, but there was no indication of a source of sustained limit cycles. Thus, the source of the oscillation remained a mystery until the spacecraft entered its first eclipse some twenty days after launch.

The oscillation on OGO-IV stopped when the vehicle entered eclipse. This observation led to the conclusion that the oscillation was thermally induced by the sun. A computer simulation confirmed the likelihood of thermally-induced boom vibration as the cause for the OGO-IV behavior. The following explanation is an attempt to construct a plausible physical model for the boom's "solar flutter."

The SOEP antenna, a STEM boom manufactured by Spar Aerospace Products Ltd., consists of an open tubular structure made of rolled-up, 2-in. -

wide, beryllium-copper strip. Under solar heating, a temperature difference is developed between the sun and anti-sun facing sides of the boom which causes it to bend. As the boom bends, it also rotates because of the shear center offset, and thereby exposes some of its cooler side to the sun. Consequently, the temperature gradient is reduced, and the boom tends to straighten out. Then the temperature difference increases again and the cycle repeats itself.

A considerable amount of study on the thermo-elastic effects of booms has taken place since the launch of OGO-IV. An initial attempt at modeling the phenomena is documented in Reference 24. While the thermal model indicated some general trends, significant inaccuracies were found. Reference 25 presents a detailed analysis of static thermo-elastic effects. An extension of this work to dynamic conditions is currently under way.

It must be pointed out here that OGO-I and -III had 30-ft antennas and OGO-II had a 60-ft antenna. OGO-I had a motor-driven deployment mechanism which failed to extend the antenna more than a few feet. The antenna on OGO-II was not deployed until nearly all the ACS gas had been depleted. Therefore, there was only a brief period of Mode 3 operation and no oscillation was observed in the flight data. On OGO-III, the antenna was deployed soon after earth lock was achieved. While the period of Mode 3 operation was cut short by the magnetic amplifier failure, again no oscillation was detected. Thus, OGO-IV was the first spacecraft to have flown with the 60-ft antenna with any extended period of normal Mode 3 operation.

The flight experience of OGO-III and several analytical studies indicated that shortening the SOEP antenna would alleviate the oscillation problem. Current improvements in boom design which increase torsional rigidity and/or bending stiffness were also considered. However, time did not permit qualification of the new booms prior to the OGO-V flight. Therefore, OGO-V has two 30-ft booms, one on each solar paddle. The second antenna was added for another experiment.

5.4.3 Moon Tracking

The OGO-IV flight has vividly demonstrated another extraneous source of gas consumption. When the sun, earth, and moon are approximately in the same plane and the moon is fully illuminated, the A scanner head tracks the moon. As the moon rises above the earth's horizon after eclipse, it pulls the A head off the earth's edge. Eventually, the scanner loses track of the moon, but not until a large roll error has developed. The recovery to correct earth pointing is a potential source of significant gas usage. On OGO-IV, the gas is disabled so no gas is lost.

Moon tracking produces nearly pure roll motion since the A head is used only to compute roll error. Figure 29 shows the relative positions of the moon, sun, earth, and spacecraft for moon tracking. Note that the moon is fully illuminated by the sun. As the spacecraft proceeds in orbit, the moon appears to be rising above the earth's horizon. OGO-IV flight data indicated that the A scanner head may remain locked on the moon until the moon is as much as 35° above the earth's horizon.

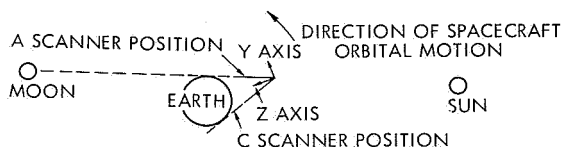


Figure 29. Moon-Earth-Sun Spacecraft Positions for Moon Tracking

The conditions which favor moon tracking occur much more frequently in a POGO orbit than in an EGO orbit. With the rather low probability of moon interference for an EGO orbit, the possible gas consumption from this disturbance is slight. In contrast, for a POGO orbit it is estimated that moon tracking might consume 16% of the available gas supply during the operational lifetime of the observatory.

The proposed solution to the moon-tracking problem is an individual gas jet control for OGO-F (not launched yet). When moon interference occurs from the A head, the spacecraft should be operated with the roll gas inhibited. Since it is possible to predict the periods when moon tracking is most likely, operation in this way should not be difficult.

5.5 OGO-V

OGO-V, launched 4 March 1968, is the first spacecraft which has completely met or exceeded all ACS specifications outlined in Section 2.

Improvements in the thermal design of the visco-elastic tape on the EP-5 and EP-6 booms has apparently improved boom damping. EP-5 motion on OGO-IV has been observed by the magnetometer experimenter to be as much as ± 1.5 in. whereas the motion is less than 0.25 in. on OGO-V.

The 30-ft experiment antennas on OGO-V did exhibit a low-level sustained oscillation immediately after deployment. The motion could not be detected in the pitch error signal because of the extremely low amplitude. However, by rotating the OPEP shaft so that the OPEP gyro measured body pitch rate, the effects of the boom motion were observable.

Figure 30 shows the pitch reaction wheel tachometer and the OPEP error before and after deployment of the antenna on the -X solar paddle. The OPEP shaft was at approximately -80° . Before deployment, the OPEP error telemetry shows the sawtooth variation in pitch rate due to normal reaction wheel limit cycles. Ten minutes after boom deployment, a sine wave with a period of 14.0 sec and amplitude of $\pm 0.02^\circ/\text{sec}$ is superimposed upon the sawtooth pitch rate variations. The period is near the predicted value for the 30-ft boom. The angular rate corresponds to a pitch angular motion of approximately $\pm 0.045^\circ$ and a boom tip motion of approximately ± 0.75 ft. Fifty minutes after deployment, the

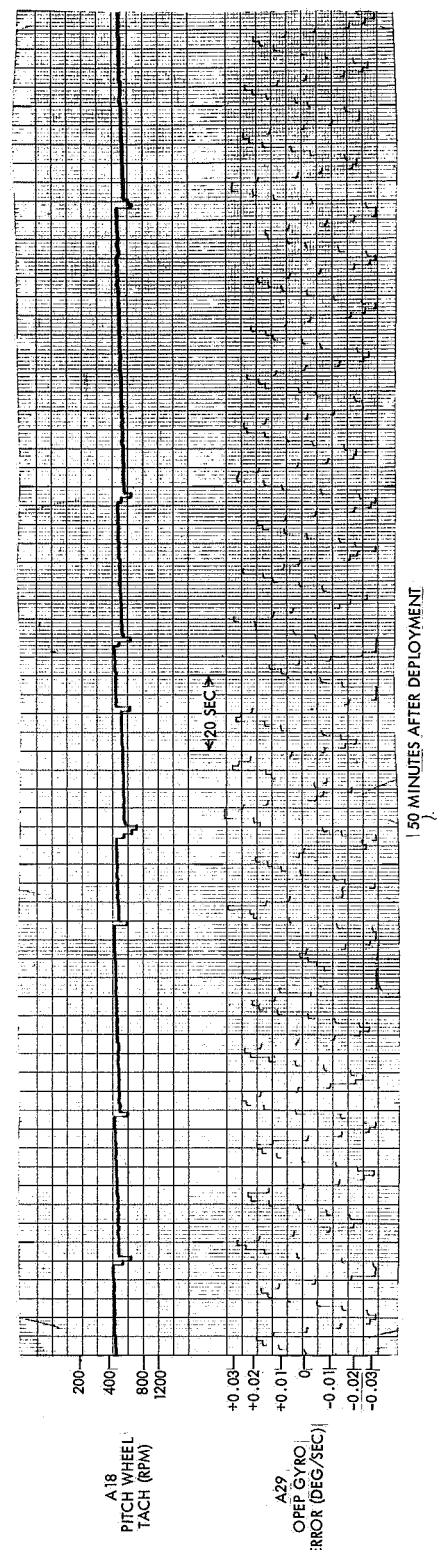
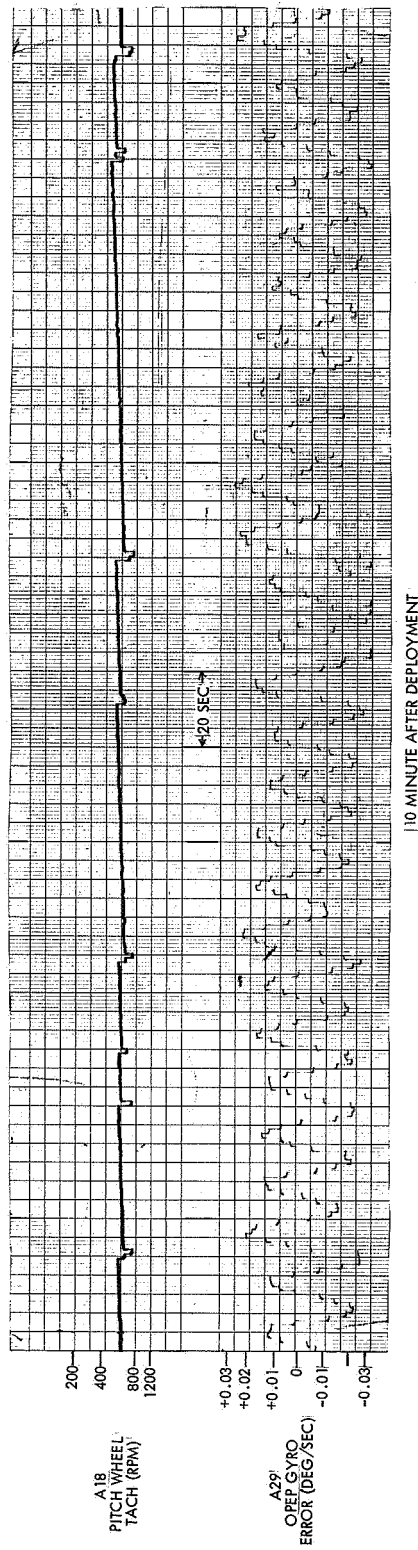
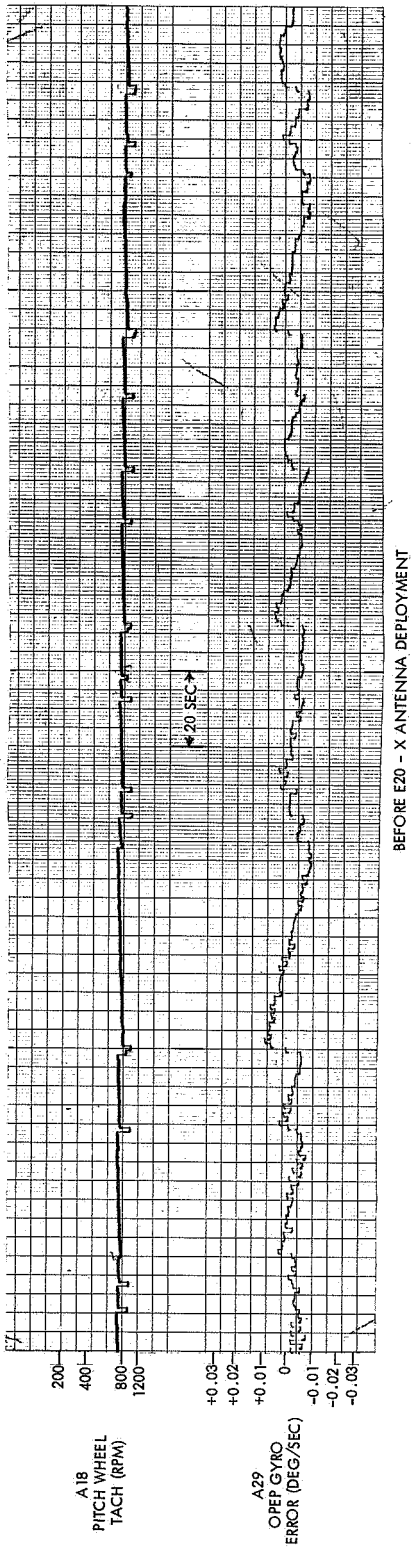


Figure 30. Telemetry of OGO-V -X SOEP Antenna Oscillation

oscillation amplitude increased slightly. On one occasion the pitch wheel actually drove downward on a positive rate peak. The oscillation persisted until the spacecraft passed into eclipse approximately five hours later. After leaving eclipse, the oscillation reappeared but completely died out within 1 hr. From that point until the +X antenna deployment, no oscillations were observed.

The pitch reaction wheel tachometer and OPEP error before and after deployment of the +X antenna are shown in Figure 31. (Note that the sample rate of OPEP error in Figure 31 is much lower than in Figure 30.) Prior to deployment of the +X antenna, the OPEP error was quiet. A portion of the pitch tachometer data taken after deployment is shown in Figure 31. While no "hard" wheel limit cycle exists, the wheel pulsing during the normal rundown type of limit cycle tends to occur in a periodic fashion with a period of 13 sec. The OPEP error trace also indicates an oscillation existed. Although obscured somewhat by the sample rate, the oscillation appears to be larger in magnitude than after the -X antenna deployment, but with both antennas deployed, this is not surprising.

The oscillation persisted again to perigee, but ceased shortly after the end of eclipse. Figure 31 also shows the OPEP error at approximately 1640 GMT, 17 March, about two hours after the end of eclipse. On occasions, some small 13-sec period motion can be observed in the data, but no sustained oscillation appears. The two bursts of activity seen in the data are due to array drive activity.

5.6 REVIEW OF IN-FLIGHT PROBLEMS AND RELATION TO DESIGN APPROACH

The major difficulties encountered in the first four OGO flights lie in the area of attitude control. So far only OGO-V has acquired and maintained the specified orientation in a completely satisfactory manner. The attitude control systems in the first four OGO's

operated as designed, but were not designed to handle all the disturbances experienced in orbit. The ACS deficiencies primarily go back to the design concept stage.

The history of OGO-I, -II, -III, and -IV offers a unique succession of flight problems. Each failure prevented the next one from being observed. On OGO-I, the experiment boom blocking the field-of-view of the horizon scanner made it impossible to discover the cold-cloud phenomena. On OGO-II, tracking of cold clouds was responsible for the premature depletion of all control gas, and attitude control terminated before the magnetic amplifier could overheat and fail. On OGO-III, continuous operation of the roll magnetic amplifier caused it to burn out because of its poor thermal design. All these design problems were present in OGO-I, but it took three OGO flights to detect them. The thermally induced oscillations of the OGO-IV SOEP antenna were also not detected in earlier flights. Although OGO-II flew with a 60-ft antenna, Mode 3 control was maintained for only a short period after the SOEP antenna deployment and the antenna oscillations were not detected. The shorter antenna flown on OGO-III did not exhibit the thermal instability.

Two malfunctions occurred as a result of inadequate designs for a specified performance: the partial deployment of the experiment boom EP-1 and the magnetic amplifier failure.

The other major flight problems arose from obscure and mostly unpredictable sources. Cold-cloud tracking and thermally induced boom oscillations certainly were not well-known phenomena before they were revealed by OGO experience. Consequently, no one anticipated these problems. The saving factor for both OGO-III and -IV was the increased capability of the spacecraft to handle unforeseen disturbances by ground command. The need for control flexibility is greatest in the first launch because at that time

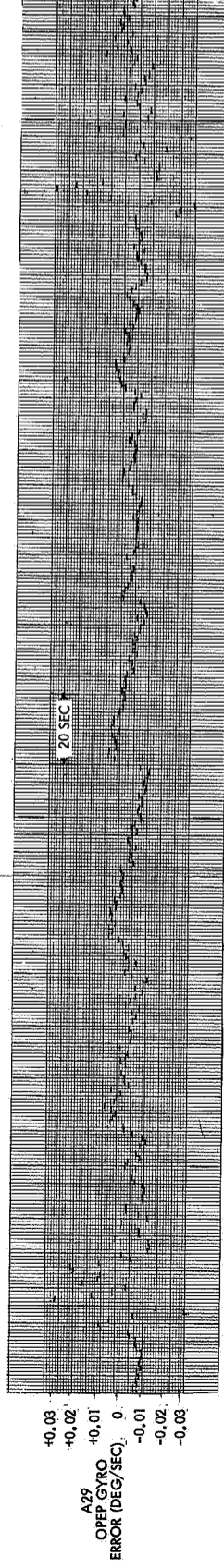
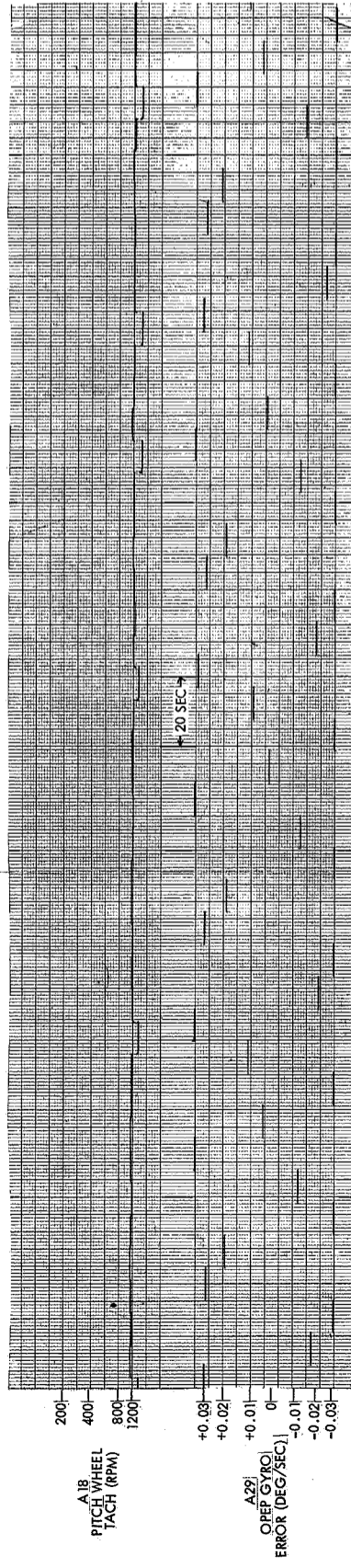
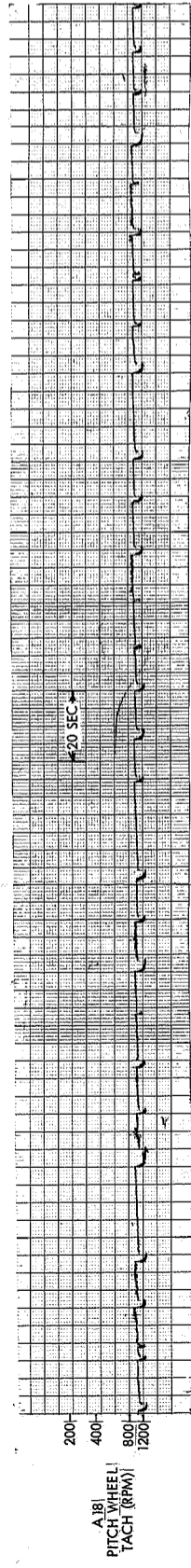
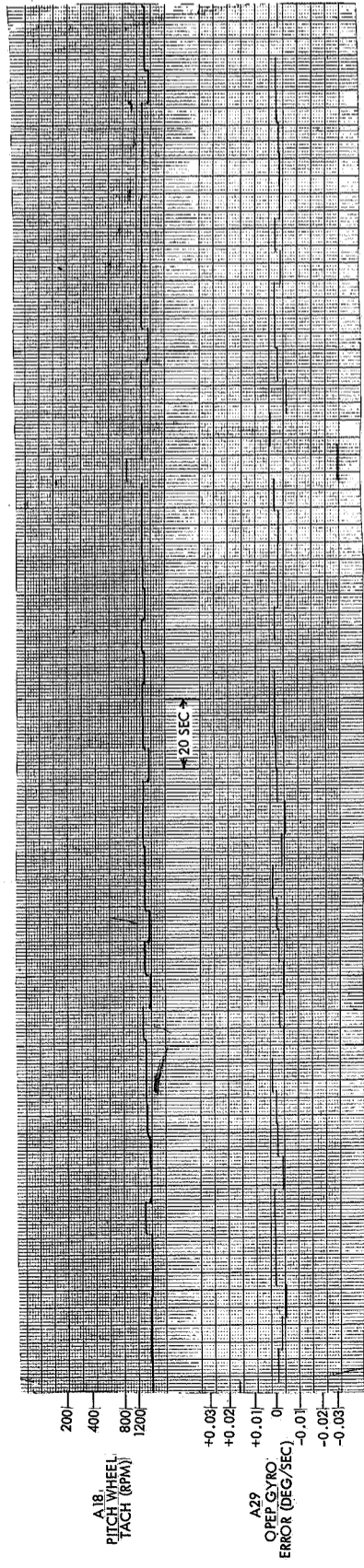


Figure 31. Telemetry of OGO-V +X SOEP Antenna Oscillation

the least information about possible difficulties is available. OGO-I was visualized as a fully automatic spacecraft. The observatory deployed automatically over Darwin, Australia, and then tumbled into an uncontrolled spin with subsequent data noise that complicated ground operations at Greenbelt.

The OGO-I experience impressed the need for real time data of crucial spacecraft maneuvers. One common plague of the first four OGO spacecraft was excessive use of gas. If close watch is not kept on flight operations, gas may be wasted rapidly by transient disturbances. To prevent unnecessary gas consumption, a clear picture of all significant flight data must be available. Good data is the prerequisite for successful manual intervention in spacecraft attitude control.

Another feature of the telemetry system design which proved very valuable for OGO was the tape recorder

on board the vehicle. Certain parts of the orbit, particularly POGO, are not visible from a ground station, but during that time the tape recorder took data which was played back later. The recorder data was indispensable in analyzing spacecraft behavior.

No failure in orbit was traceable to a ground testing oversight; i. e., ground testing eliminated all obvious malfunctions before the launch. The integration and test function had apparently been performed well. The shortcomings that troubled OGO stem from sophisticated errors of concept rather than detail and from insufficient dynamic simulation. However, one cannot blame the designer for not anticipating problems beyond the state of his art. A logical countermeasure against such unpredictable disturbances is to equip the spacecraft with several manual back-up modes of attitude control operation. This is the most important lesson derived from the orbital experience of OGO.

6. NEW CONCEPTS

6.1 ACS INNOVATIONS

6.1.1 Wobble Gear

The wobble gear drive mechanism developed by TRW was a completely new application of this form of drive. The original principle of the wobble gear was used in an agricultural machine of the 1800's. However, application of the principle to a sealed drive unit suitable for use in space was a new technology.

Reliability of the unit has been excellent. None have failed on orbit. The solar array drive on OGO-I is still periodically activated to reorient the solar arrays. It has been in the space environment nearly four years.

6.1.2 Bang-Bang Reaction Wheel Control

The concept of gas jet and reaction wheel control of a spacecraft was developed by NASA's Goddard Space Flight Center. It has since been applied to other observatory class programs (i. e., Nimbus and Orbiting Astronomical Observatories). The concept of using the wheels in an on-off or bang-bang control mode was developed and implemented by TRW, however, and has subsequently been applied to other programs.

The primary advantage of the on-off wheel control approach is a conservation of power. Power is applied to the reaction wheels only to replace windage and friction losses or to provide control during maneuvers. In contrast with a so-called linear wheel system,

wheel speed is controlled proportional to the attitude error and continuous power must be applied.

The wheel unloading method used in conjunction with the bang-bang wheels was also a new concept. No special logic such as using tachometers to measure wheel speed was needed.

6.1.3 Sun Orientation Control

Using the sun as the spacecraft yaw reference was not a new concept, historically. It had been considered for the Advent Communications satellite system. However, the ultimate form of the yaw control system was a new concept, namely the use of only a reaction wheel to perform all yaw maneuvers. The same is true of the sun-then-earth acquisition sequence.

6.1.4 Horizon Scanner

The horizon scanner system developed by the ATL of American Standard used a new concept for the scanning mechanism. The positor or flexure-supported mirror was a unique method of obtaining a scanning mechanism for a space environment. This technique also allowed the use of the scanner at widely varying attitudes without modification. The concept of an edge-tracking scanner was also new, as previous scanner systems were of the conical scan type.

The positor device, despite its initial development problems, has proved highly reliable in space. No on-orbit failures of this portion of the scanner system have occurred.

6.1.5 Sun Sensor

The OGO sun sensor assemblies include two new developments: passive thermal control and the fine sensor or Radiation Tracking Transducer (RTT) innovations. Since the sun sensor assemblies were to be mounted at the tips of the solar arrays, each assembly had to have its own thermal control. The sensors were displaced too far from the main box to depend upon conduction for thermal stability. While heaters could have been used, passive thermal control was chosen for reasons of reliability. It is believed that this is the first attempt at passive thermal control of such a device. Performance on orbit of the thermal control system has been very good.

The RTT was developed by Micro Systems Incorporated. It is unique in that it senses the sun aspect in two orthogonal axes. The instrument also provides a logic signal that indicates when the sun is in its field-of-view. Although it is completely passive in that no electronics are required to drive it, electronics are required for subsequent signal amplification and logic signal processing.

6.1.6 Testing

One aspect of the test program resulted in a new and unique test technique. This was the method of testing horizon scanner response to the sun radiance. Rather than duplicate the entire solar spectrum, the horizon scanner infrared filter was removed from the optics, thus permitting a low-level heat source to be used as a sun

simulator. This test technique has been successfully utilized on a number of other TRW spacecraft programs.

6.2 FLIGHT OPERATIONS

The OGO flight operations pose perhaps the most important innovation obtained from the OGO program. Some satellite systems have been developed largely as the result of on-orbit experience, notably the Tiros series. Many cases can be cited on other programs where in-flight problems have been solved by ground control.

However, the initial OGO concept was for completely automatic operation. Experience obtained from the early OGO spacecraft clearly indicated a need for real time coverage of critical spacecraft operations and flexibility of command functions. For instance, OGO-II could have been operated in the same manner as OGO-IV had a gas jet disable command been available.

To develop a ground back-up capability prior to launch requires asking the question, "What if it doesn't work?" Human nature makes this a hard question to face. It usually means degradation of performance, which on the surface is usually not acceptable. The option may be completely useless spacecraft versus a partial success. Often a surprising amount of useful information can be derived from a spacecraft flying other than its intended mission. For instance, 17 of the 20 experiments on OGO-I obtained useful scientific data even though the spacecraft was spin stabilized.

7. THE PROGRAM IN RETROSPECT

As exemplified by OGO-V, the ACS has performed its function extremely well. There were many stumbling blocks along the way, however. For the benefit of future programs, it is hoped the following discussion will illuminate some of the lessons learned from OGO (Reference 26).

7.1 SYSTEMS DESIGN

The basic system design of the OGO ACS was sound. Similarly, the translation of that design into hardware produced, ultimately, a reliable and well functioning system. There were three flaws in the original design approach, however; the concept of completely automatic operation without backup modes of operation, the sensitivity of the gas control laws to unexpected spacecraft disturbances, and lack of adequate test data and/or analytical models (the antenna thermally induced oscillation) of the dynamic interaction of flexible appendages on the spacecraft. These flaws are not totally inseparable, but each affects a different area of systems design.

7.1.1 Ground Back-Up

The concept of complete automatic operation theoretically simplifies the flight-operations task. However, automatic operation does not allow for unexpected failures. Monitoring of critical spacecraft operations, particularly on early launches, should have been a design goal. Moreover, commands should have been provided such as were eventually included in OGO-IV and -V.

For instance, a large scale acquisition simulation was performed to study the effects of launching the spacecraft into eclipse. On OGO-V this problem was solved by simply locking the ACS in Mode 1 at launch and enabling the sun acquisition sequence when the spacecraft was in sunlight and in view of a ground station.

Manual unloading of the reaction wheels as is presently being done in OGO-IV, would probably have been considered an impossible task. But faced with the alternative of a spinning spacecraft, it has been accomplished. Interestingly, after OGO-II the idea of individual gas jet control by ground command was suggested. This would have proved invaluable in the OGO-IV operations. Such manual capability has been incorporated on OGO-F.

The need for ground control and observation is particularly important on the initial launches. As on-orbit experience is gained the requirements may be relaxed. In contrast, the OGO program provided more ground control as on-orbit experience was gained.

7.1.2 Gas Control Law Design

The ACS was designed such that the reaction wheels were to be the primary control torque source. Gas jets were to be used only during acquisition and for wheel unloading. No provisions were made for unexpected short term transients which might cause gas jet firings. This was an oversight in the

original design. OGO-I and -II demonstrated the need for being able to completely disable the gas jets. The gas delay logic incorporated into OGO-III saved that spacecraft from an early depletion of its gas supply. In fact, as the result of the OGO experience, gas jet disable commands have been incorporated into other NASA spacecraft.

7.1.3 Dynamic Interaction

The problem of dynamic interaction of flexible spacecraft appendages was not totally bypassed in the OGO system design; the emphasis was minimal, however. The boom oscillations which occurred on OGO-III were predictable. The faults in the original analysis of this problem occurred both in the acceptance of boom damping data which did not apply in the region of boom deflections of interest and in insufficient investigation of the ACS sensitivity to the damping parameters.

The OGO-IV antenna oscillation was not predictable, though a similar problem had occurred on a classified program. An unclassified paper was published on the observed phenomena (Reference 27) but it implied that no sustained oscillations existed. The prior OGO flight experience did not suggest the possibility of such a phenomenon either. Thus, it is unlikely that under the circumstances the problem could have been avoided or predicted.

The original OPEP control system design neglected the possibility of dynamic phenomena. As was pointed out in Section 4, initial testing of the assembly uncovered drive chatter caused by dynamic coupling of the shaft motion into the gyro. On-orbit performance of the OPEP in OGO-II and -III demonstrated the sensitivity of the controller to spacecraft motion induced by boom vibrations. This was corrected on OGO-IV by the installation of a filter in the control loop.

The problems of dynamic interaction on spacecraft have received wide recognition only recently. Reference 28 presents a survey of dynamic problems and methods of analysis on most of the current and earlier spacecraft programs.

7.2 EQUIPMENT DESIGN

In general, the concepts of the ACS design were translated into hardware effectively. In all cases, the ACS performed as designed without failure or degradation of performance. The distinction drawn here is that although there were faults in the original design concept, there were no faults in the hardware implementation.

7.2.1 Horizon Scanner

The largest single problem in the equipment development phase was the horizon scanner positor mechanical design. Since this was an entirely new device, it is unlikely that the problem could have been circumvented. Eventually, the performance of this unit was flawless.

Cold cloud tracking of the OGO-II scanner was not an equipment problem. The scanner performed precisely as designed. The fault was in an insufficient understanding of the dynamics of the scanner's operation in the presence of anomalies in the earth's radiance. Better knowledge of the earth's radiance model and more extensive simulation of the scanner dynamics might have avoided the problem.

The problems of sun and moon interference of the horizon scanner again were not equipment design problems. Rather, they were oversights in analysis of the design concepts.

7.2.2 Magnetic Amplifiers

The choice of magnetic amplifiers for the ACS was made solely on the basis of reliability. Indeed, the use of magnetic amplifiers significantly re-

duced the number of components in the system. If the design were to be implemented today, however, solid-state circuits would inevitably be chosen. Increased parts reliability and the significant weight savings would dictate such a decision.

Magnetic amplifiers have long been regarded as a reliable system element. As a result, the thermal and electrical design problems associated with spacecraft applications were not fully appreciated early in the OGO program. This led ultimately to the failure of the motor driver magnetic amplifiers on OGO-III. Again, the magnetic amplifiers performed as designed by the manufacturer; however, they were not intended for 100-% duty cycle cyclic operation.

7.2.3 System Testing

The individual unit testing approach on OGO is, for the most part, standard throughout the industry. No change in this approach would appear warranted. System test philosophy varies from program to program, however. The most valuable of the OGO systems tests was the subsystem laboratory test. It provided verification of the entire system operation under closely controlled conditions. The value of this test decreased in later flight systems simply because the earlier tests verified that the individual units, when constructed according to their specifications, performed properly as a system.

The torsion wire tests were of questionable value although they did lend confidence in the bang-bang reaction wheel design concepts.

Similarly, the air-bearing test provided little useful dynamic design information. The air bearing and associated equipment were expensive. Although no quantitative data were obtained from the test, several mode-switching failures were discovered and corrected. In retrospect, although the use of air-bearing tests for space simulation is valuable, these tests did not provide the dynamic design information and performance evaluation originally anticipated.

7.2.4 Mission Changes

OGO experience has shown that changes in mission (orbit) late in the program may provide unexpected consequences. Because of timing, the revised orbits produce an effect on performance which may not be recognized by personnel active at the time. Two such changes have been described.

1. The POGO orbit perigee objective was lowered to 140 n. mi. at one point and remained there for several years without anyone realizing that gas available would not support one year life. At the last minute, perigee had to be raised to avoid short spacecraft life.
2. Apogee was raised above the design objective (60,000 n. mi.) prior to launch of OGO-III. In this case, a scanner redesign for small earth margin was recognized but could not be implemented until OGO-V. Thus, apogee had to be reduced to near the 60,000 n. mi. value again.

8. REFERENCES

1. "Final Report, Orbiting Geophysical Observatories I, II, and III," TRW Systems Report No. 00063-6009-R000, 19 December 1965.
2. Otten, D.D., "OGO Attitude Control Subsystem Description, Logic, and Specifications," TRW Systems Report No. 2313-0004-RU000, 4 December 1961.
3. "OGO Attitude Control Subsystem Operations Manual," Revision 1, TRW Systems IOC No. 7231.4-18, 12 February 1968.
4. Hutchings, P.B., "OGO Sun-Sensor Assembly Technical Description," TRW Systems Report No. 2313-6019-TU000, 28 October 1963.
5. Priorie, K.C., "OGO Horizon Scanner Assembly Technical Description," TRW Systems Report No. 2313-6012-KU000, Revised 6 January 1965.
6. Field, G.R., "OGO Pitch Rate Gyro Assembly Technical Description," TRW Systems Report No. 2313-6020-KU000, 1 July 1963.
7. Keller, W.N., "OGO Sensor Electronics and Logic Assembly Technical Description," TRW Systems Report No. 2313-6005-KU000, 22 October 1962.
8. Sherman, J.P., "OGO Attitude Control Assembly Technical Description," TRW Systems Report No. 2313-6016-KU000, 13 September 1963.
9. Sherman, J.P., "OGO Solar Array and OPEP Drive Electronic Assembly Technical Description," TRW Systems Report No. 2313-6015-KU000, 13 September 1963.
10. Richardson, J.M., "OGO Inverter Assembly Technical Description," TRW Systems Report No. 2313-6018-KU000, 4 November 1963.
11. Wattenbarger, R.L., "OGO Reaction Wheels Technical Description," TRW Systems Report No. 2313-6024-TU000, 17 January 1964.
12. Warne, D., "OGO Solar Array and OPEP Drive Assembly Technical Description," TRW Systems Report No. 2313-6017-KU000, September 1963.
13. "Orbiting Geophysical Observatory, Part I Technical Proposal," TRW Systems Proposal No. 60-63, 23 September 1960.
14. "Preliminary Specifications for the Orbiting Geophysical Observatories," NASA Goddard Spaceflight Center, 23 August 1960.
15. "Final Report, OGO Design Modification and Evaluation Study, Volumes I and II," TRW Systems Report No. 2310-0001-RU000, March 1961.
16. "Program Plan for Development of OGO Attitude Control and Stabilization Subsystem," TRW Systems Report No. 9313.9-1, 3 February 1961.

17. "Specifications for the Orbiting Geophysical Observatory, S0-S49/50-1, " Revision 1, NASA Goddard Space Flight Center, August 1962.
18. "Final Report, Investigation of OGO-A Malfunction, " TRW Systems Report No. 2311-6094-SU000.
19. "Final Report, OGO-I Flight Evaluation, " TRW Systems Report No. 2311-6098-SU000, 3 February 1965.
20. "Final Report, Investigation of OGO-II Malfunctions, Volume I Attitude Control, " TRW Systems Report No. 2360-6002-R0000, 1 March 1966.
21. McKenna, K.J., "Final Report, The OGO Attitude Control Subsystem Redesign as a Result of the OGO-III Experience, Volume I Subsystem Analysis, " TRW Systems IOC No. 67-7231.7-116, 30 January 1967.
22. "Final Report, The OGO Attitude Subsystem Redesign as a Result of the OGO-III Experience, Volume II Hardware Redesign Data, " TRW Systems IOC No. 67-7234.1-51, 17 July 1967.
23. "Operations Summary Report, OGO-IV 28 July to 7 August 1967, " TRW Systems Report No. 08672-6006-T000.
24. Koval, L.R. and Mueller, M.R., "Formulation of Equations for the OGO-IV Boom Problem, " TRW Systems IOC No. 67-3341.1-188, 30 November 1967.
25. Frisch, Harold P., "Thermal Bending Plus Twist of a Thin Walled Cylinder of Open Section with Application to Gravity Gradient Booms, " NASA TN D-4069, August 1967.
26. Fraser, R.E., "The Lessons of OGO, " 15 March 1968.
27. Fischell, R.E. and Mobley, F.F., "A System for Passive Gravity Gradient Stabilization of Earth Satellites, " Paper No. 63-326, presented at AIAA Guidance and Control Conference, 12-14 August 1963.
28. Farrenkopf, R.L., "A Survey of Case Histories Involving Spacecraft Dynamic Interaction, " TRW Systems Report No. 06314-6007-R000, 30 March 1968.